Smart Mitigation of flow-induced Acoustic Radiation and Transmission for reduced Aircraft, Surface traNSport, Workplaces and wind enERgy noise

Aerodynamic Noise Reduction with Flow Control Devices

R. Zamponi, T. Suresh, C. Teruna, L. T. Lima Pereira, G. Bampanis, I. Zurbano Fernández

SA Public Workshop, 26 November 2020

H2020 MARIE SKŁODOWSKA-CURIE ACTIONS

Outline

- Introduction
- Leading-Edge Noise Treatments
- Trailing-Edge Noise Treatments
- Boundary-Layer Separation control
- Industrial Perspective and Applications
- Q&A

I. INTRODUCTION

Aerodynamic Noise is Everywhere

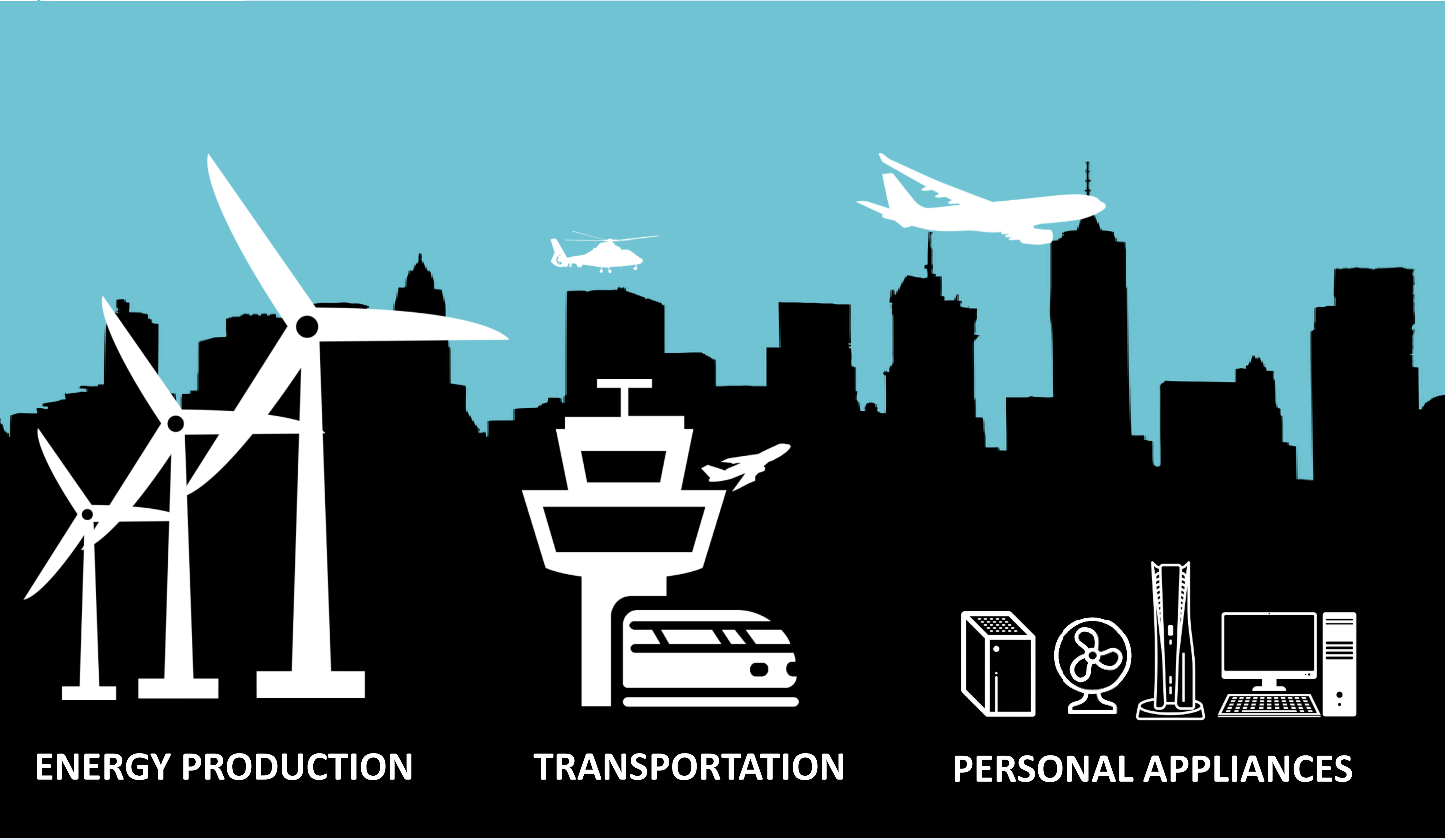

Can We Blame Turbulence?

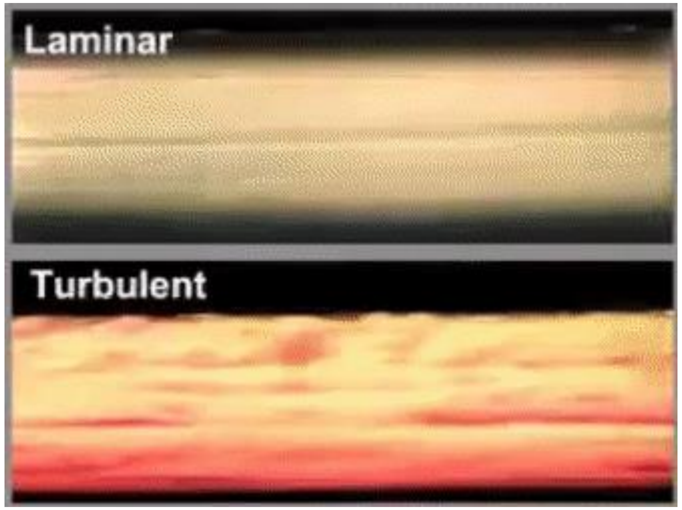

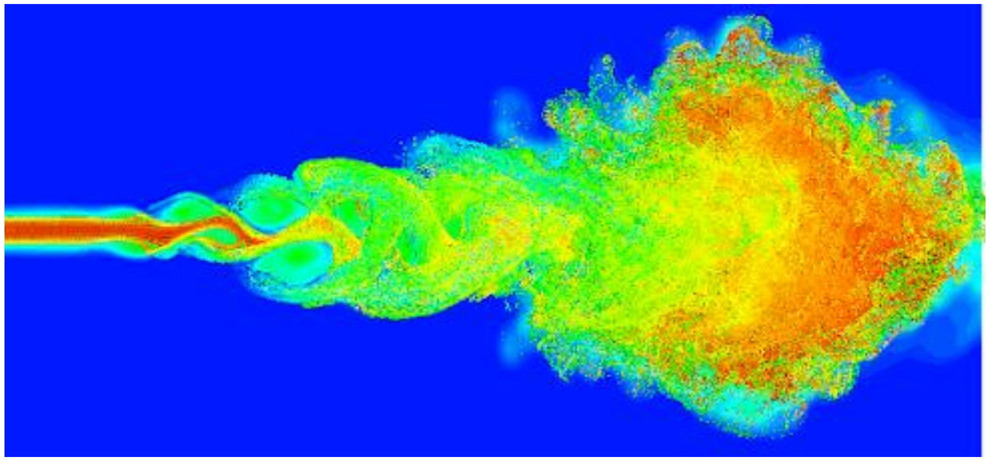

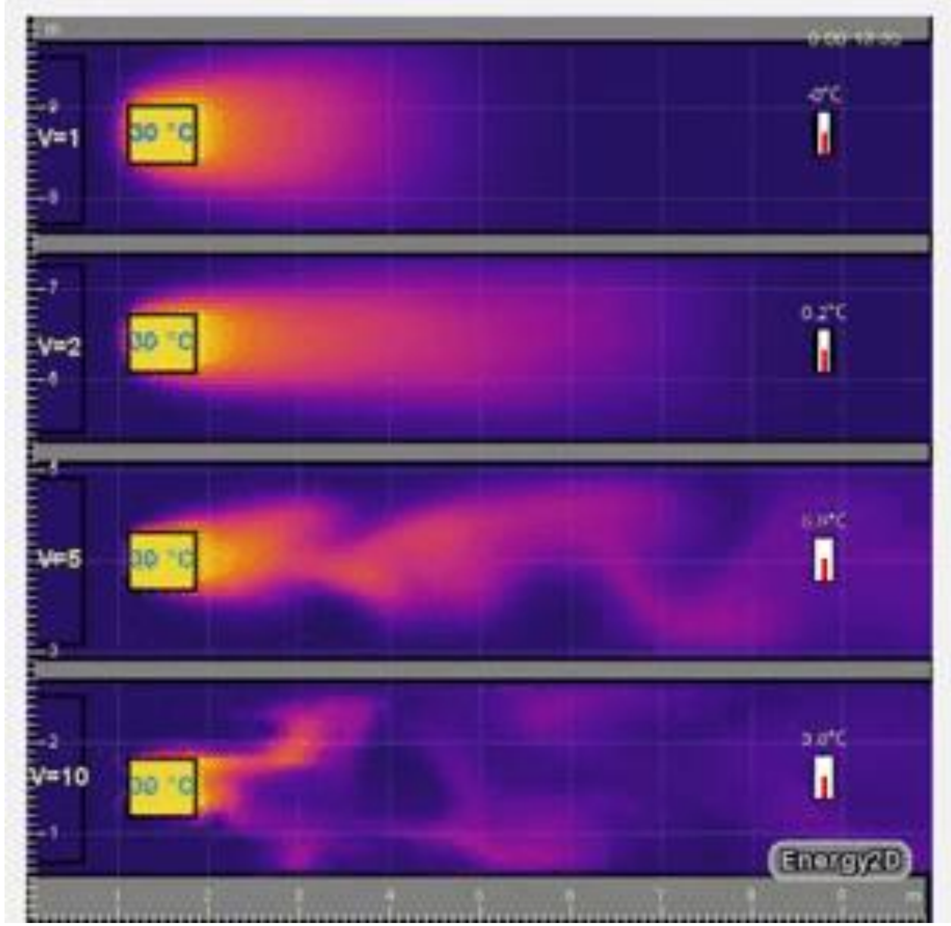

High Reynolds number→ turbulence

[1] http://www.2decomp.org/dstar.html
[2] https://images.app.goo.gl/CDy38ig5yotfVNYc9
[3] https://www.sciencealert.com/the-internet-is-obsessing-over-this-impossible-water-stream

Turbulence-Interaction Noise

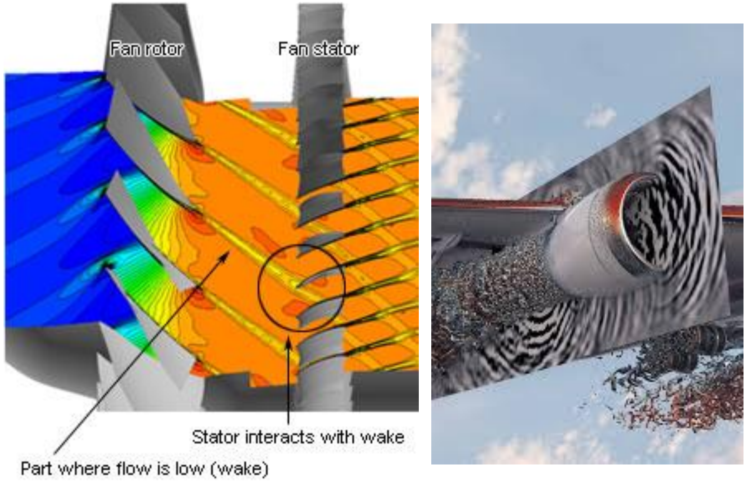

Sound radiation from a turbofan fan stage [1]

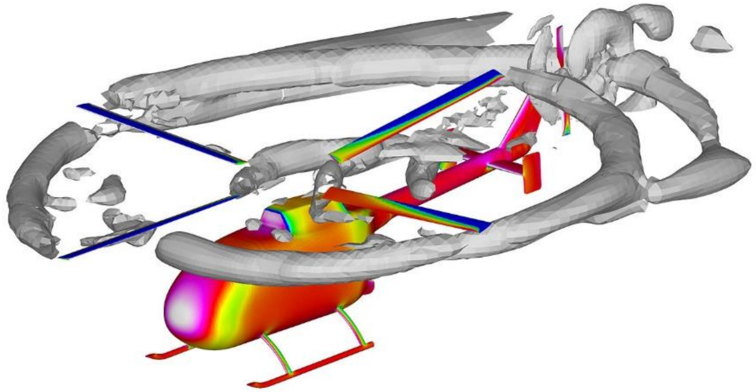

Blade-vortex interaction on helicopter [2]

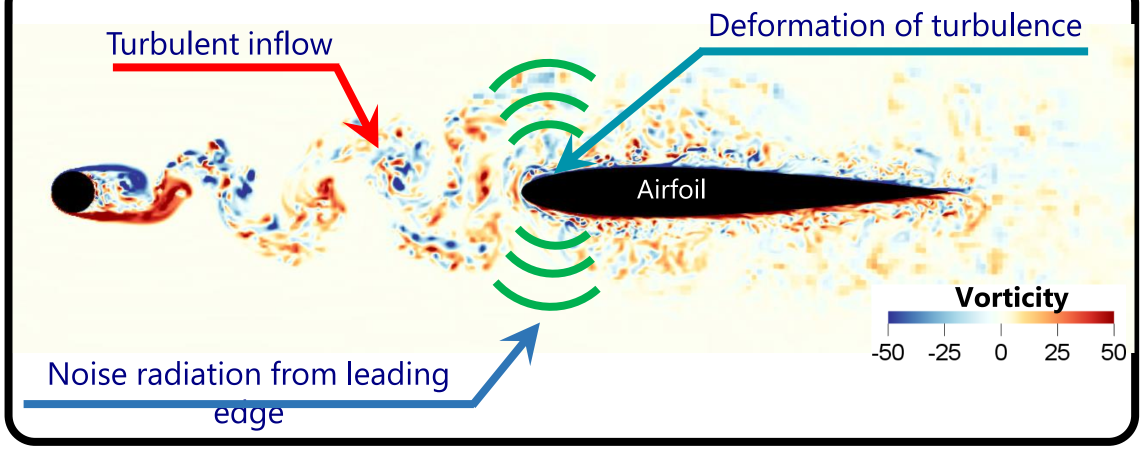

[1] https://www.aero.jaxa.jp/eng/publication/magazine/apgnews/2012_no24/apn2012no24_02.html
[2] http://www.dlr.de/media/en/desktopdefault.aspx/tabid-4985/8422_read-19451

Airfoil Self-Noise

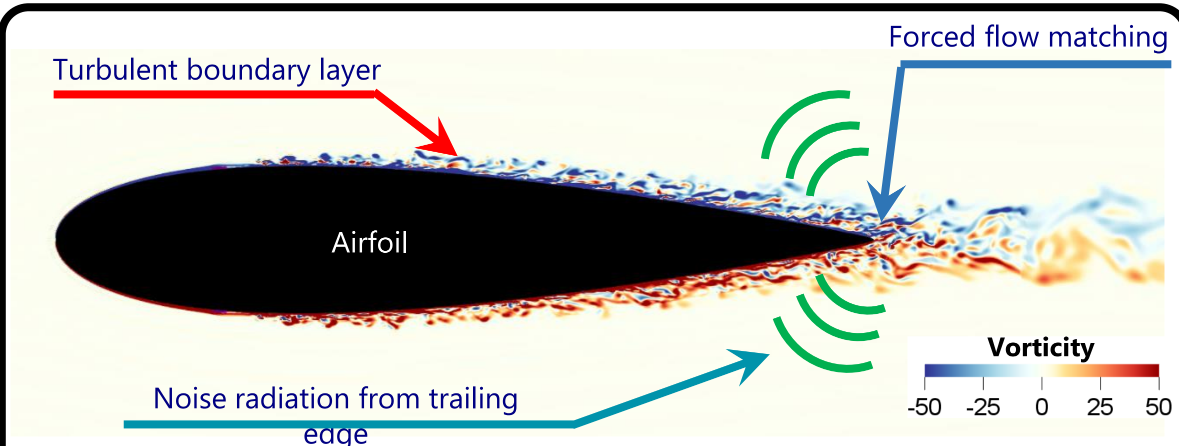

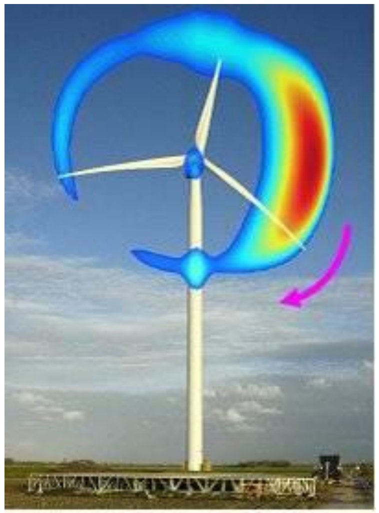

Wind turbine sound source map [1]

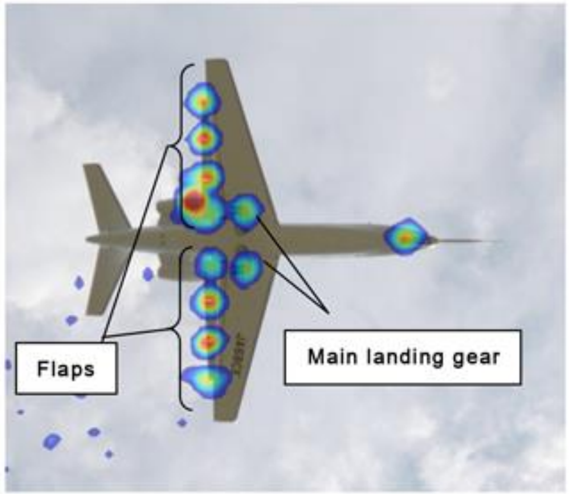

Aircraft-on-approach source map [2]

[1] Oerlemans, S., Sijtsma, P., & López, B. M. (2007). Location and quantification of noise sources on a wind turbine. *Journal of sound and vibration*, *299*(4-5), 869-883.

[2] Yamamoto, K., Takaishi, T., Murayama, M., Yokokawa, Y., Ito, Y., Kohzai, M., & Tsuchimoto, Y. (2018). FQUROH: A Flight Demonstration Project for Airframe Noise Reduction Technology–the 2nd Flight Demonstration. In *2018 AIAA/CEAS Aeroacoustics Conference* (p. 4087).

Wind Turbine Noise and Complaints

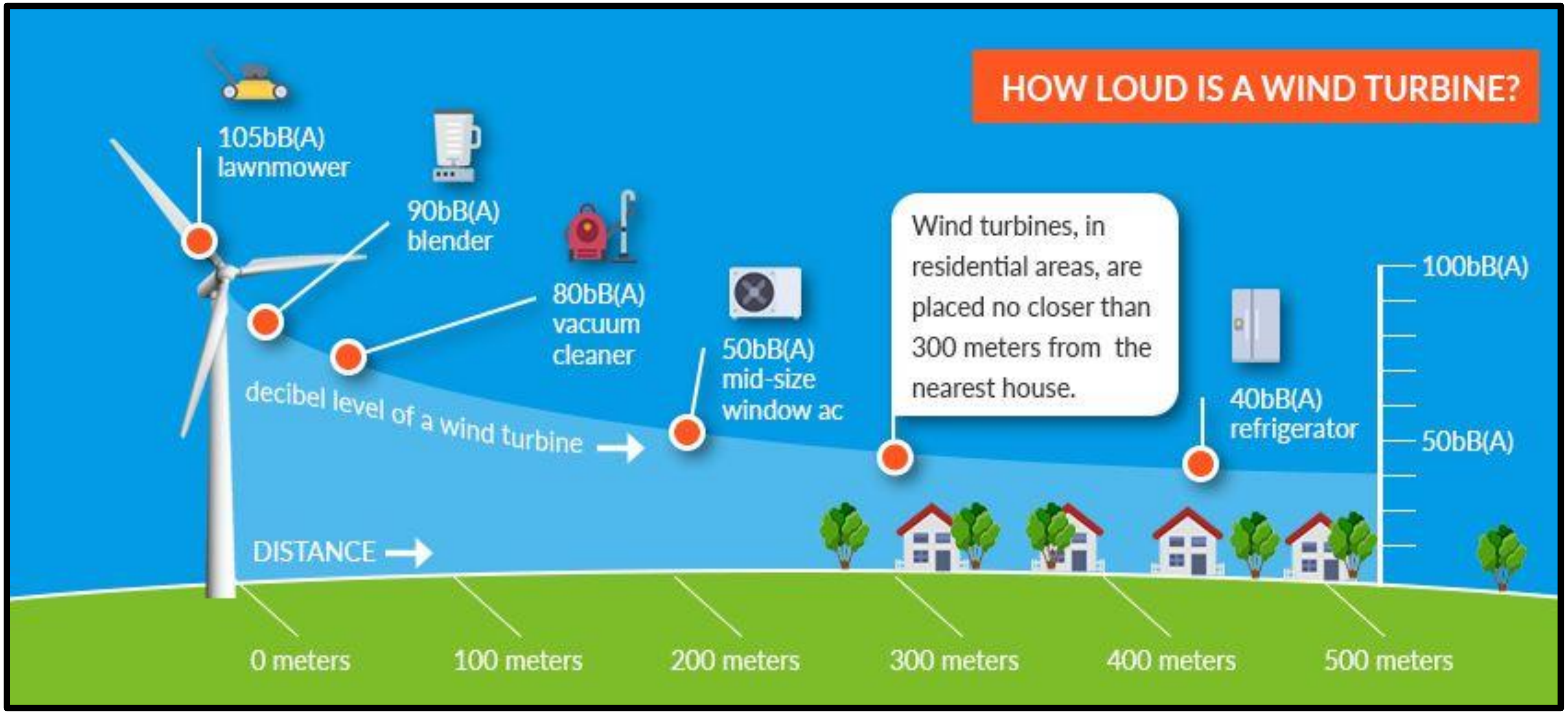

[1] https://blogs.sw.siemens.com/simcenter/not-in-my-backyard-how-annoying-is-wind-turbine-noise/
[2] https://www.wind-watch.org/documents/wind-turbine-noise-complaint-predictions-made-easy/

Wind Turbine Noise and Complaints

De Telegraaf

NIEUWS SPORT ENTERTAINMENT FINANCIEEL VROUW LIFESTYLE WAT U ZEGT

Eerste NL'se klimaatvluchtelingen een feit: 'Windangst, het lawaai is niet te harden'

Door EDWIN TIMMER
31 okt. 2020 in BINNENLAND

Lees voor

AMSTERDAM - De eerste Nederlandse klimaatvluchtelingen zijn een feit. Niet vanwege natte voeten, maar omdat burgers het geluid van windparken niet kunnen harden. Ook omwonenden van biomassacentrales klagen steen en been. Zijn gezondheid en milieu in Nederland ondergeschikt aan onze klimaatdoelen? „Ik zie wel een overeenkomst met het Groninger gas en de Limburgse mijnen: energiebelangen wegen zwaarder dan andere belangen."

[1] https://blogs.sw.siemens.com/simcenter/not-in-my-backyard-how-annoying-is-wind-turbine-noise/
[2] https://www.wind-watch.org/documents/wind-turbine-noise-complaint-predictions-made-easy/

Why Noise Mitigation is Important?

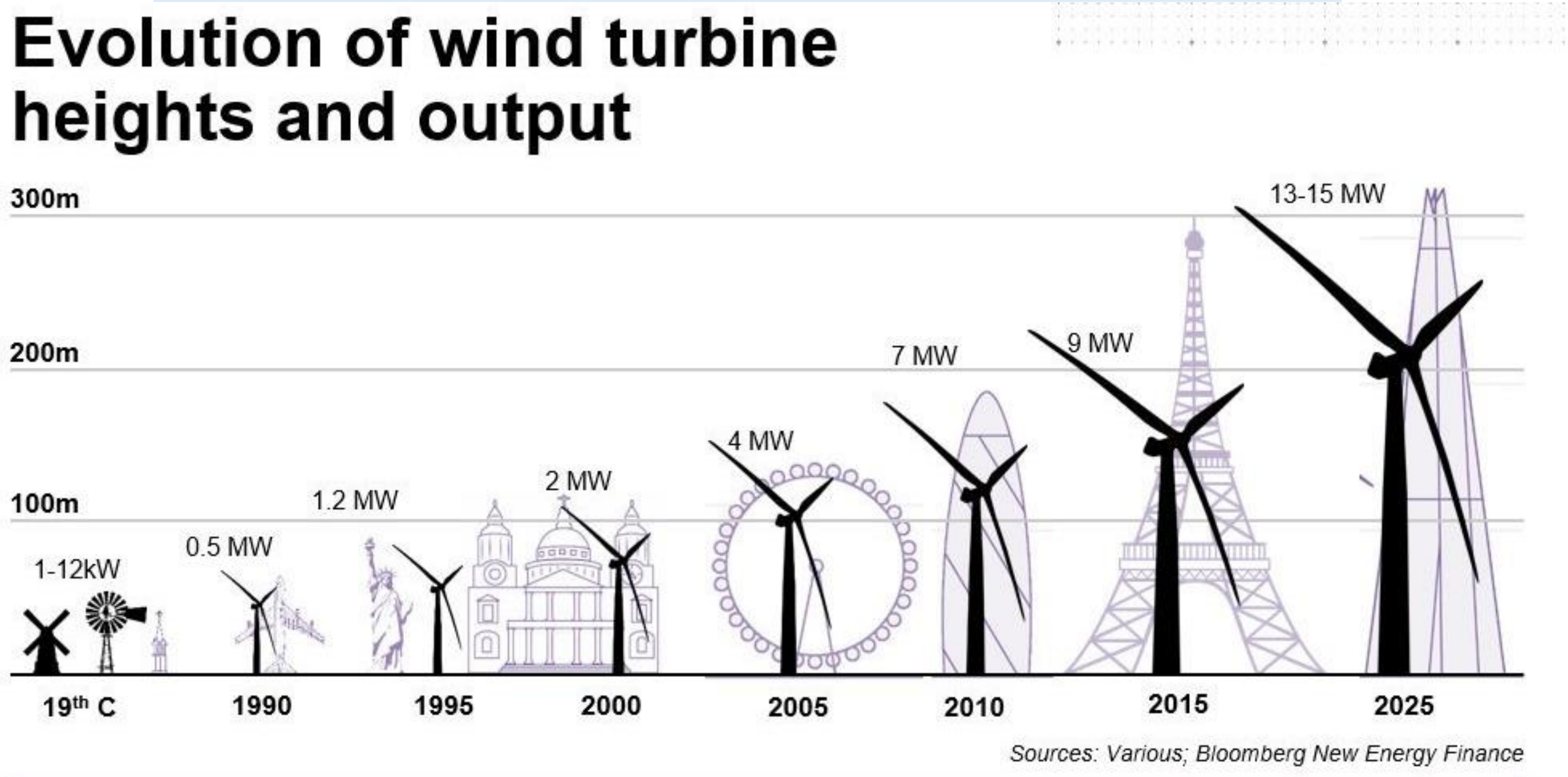

Why Noise Mitigation is Important?

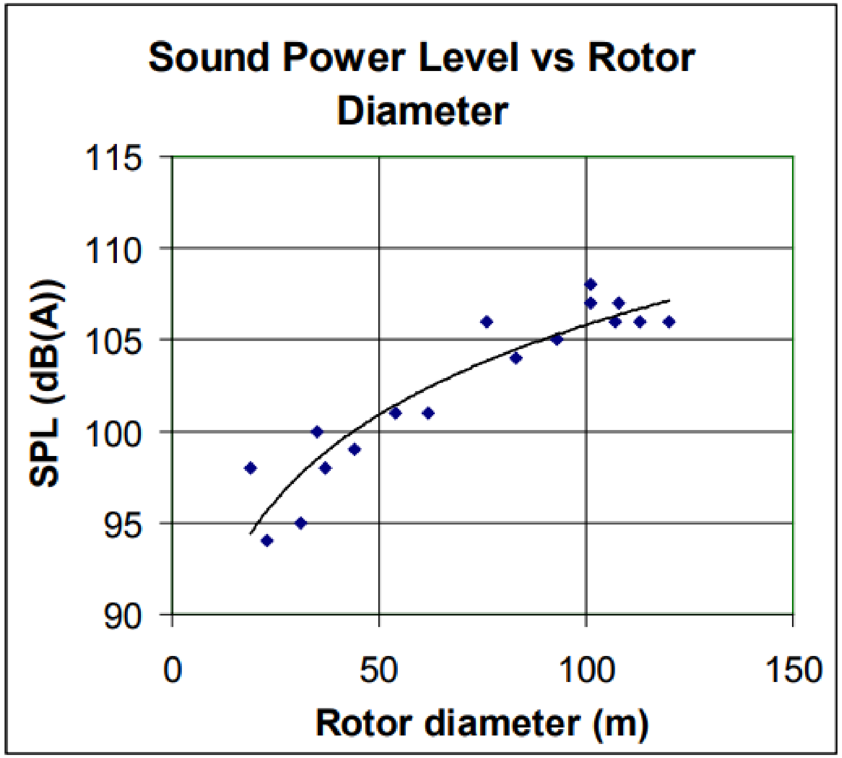

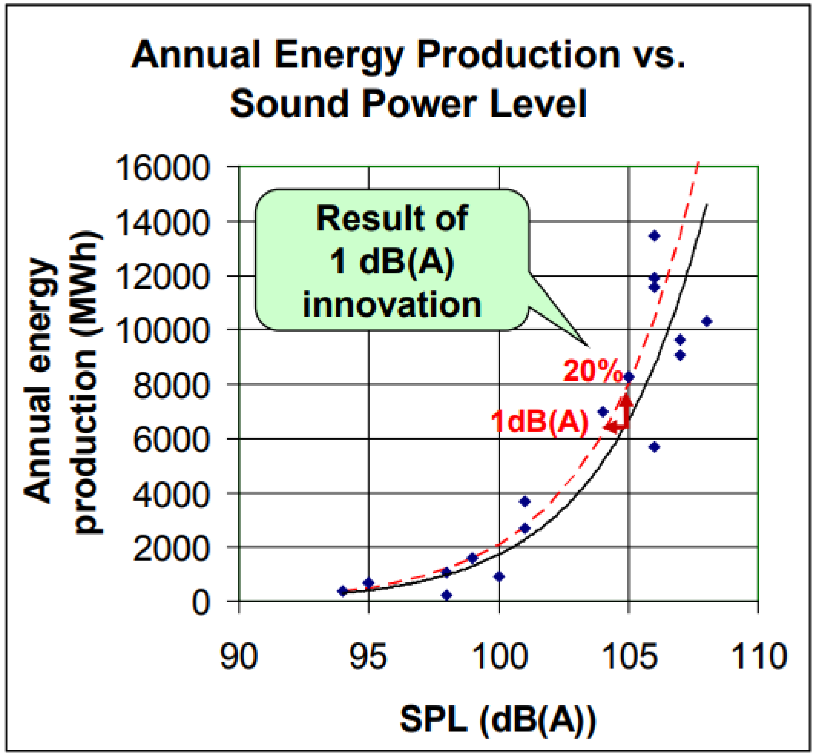

Power curtailment is no longer needed

Or

Higher energy production within the noise limit

Aircraft Noise

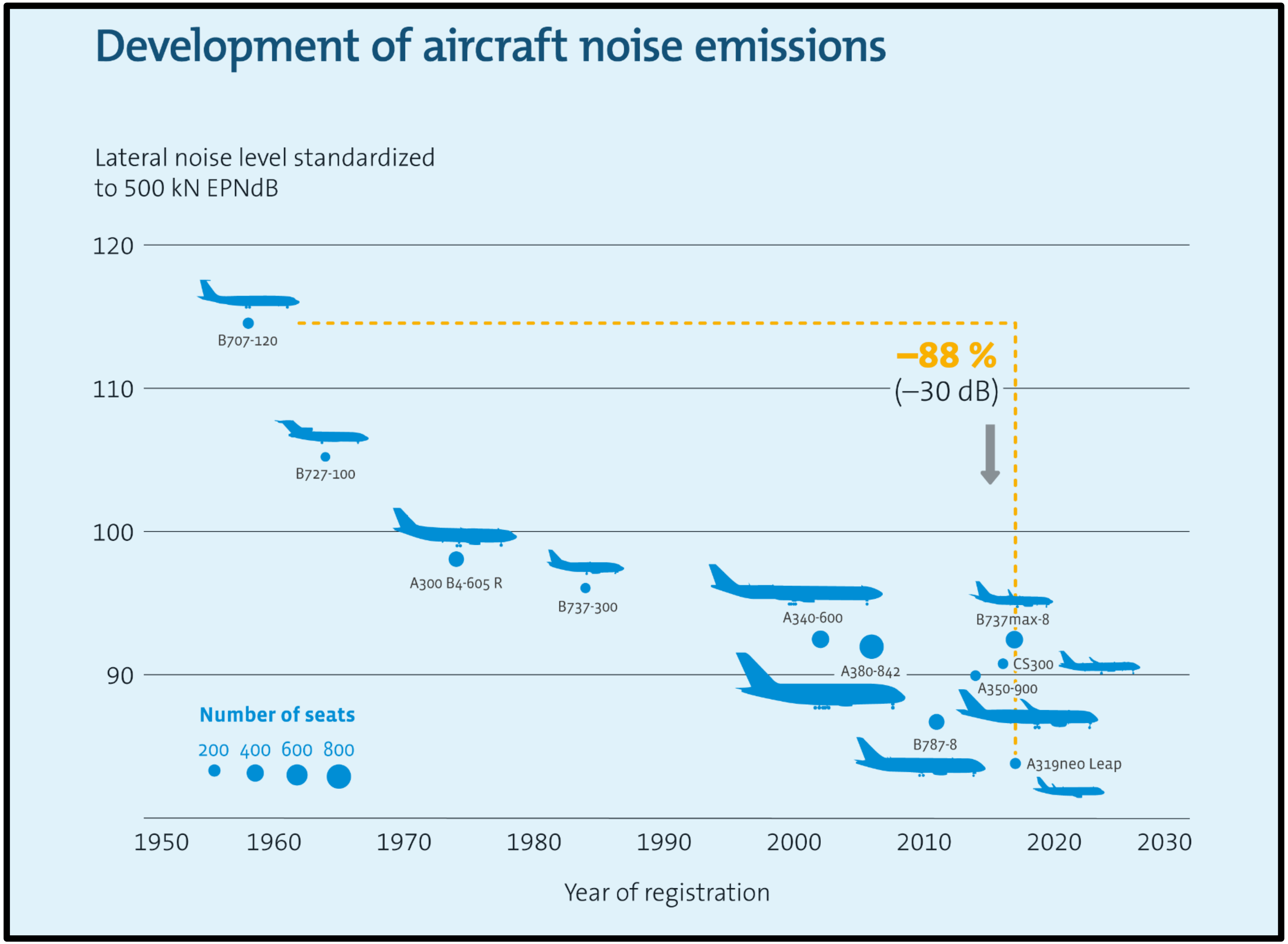

[1] https://www.bdl.aero/en/topics-and-positions/sustainability/aircraft-noise/

Aircraft Noise

1960s → 2000s

Boeing 707[1]
Turbojet

Boeing 777[2]
High-bypass turbofan

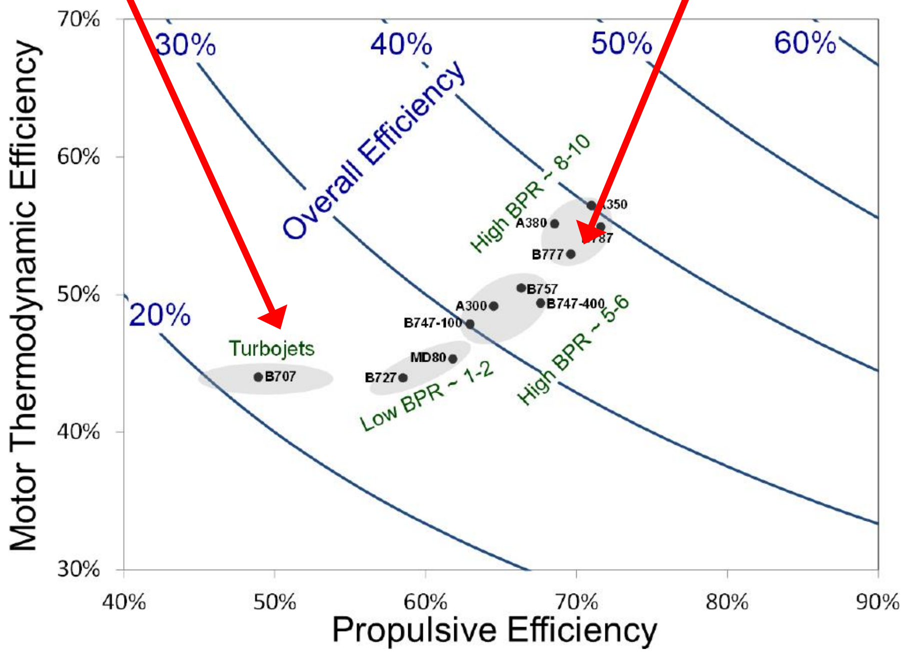

[1] Kuwait airways 707, Pinterest
[2] https://blog.klm.com/jet-engines-are-hot-in-at-least-4-ways/
[3] https://www.nap.edu/read/23490/chapter/6#36
[1] https://www.bdl.aero/en/topics-and-positions/sustainability/aircraft-noise/

Aircraft Noise

Boeing 707[1]
Turbojet

1960s → 2000s

Boeing 777[2]
High-bypass turbofan

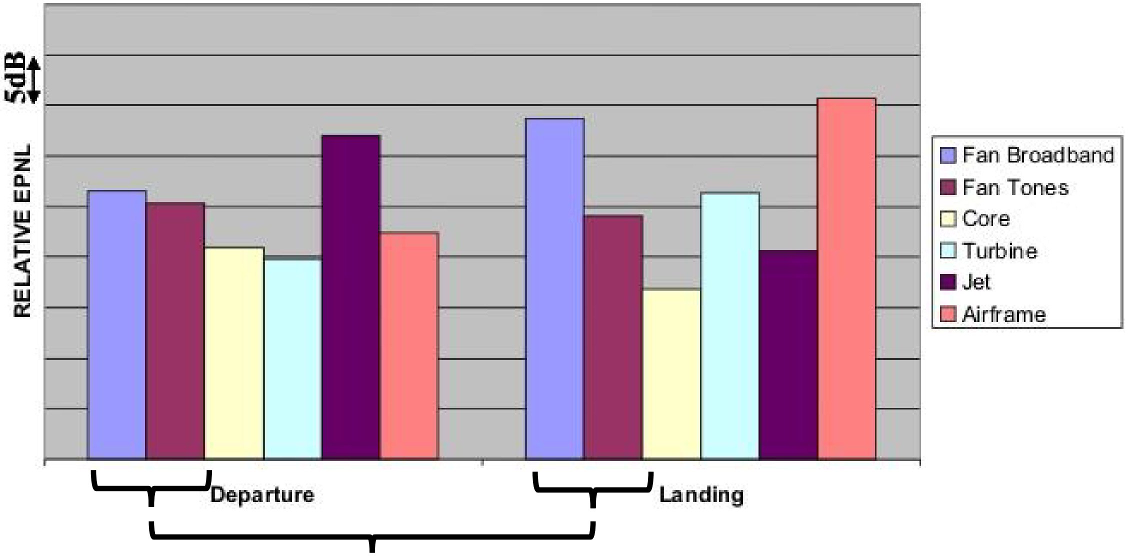

Fan noise

[1] Kuwait airways 707, Pinterest
[2] https://blog.klm.com/jet-engines-are-hot-in-at-least-4-ways/
[3] https://www.nap.edu/read/23490/chapter/6#36
[4] Lecture 6 Turbojet Turbofan Increasing thrust, CHALMERS
[1] https://www.bdl.aero/en/topics-and-positions/sustainability/aircraft-noise/
[5] http://www.cimne.com/vpage/2/2189/Objectives

HOW CAN WE ACHIEVE NOISE REDUCTION?

1. Sound absorption
2. Noise source intensity attenuation
3. Acoustic interference

PROMISING FLOW CONTROL DEVICES ?


Porous materials

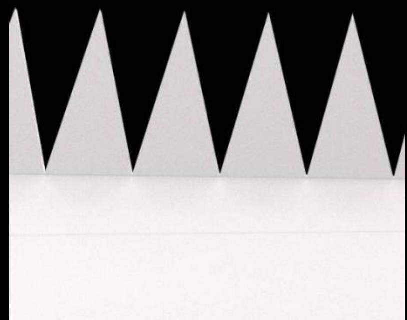
Serrations


Vortex Generators

II. LEADING-EDGE TREATMENTS

TIN Reduction by Wavy Leading Edge Serrations

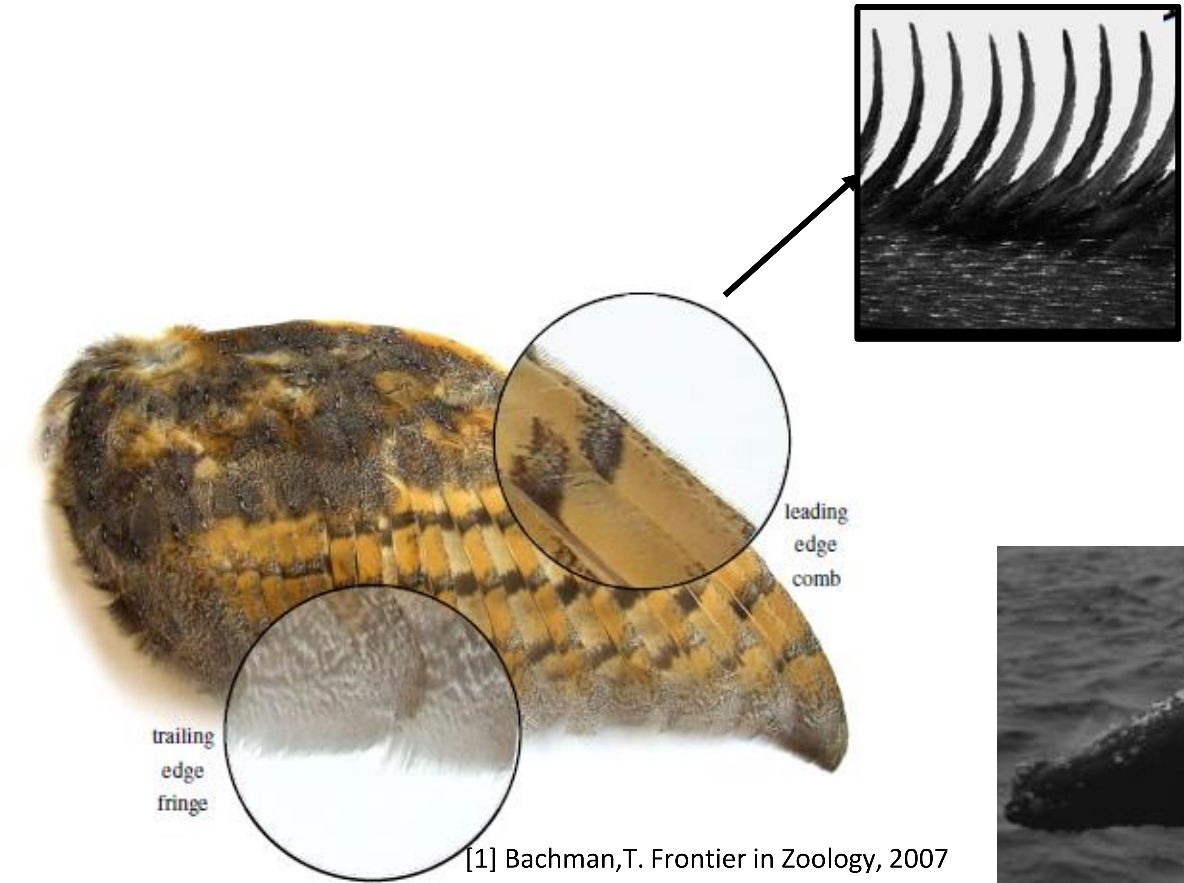

[1] Bachman,T. Frontier in Zoology, 2007
[2] Geyer,T. AIAA, 2014

[3] Fish, Integrative and Comparative Biology, 2011

TIN Reduction by Wavy Leading Edge Serrations

Flat-plate

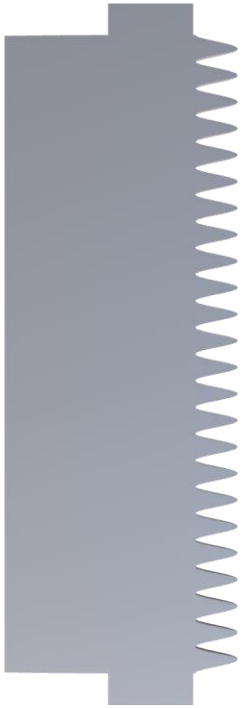

NACA 0012

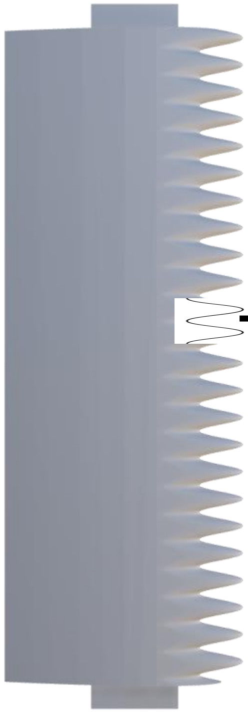

'Tuned' serrations,

Λ

$$L \leq 4\Lambda$$

P. Chaitanya et al. JFM, 2017

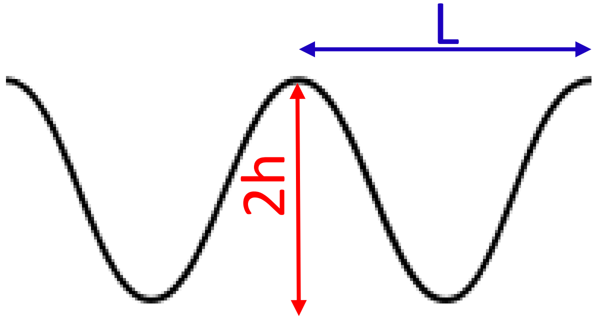

Basic Noise Reduction Mechanisms

- Destructive interference of the scattered surface pressure [1]

- Cutoff effect due to the oblique edge [2]

[1] S. Narayanan, P. Chaitanya, S. Haeri, P. Joseph, J. W. Kim, and C. Polacsek, “Airfoil noise reductions through leading edge serrations,” *Phys. Fluids*, vol. 27, no. 2, 2015.
[2] J. W. Kim, S. Haeri, and P. Joseph, “On the reduction of aerofoil-turbulence interaction noise associated with wavy leading edges,” *J. Fluid Mech.*, vol. 792, pp. 526–552, 2016.

Basic Noise Reduction Mechanisms

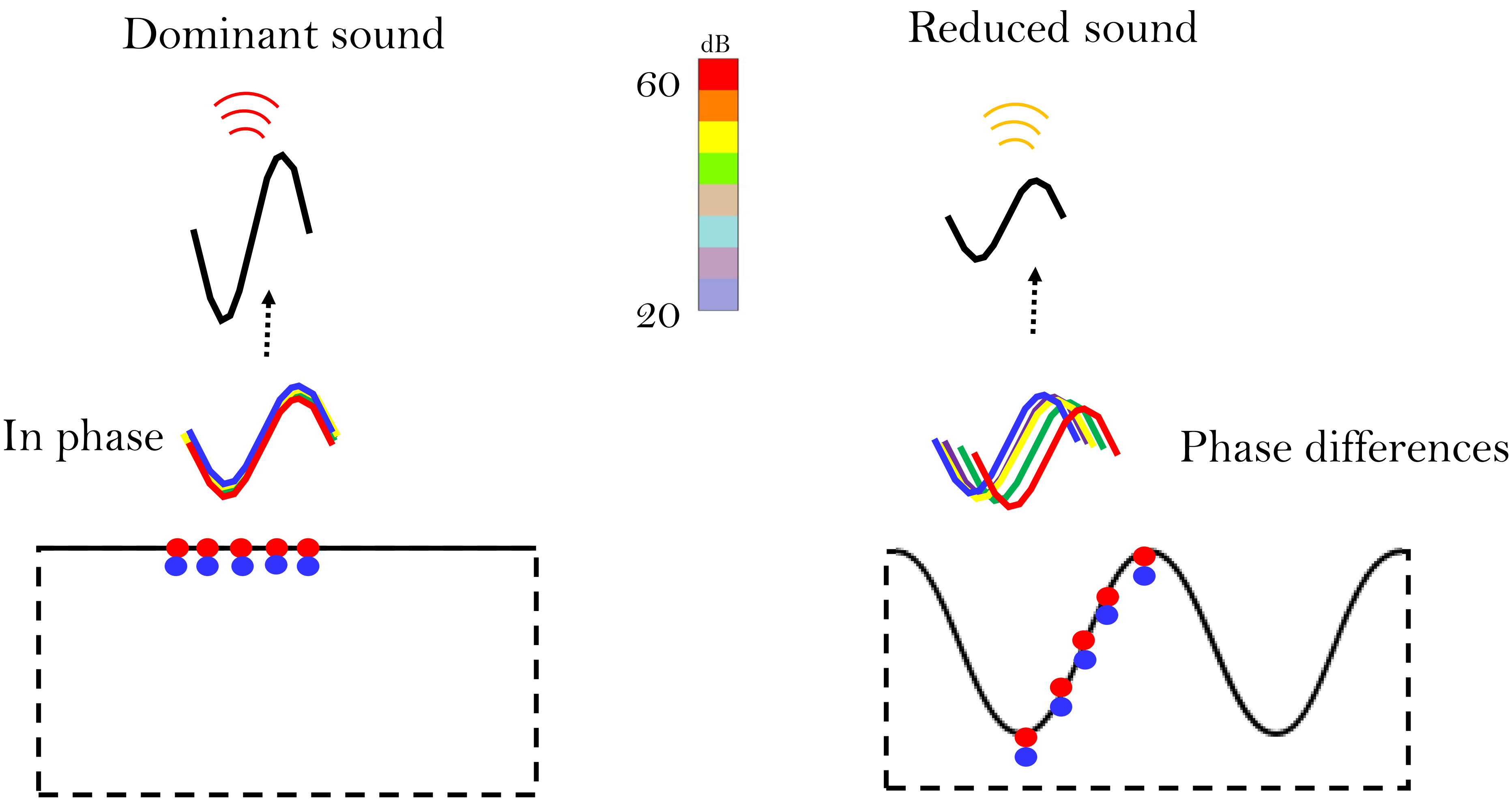

[1] S. Narayanan, P. Chaitanya, S. Haeri, P. Joseph, J. W. Kim, and C. Polacsek, "Airfoil noise reductions through leading edge serrations," *Phys. Fluids*, vol. 27, no. 2, 2015.
[2] J. W. Kim, S. Haeri, and P. Joseph, "On the reduction of aerofoil-turbulence interaction noise associated with wavy leading edges," *J. Fluid Mech.*, vol. 792, pp. 526–552, 2016.

Experimental Results
Baseline versus Serrated Flat-Plates

Baseline
Serrations

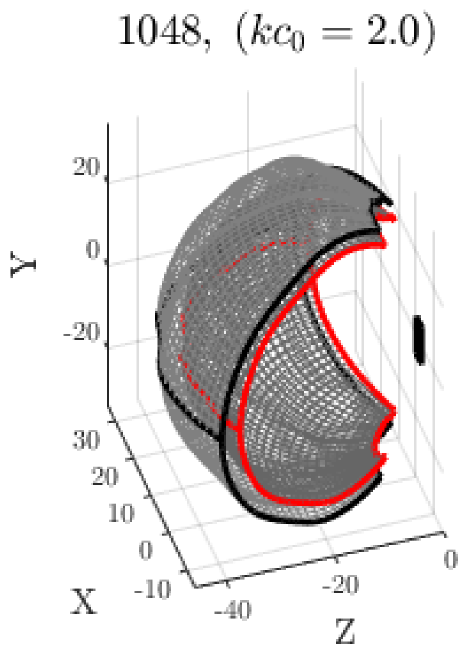

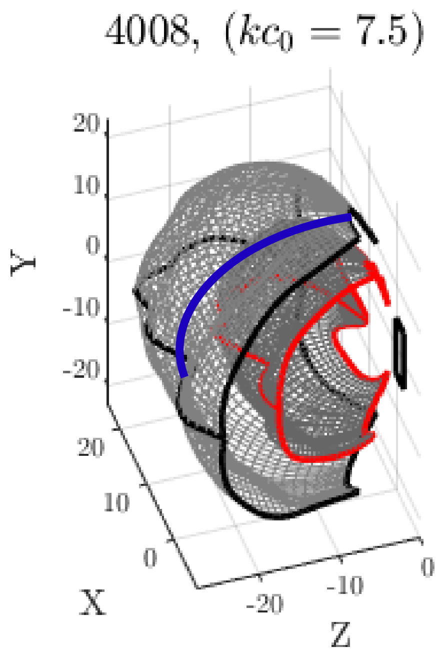

- Higher noise reductions occur at ~5 kHz over all radiation angles

Experimental Results
Baseline versus Serrated Flat-Plates

Baseline
Serrations

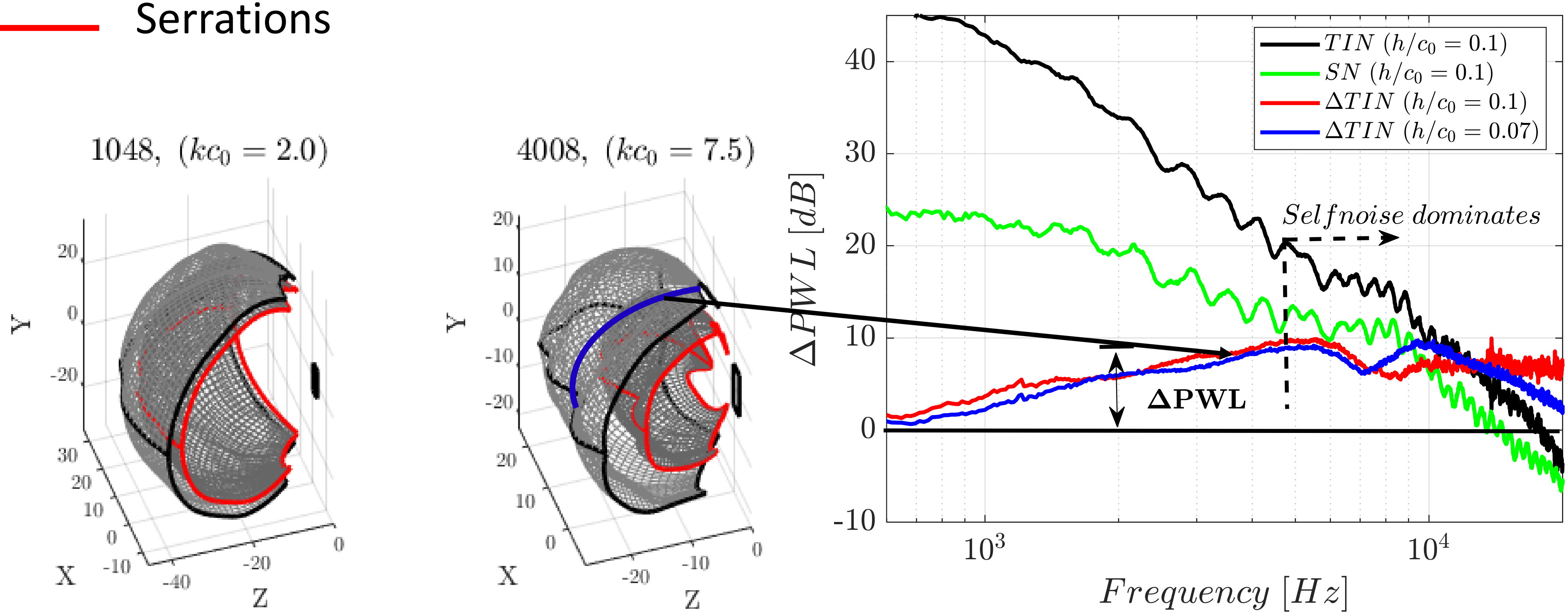

- Higher noise reductions occur at ~5 kHz over all radiation angles

Airfoil TEN contribution to the Total Airfoil Noise

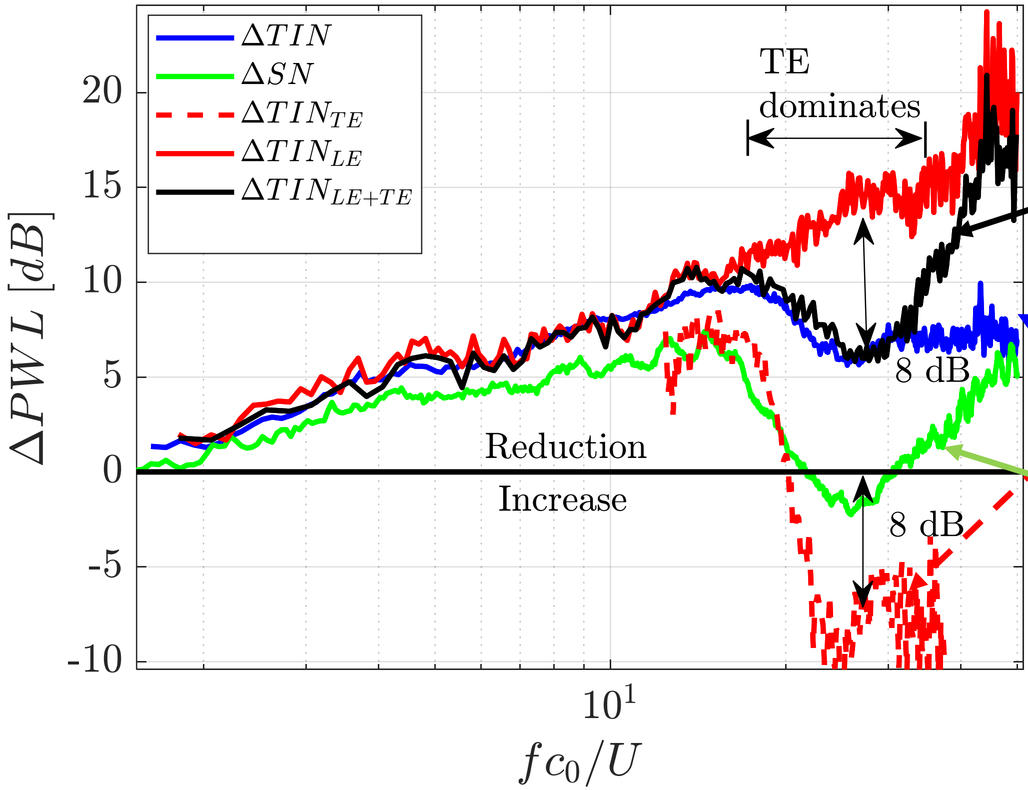

Beamforming

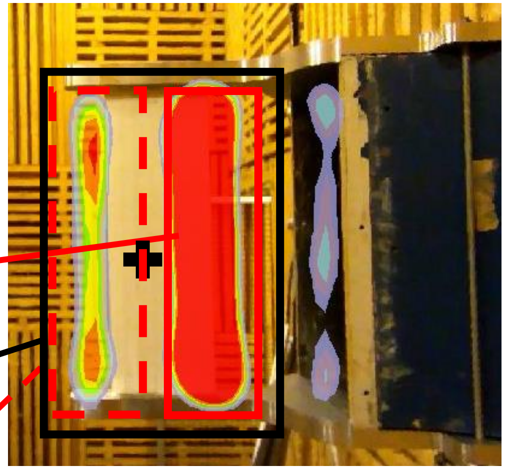

Far-field microphone

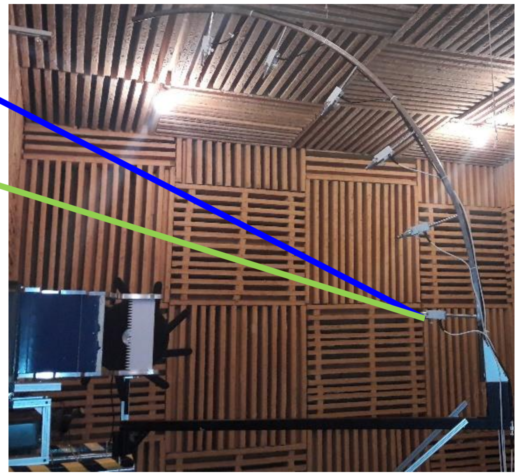

Bampanis *et al.*, AIAA 2019

Comparison of Predictions with Experiments

Flat plate baseline

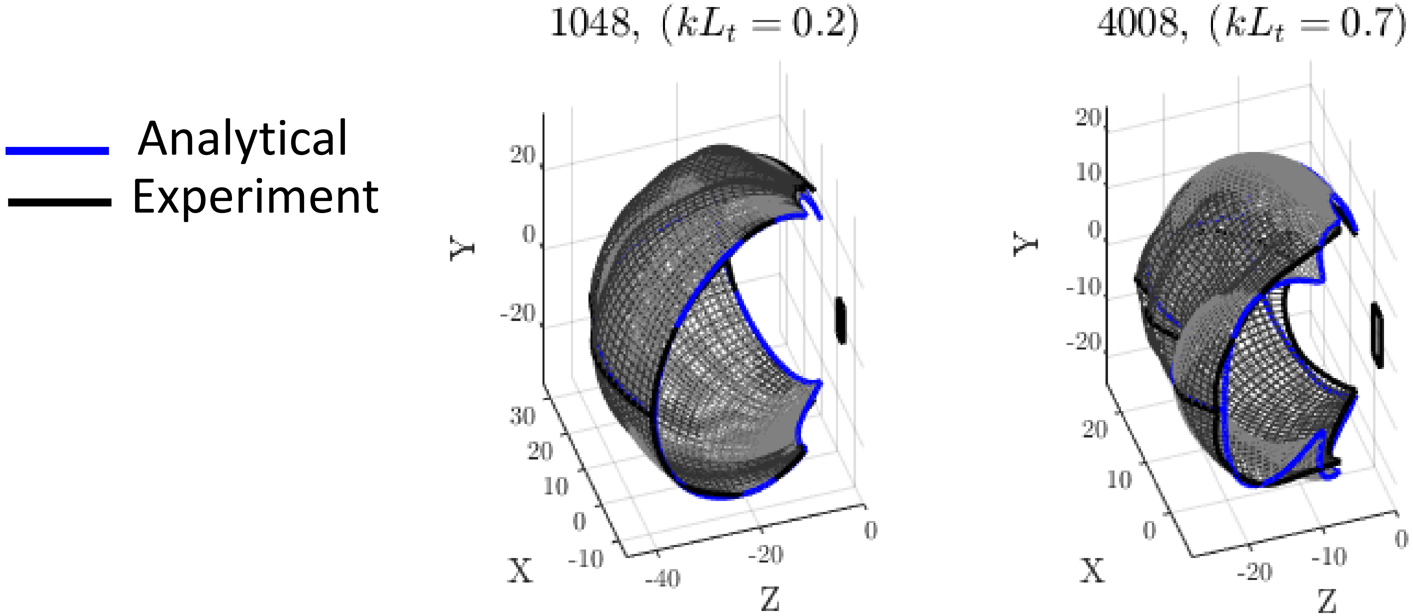

- Good agreement at low and mid frequencies
- Possible future improvement by applying a shear-layer refraction correction.
- Discrepancies at high frequencies due to the trailing-edge noise contribution. (TEN is not included in the analytical modelling).

ECL Porous Airfoil

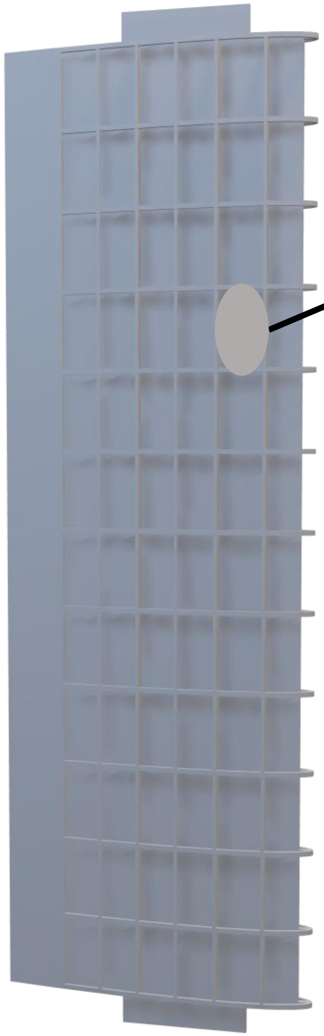

Metal wool

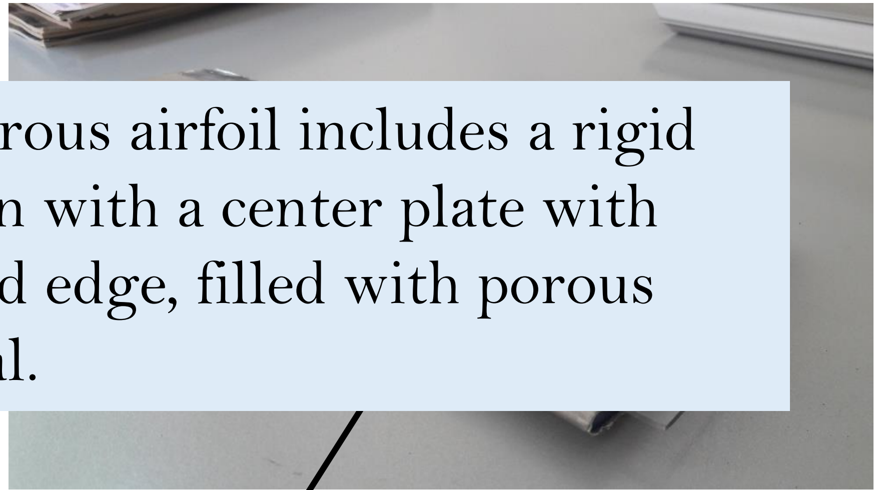

The porous airfoil includes a rigid skeleton with a center plate with recessed edge, filled with porous material.

Metal wiremesh

A smooth surface is ensured by covering the assembly with a wiremesh.

Far-Field Estimates of TIN Reduction on Porous Airfoils

Full-chord center plate (V1)

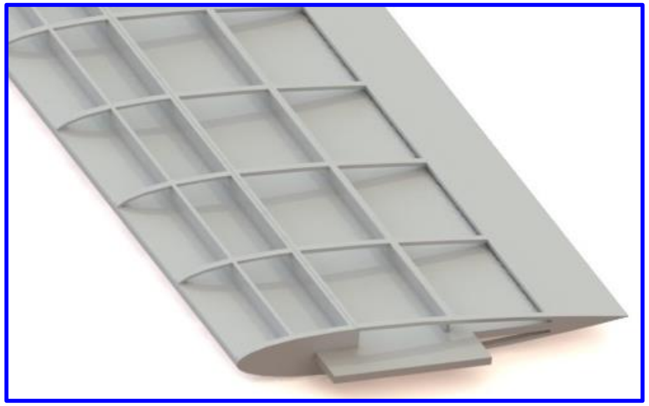

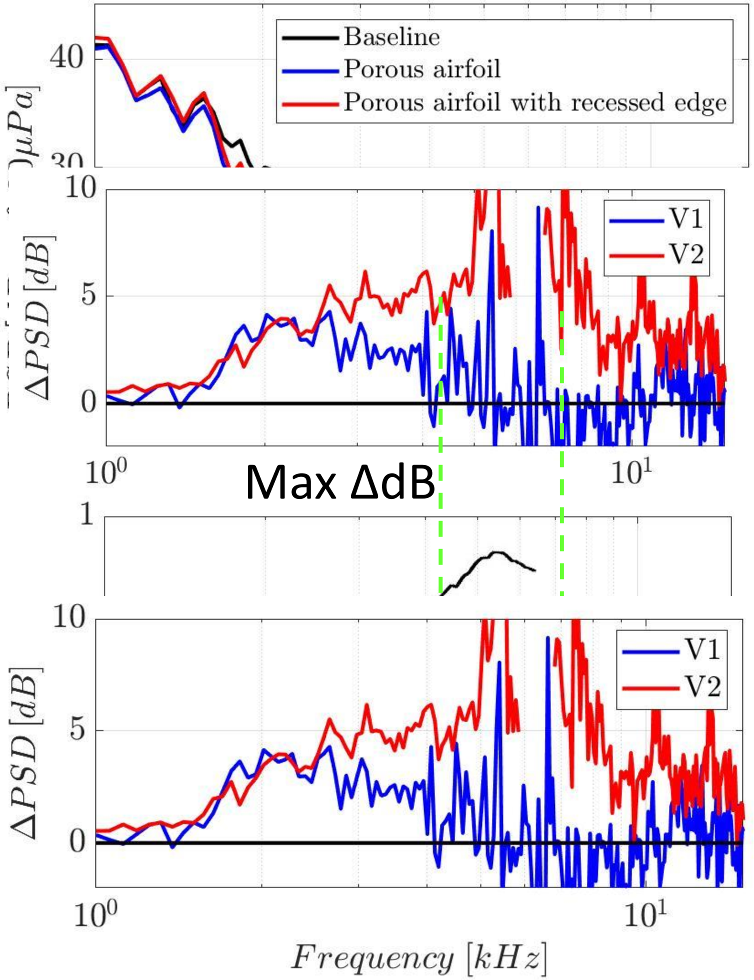

Recessed-edge center plate (V2)

Bampanis & Roger (AIAA 2020)

Full sample —

Melamine foam with frame —

Melamine foam —

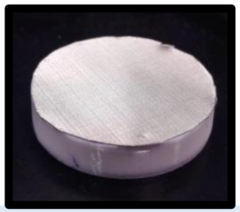
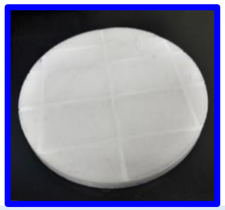


- Flow speed: 32 m/s
- 0° AOA

Rotor-Stator Interaction Noise

Rotor-stator interaction in turbofan

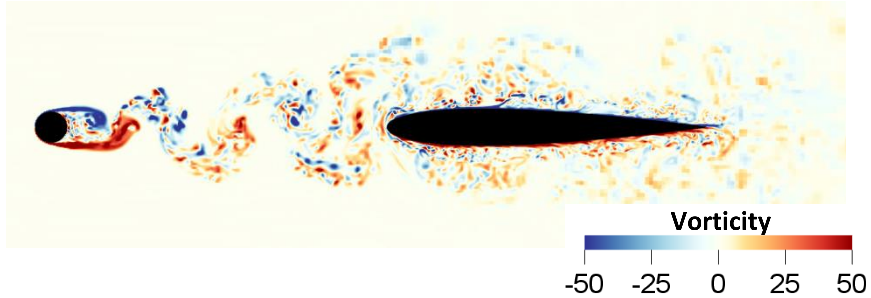

Rod-airfoil configuration [1]

SIMULIA

PowerFLOW®

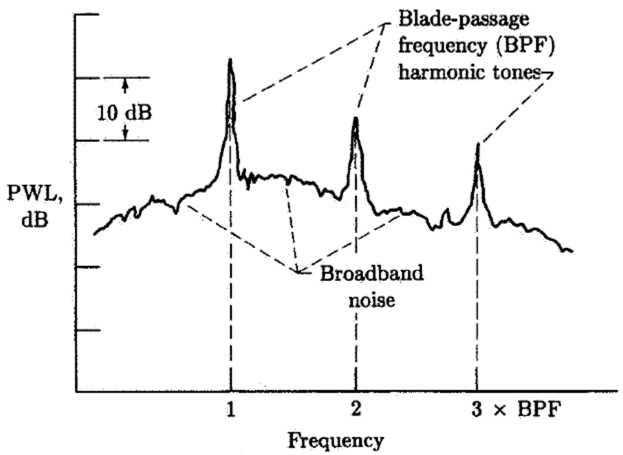

Typical turbofan noise power spectra

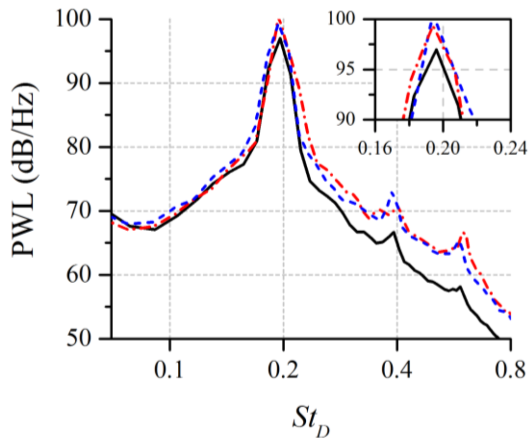

Noise spectra of rod – airfoil configuration @ 75m/s [1]

[1] Teruna, C., Avallone, F., Casalino, D., & Ragni, D. (2020). Numerical Investigation of Leading Edge Noise Reduction on a Rod-Airfoil Configuration Using Porous Materials and Serrations. Journal of Sound and Vibration, 115880.

Noise and LE Treatment Types

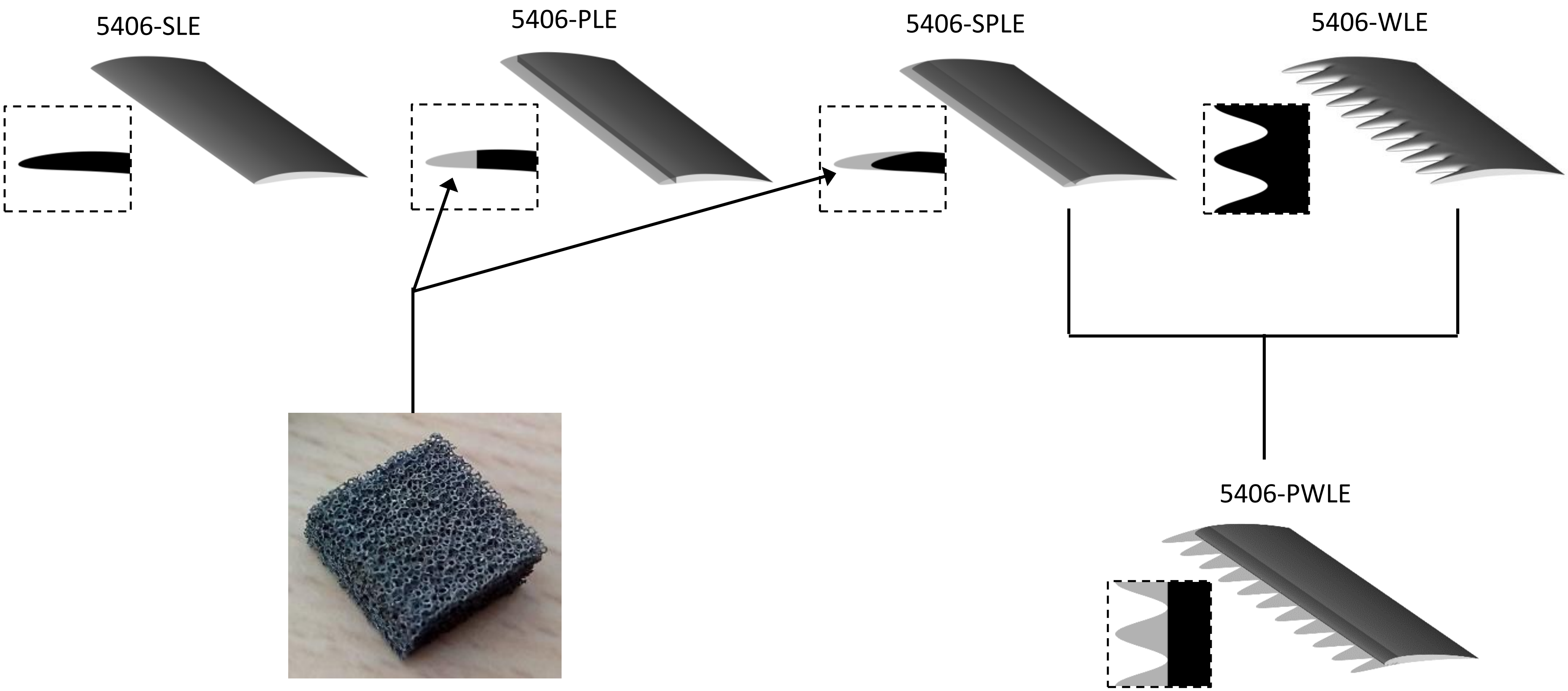

Ni-Cr-Al metal foam block

[1] Teruna, C., Avallone, F., Casalino, D., & Ragni, D. (2020). Numerical Investigation of Leading Edge Noise Reduction on a Rod-Airfoil Configuration Using Porous Materials and Serrations. Journal of Sound and Vibration, 115880.

Noise and LE Treatment Types

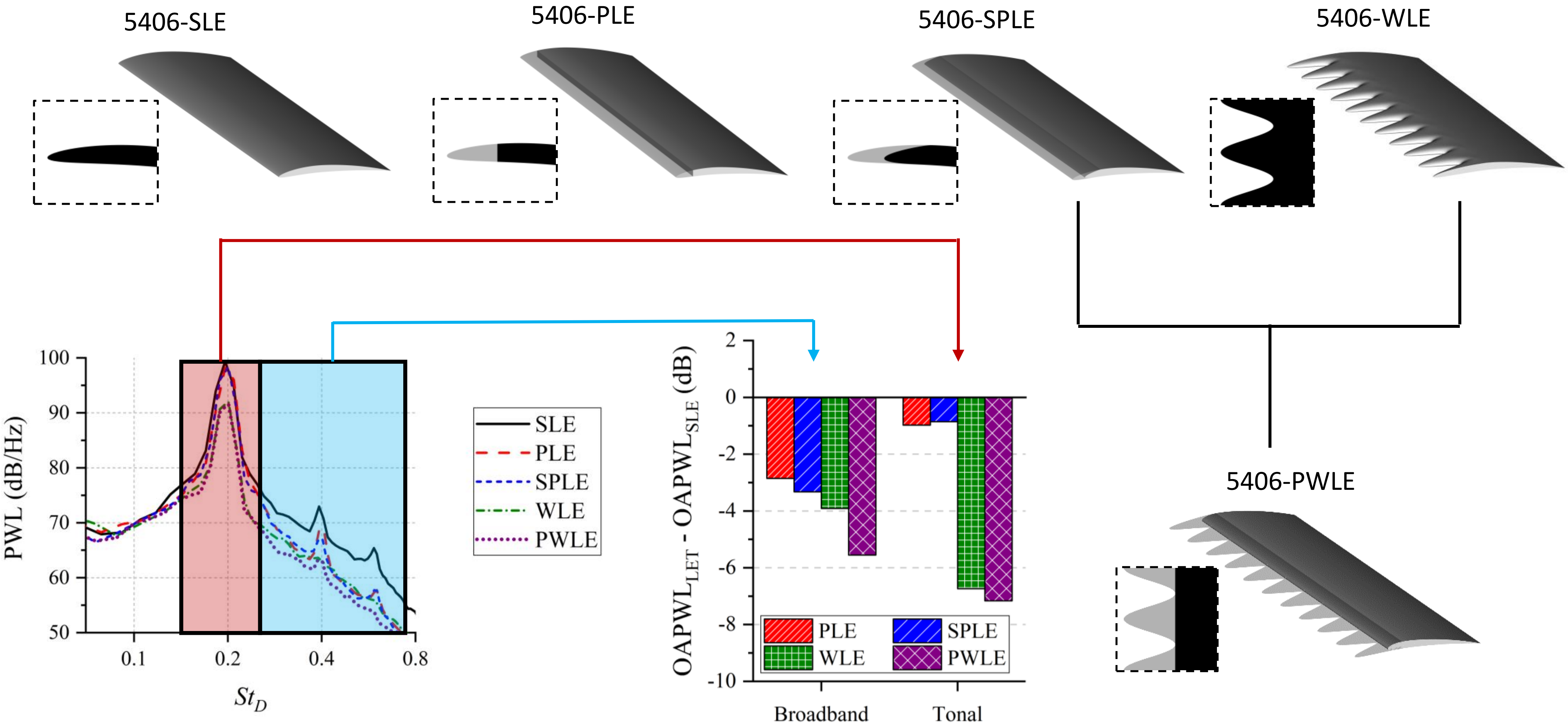

Comparison of source power level (PWL)

PWL reduction for different LE treatments

[1] Teruna, C., Avallone, F., Casalino, D., & Ragni, D. (2020). Numerical Investigation of Leading Edge Noise Reduction on a Rod-Airfoil Configuration Using Porous Materials and Serrations. Journal of Sound and Vibration, 115880.

Aerodynamic Analysis

5406-PLE

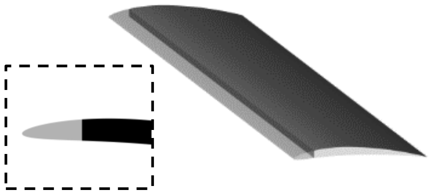

5406-SPLE

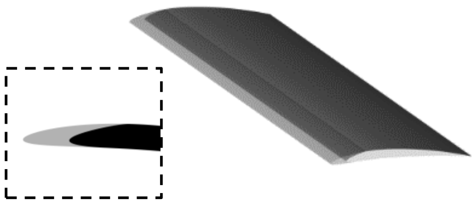

5406-WLE

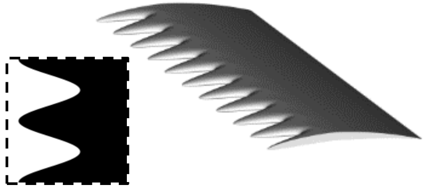

5406-PWLE

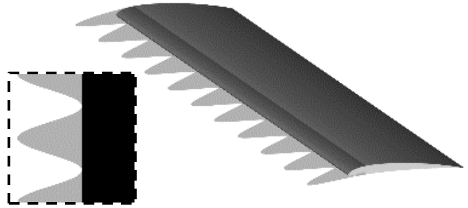

Aerodynamic penalty comparison

	$\Delta C_{l,\mathrm{mean}}$ (%)	$\Delta C_{d,\mathrm{mean}}$ (%)
5406-WLE	-5.36	+5.73
5406-PLE	-23.21	+56.70
5406-SPLE	-20.68	+55.24
5406-PWLE	-13.28	+35.35

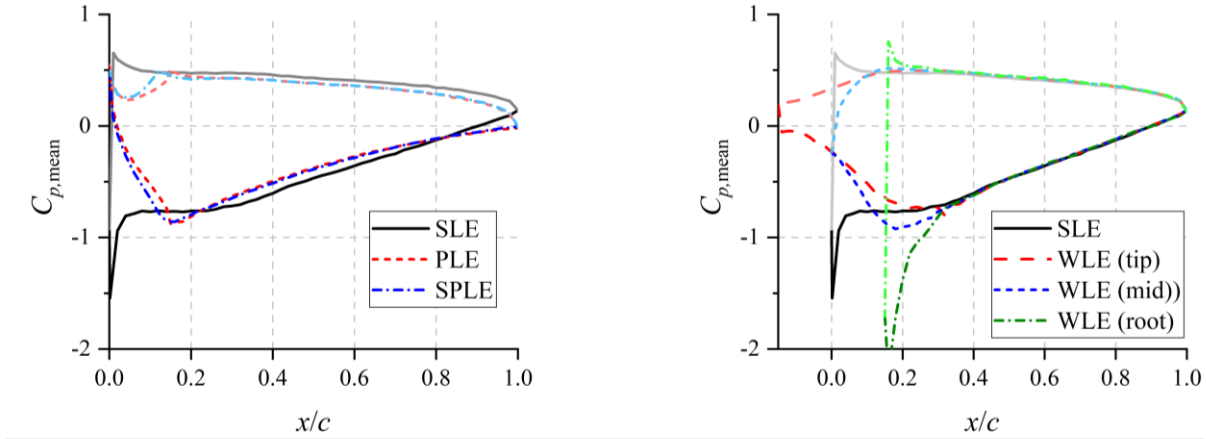

Comparison of mean surface pressure distribution

[1] Teruna, C., Avallone, F., Casalino, D., & Ragni, D. (2020). Numerical Investigation of Leading Edge Noise Reduction on a Rod-Airfoil Configuration Using Porous Materials and Serrations. Journal of Sound and Vibration, 115880.

Aerodynamic Analysis

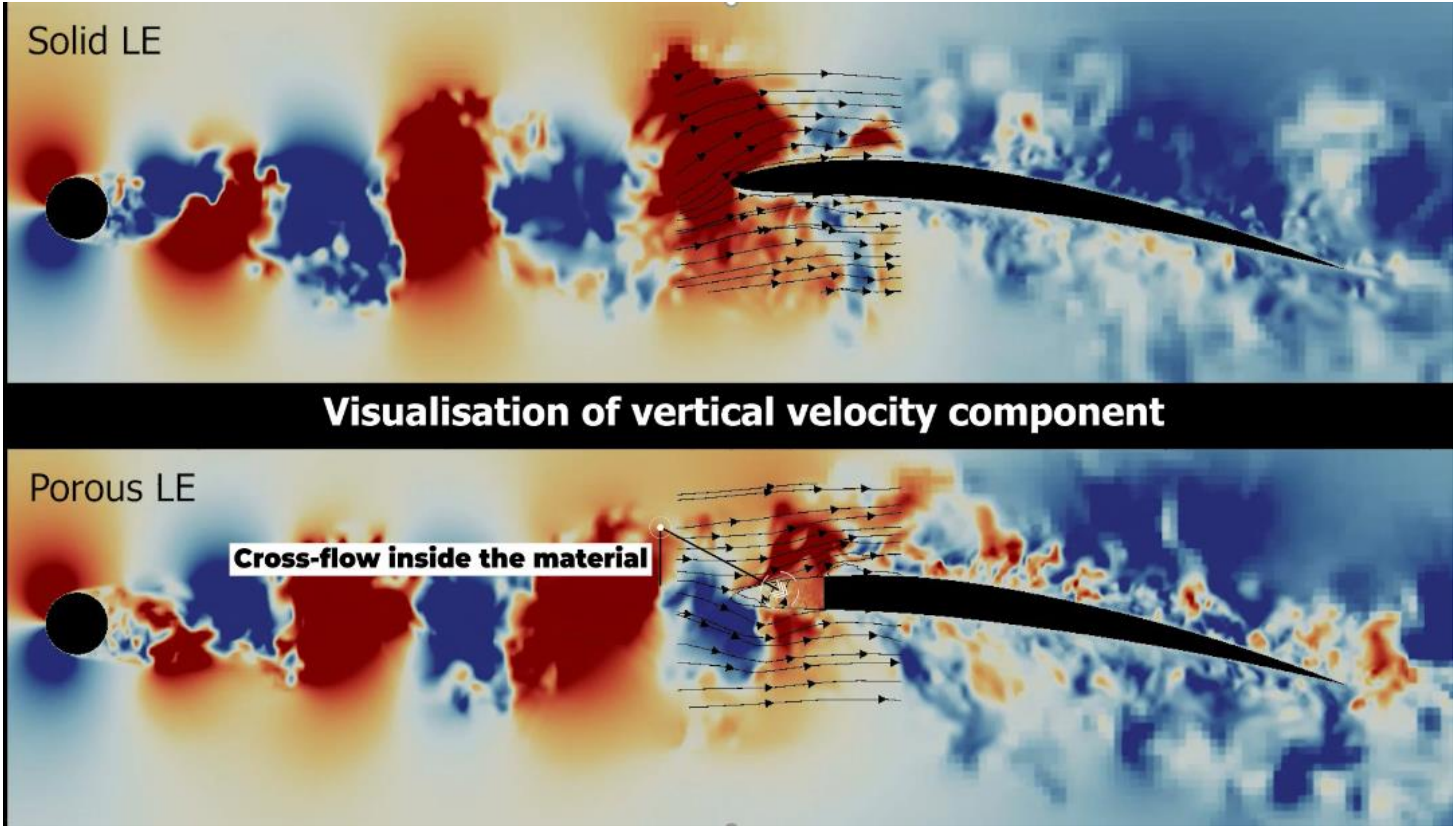

[1] Teruna, C., Avallone, F., Casalino, D., & Ragni, D. (2020). Numerical Investigation of Leading Edge Noise Reduction on a Rod-Airfoil Configuration Using Porous Materials and Serrations. Journal of Sound and Vibration, 115880.

Aerodynamic Analysis

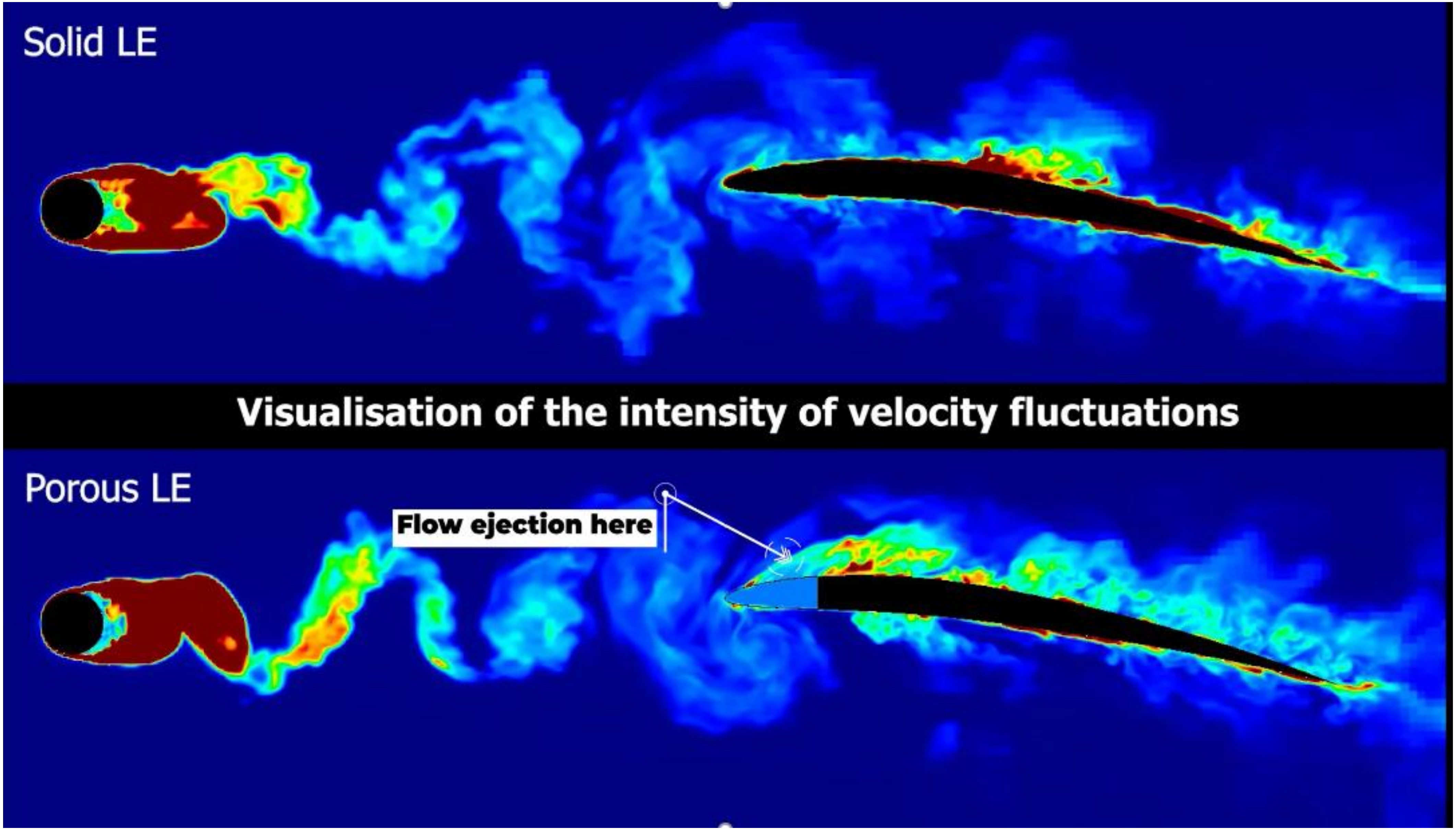

[1] Teruna, C., Avallone, F., Casalino, D., & Ragni, D. (2020). Numerical Investigation of Leading Edge Noise Reduction on a Rod-Airfoil Configuration Using Porous Materials and Serrations. Journal of Sound and Vibration, 115880.

VKI rod-airfoil configuration

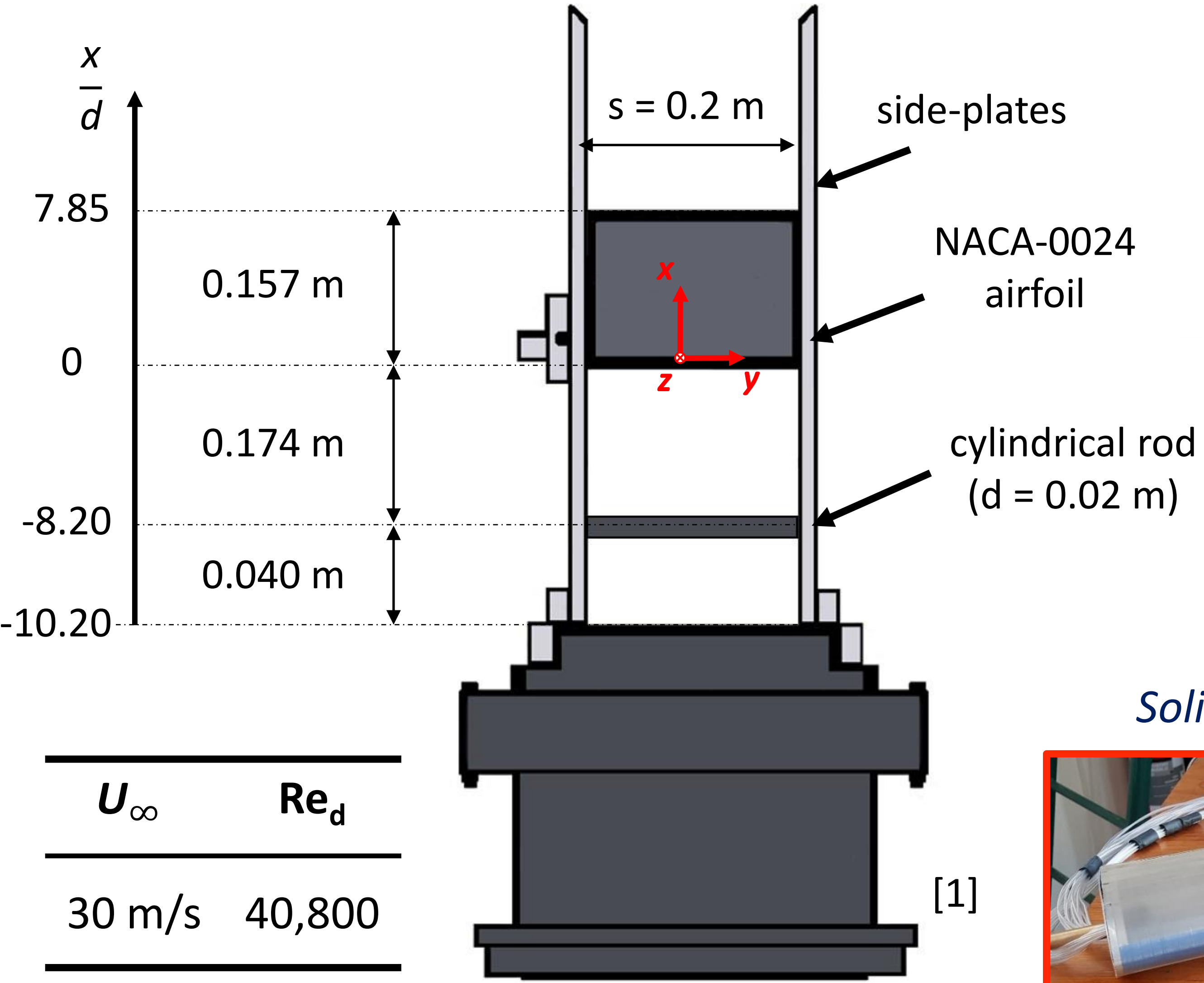

[1]

U_∞	Re_d
30 m/s	40,800

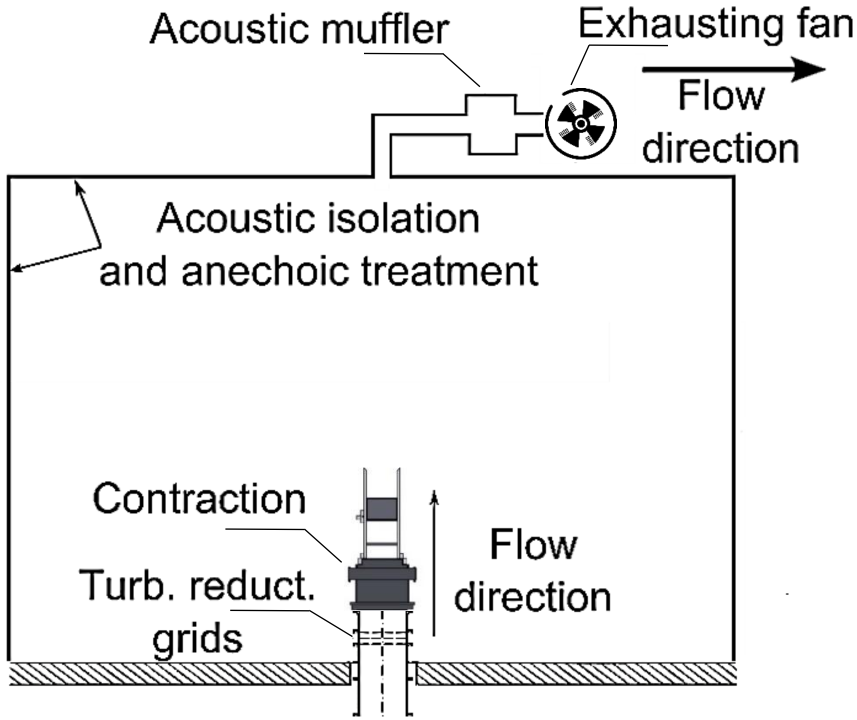

Solid airfoil

Porous airfoil

[1] Zamponi *et al., 25th AIAA/CAES,* 2019

VKI porous airfoil

NACA-0024 profile

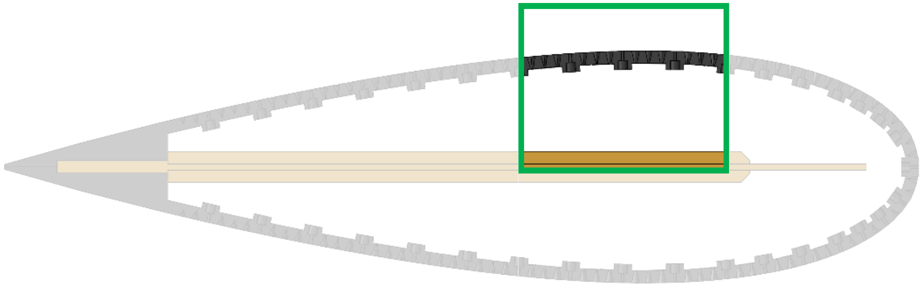

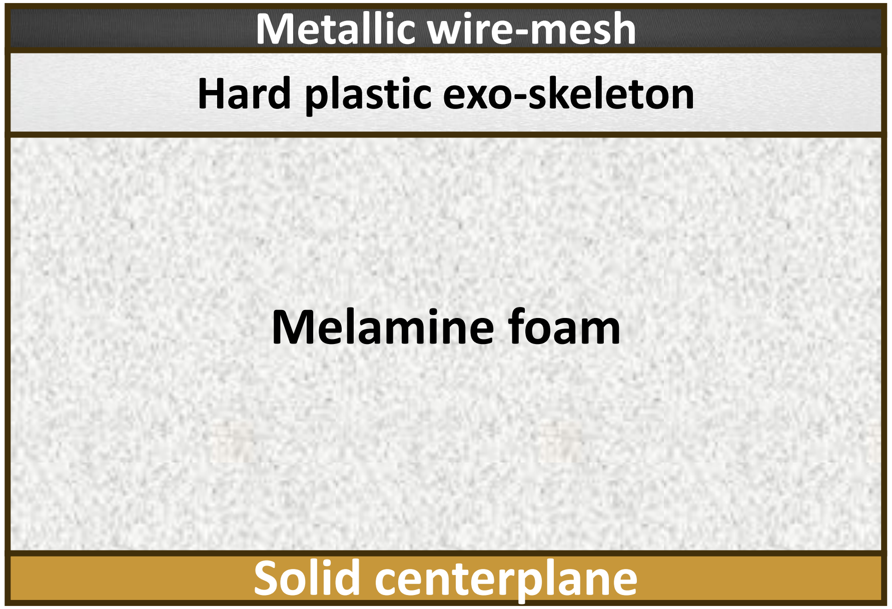

LAUM

Determination of melamine foam parameters according to the JCAL model[1-3]

Material	ϕ [%]	σ [Pa s m^{-2}]	α_∞ [-]	Λ [m]	Λ' [m]	k' [m^2]
Melamine foam	98.6	8,683	1.02	1.344×10^{-4}	1.942×10^{-4}	2.305×10^{-9}
Exo-skeleton	80.0	~ 0	~	~	~	~
Wire-mesh	60.8	~ 0	~	~	~	~

[1] Johnson *et al.*, *J. Fluid Mech.*, 1987 **[2]** Champoux and Allard, *J. Appl. Phys.*, 1991 **[3]** Lafarge *et al.*, *J. Acoust. Soc. Am.*, 1997

Airfoil layers characterization

4 samples of **melamine foam** are characterized by means of an **impedance tube** to analyze the **sound absorbing behavior** of the porous material[1]

Absorption coefficient

$$\alpha = 1 - R^2$$

Reflection coefficient

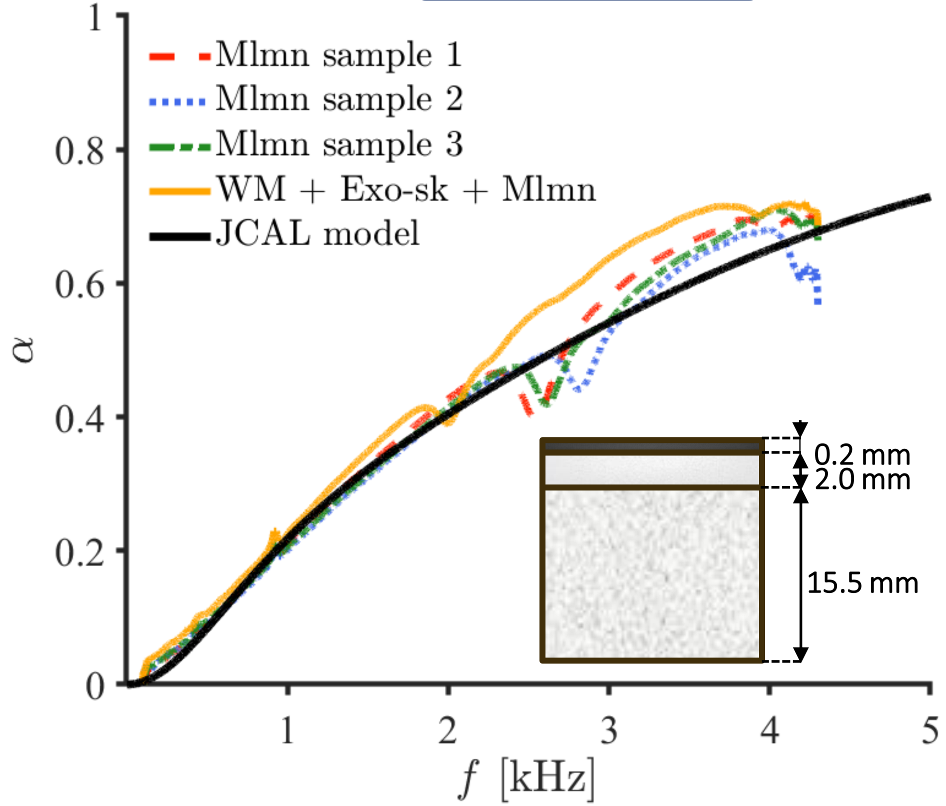

Emitted signal	Emission frequency range	Acquisition frequency range
White noise	50 - 5.000 Hz	80 - 4.300 Hz

[1] Satcunanathan *et al.*, *INTER-NOISE*, 2019

Source Distribution Isolation

Acoustic beamforming proved to be an effective tool to properly **isolate** noise source contributions and evaluate **airfoil-turbulence interaction noise**[1]

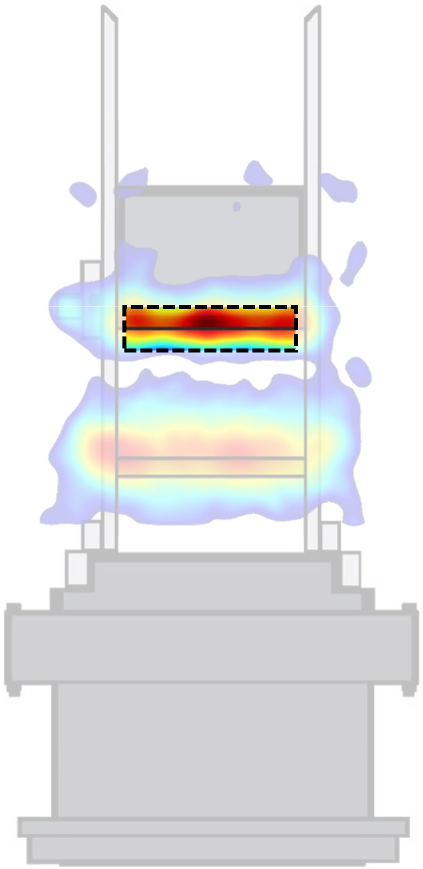

Absolute sound pressure levels

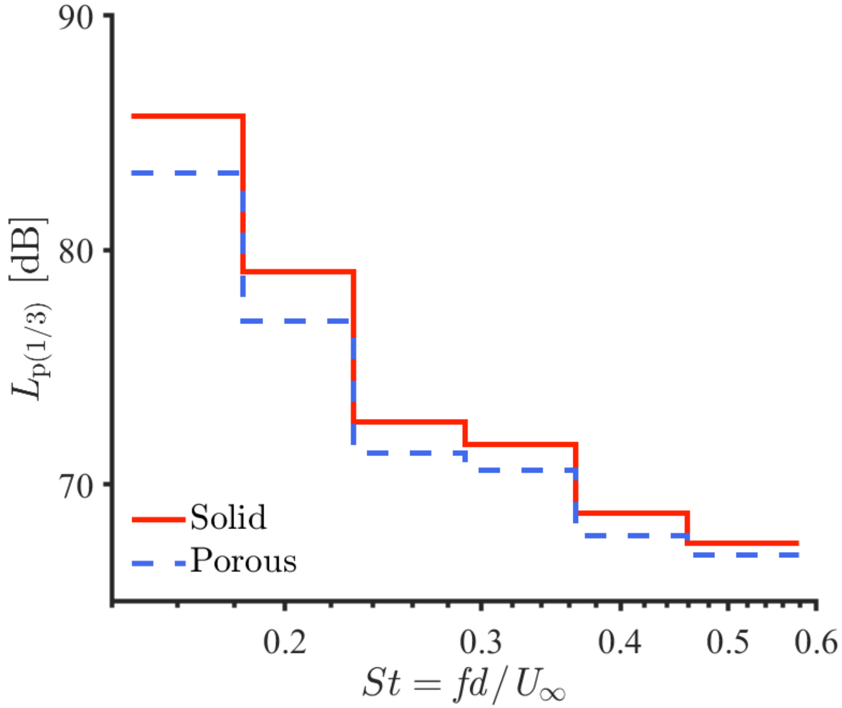

Relative sound pressure levels

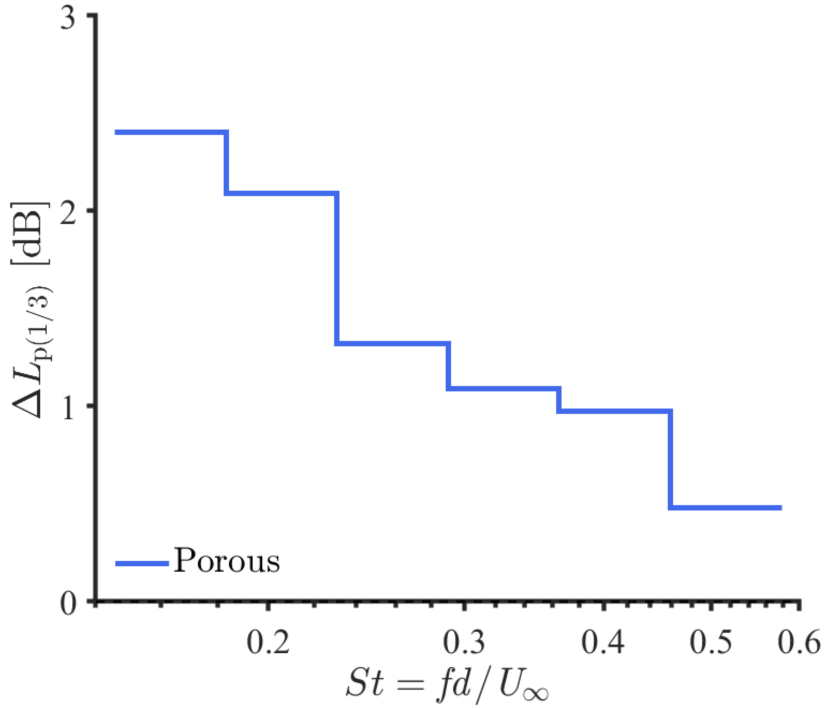

What is the origin of the noise reduction?

[1] Zamponi *et al.*, *Journal of Sound and Vibration*, 2020

How Does Porosity Affect the Flow?

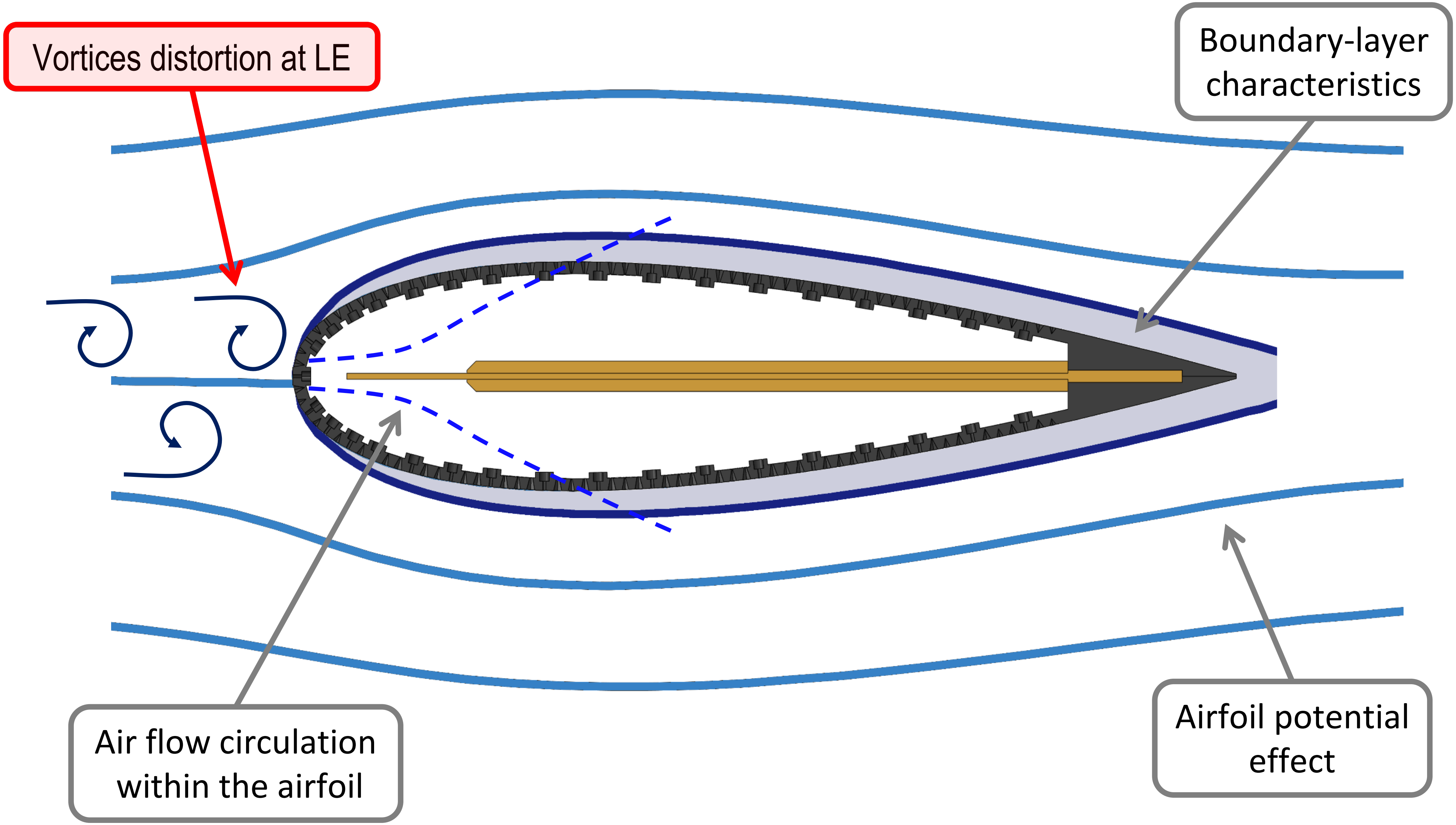

Unsteady Flow-Field Investigation

The **flow field** in the stagnation region is studied through LES[1]

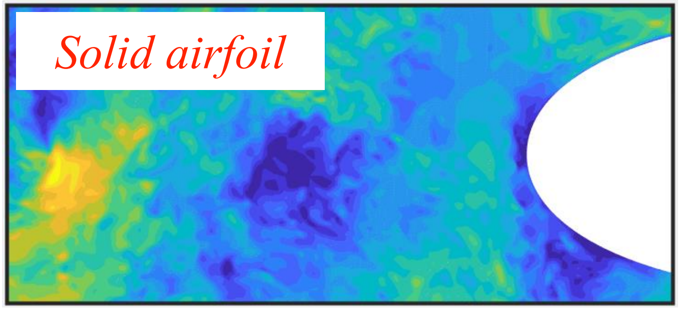

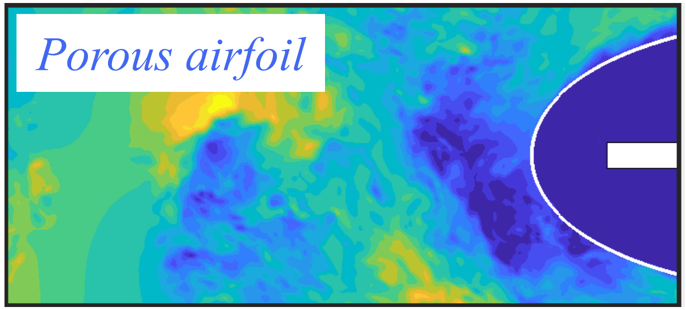

Turbulence intensity

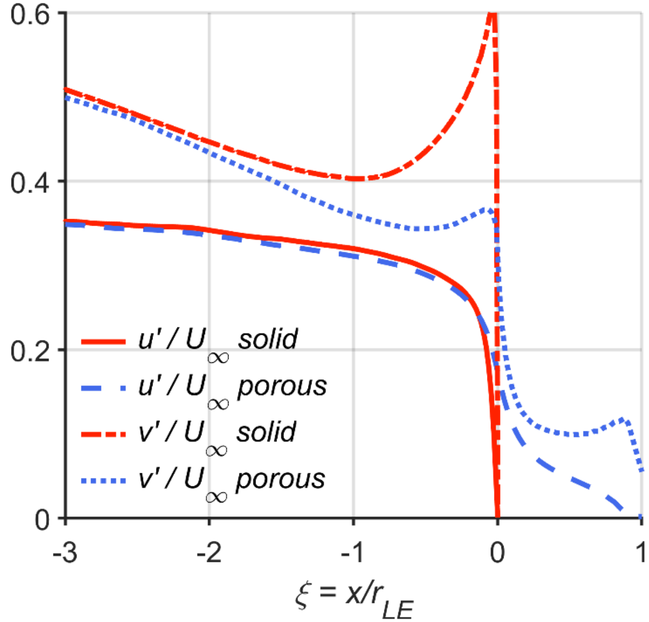

Turbulent Kinetic Energy (TKE)

Solid airfoil

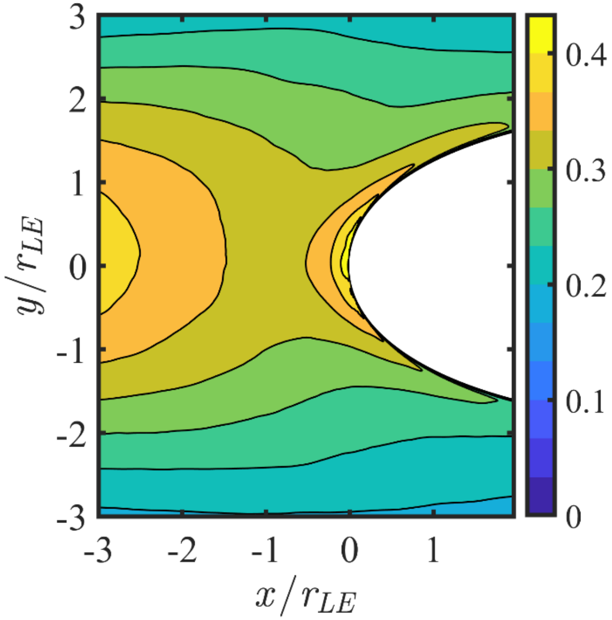

Porous airfoil

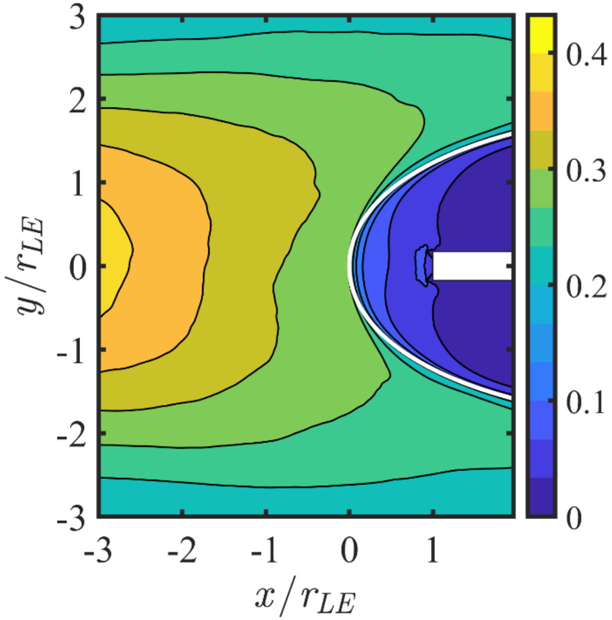

[1] Zamponi *et al.*, *Journal of Sound and Vibration*, 2020

Turbulent Velocity Spectra Comparison

The **turbulence distortion** is attenuated for a porous airfoil[1]

Turbulence distortion mechanisms[2]

- Blocking of velocity fluctuations by the pressure of the body
- Distortion of vorticity field by the mean flow

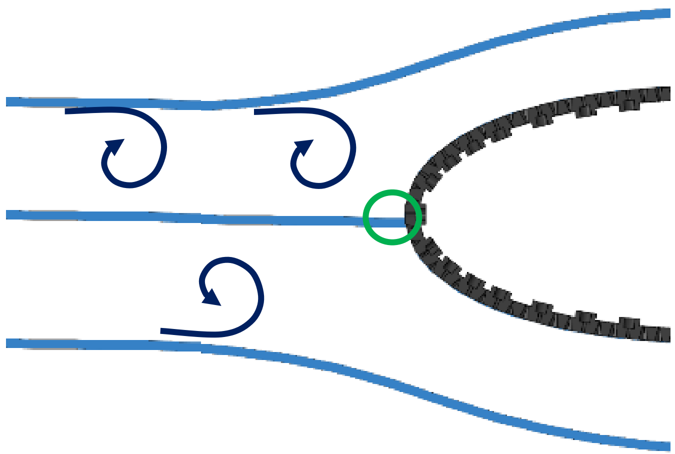

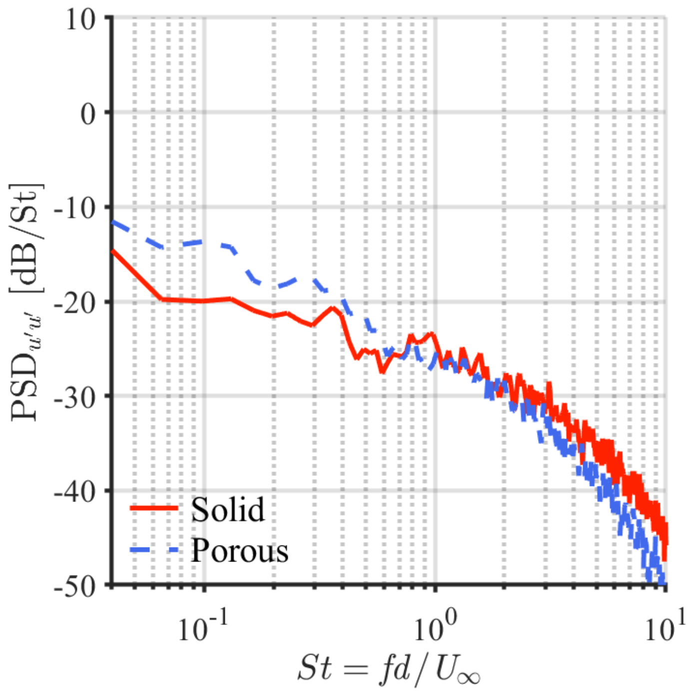

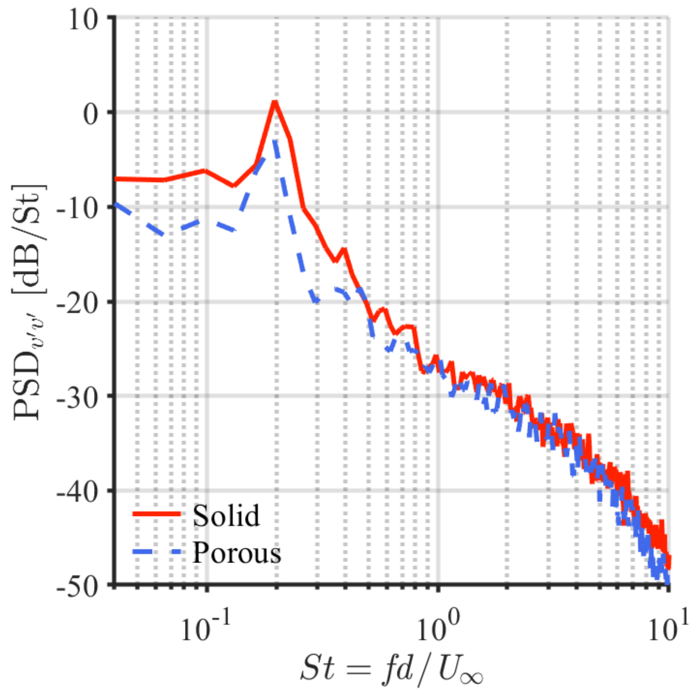

[1] Zamponi *et al.*, *Journal of Sound and Vibration*, 2020

[2] Zamponi *et al.*, *Journal of Fluid Mechanics*, Under review

Wall-Pressure Fluctuations

Solid airfoil

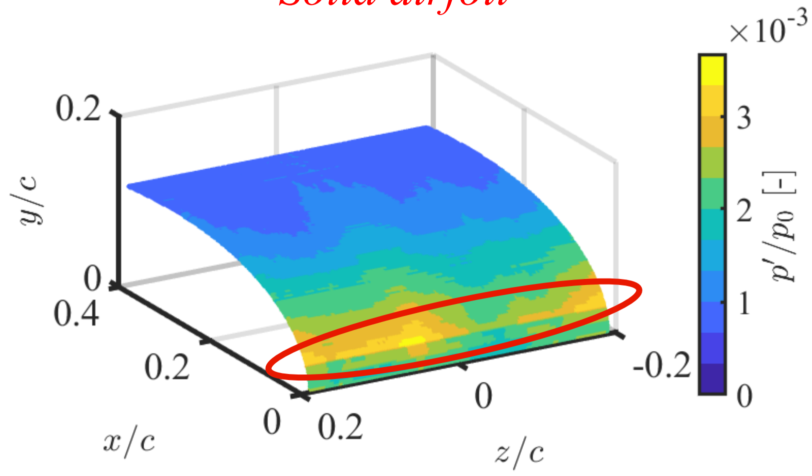

Porous airfoil

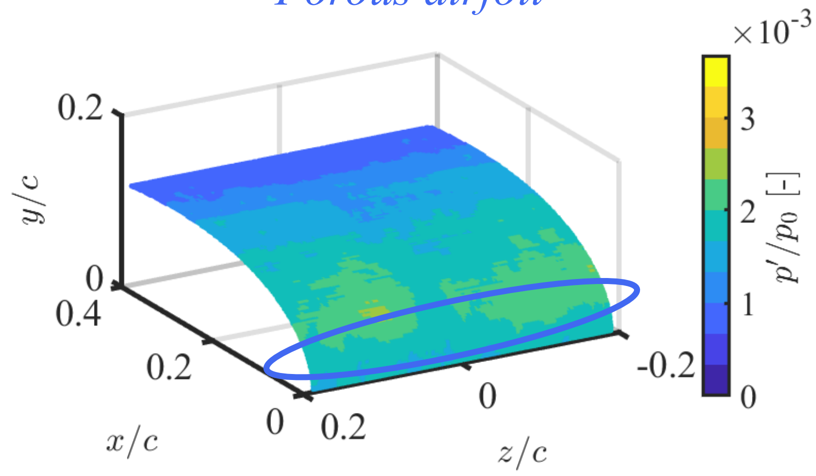

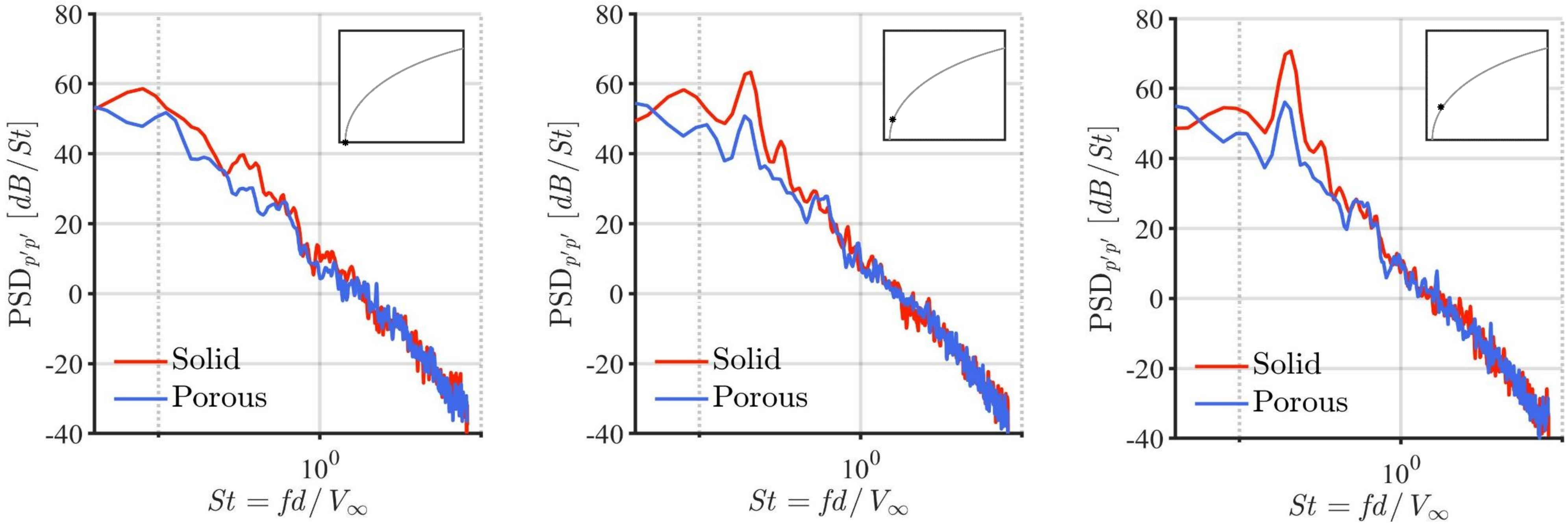

III. TRAILING-EDGE TREATMENTS

Trailing-edge serrations


[1]

- Trailing edge serrations are widely used noise reduction devices;
- Still there is a lack of information on the effects of the flow on the noise reduction:
  - High spatial and temporal resolution information required;
- Well designed trailing edge serrations can improve noise reduction in respect to the standard sawtooth.

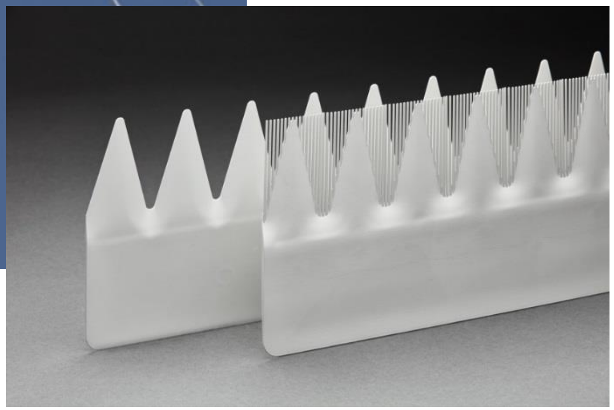
[2]

[1] Oerlemans, S. et al (2009) Reduction of Wind Turbine Noise Using Optimized Airfoils and Trailing-Edge Serrations. AIAA Journal
[2] Siemens website (2020) Dino Tails Next Generation.

Goal

Novel flow diagnostics for trailing-edge serration assessment

- Unsteady flow (pressure) over trailing-edge serrations;
- High spatial and temporal resolution required for aeroacoustic study.

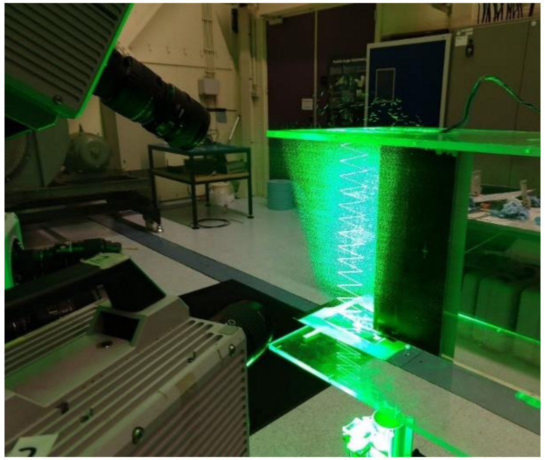

Time-resolved 3D-PIV

- Lower temporal resolution;
- Higher spatial resolution;
- Velocity field only (reconstruct pressure);
- Restricted interrogation volume;
- Post processing chain.

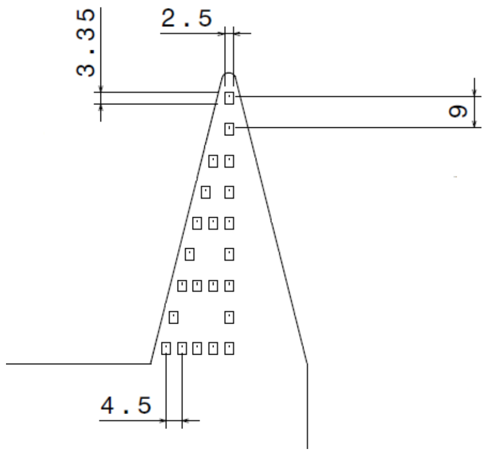

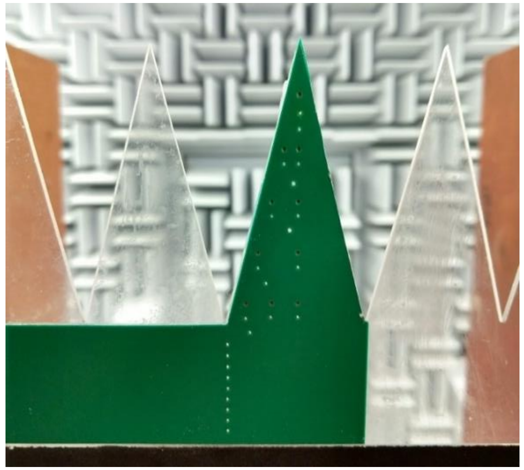

Unsteady surface pressure sensors

- High temporal resolution;
- Limited spatial resolution;
- Pressure field;
- Model installation.

3D-PIV - Post Processing

Particles → Pressure

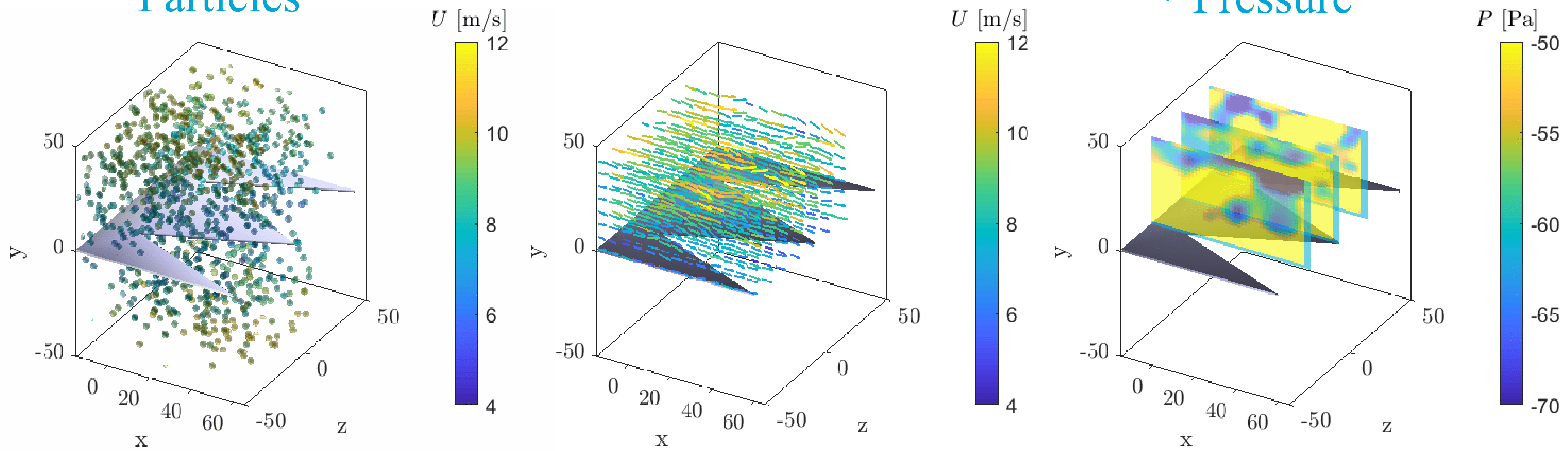

- 3D-PIV using Helium Filled Soap Bubbles:
  - Flow measurements in a large domain;
- Shake the box particle tracking (3D-LPT):
  - Particle location and velocity;
- VIC+:
  - Gridded velocity field;
- Pressure reconstruction:
  - $\nabla^2 P = -\rho \nabla . \frac{D\vec{V}}{Dt}$.

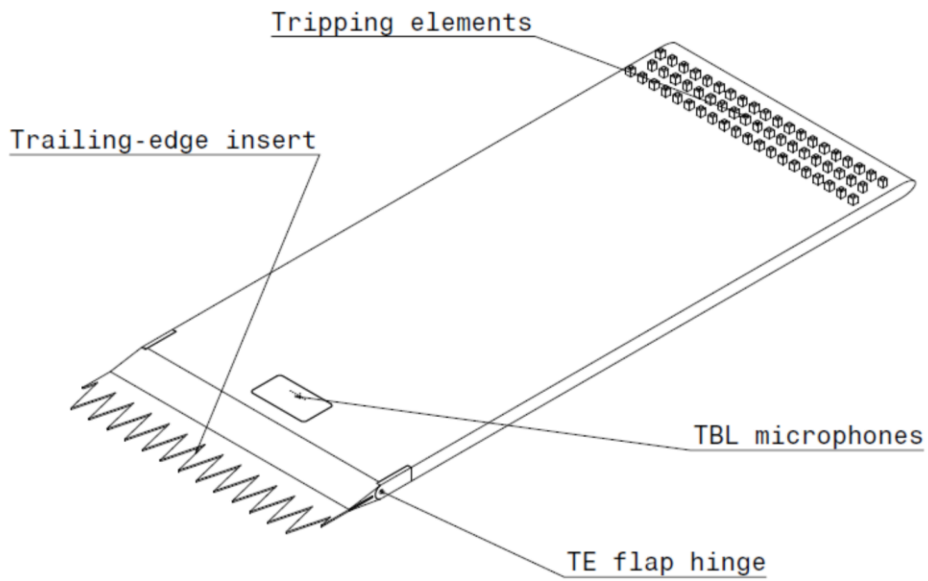

Aerodynamic measurements

- Secondary flow formed on the serrations undergoing aerodynamic loading (vortex pairs along the serration);
- Alterations of the pressure fluctuations along the serration;
- Implications on far-field noise.

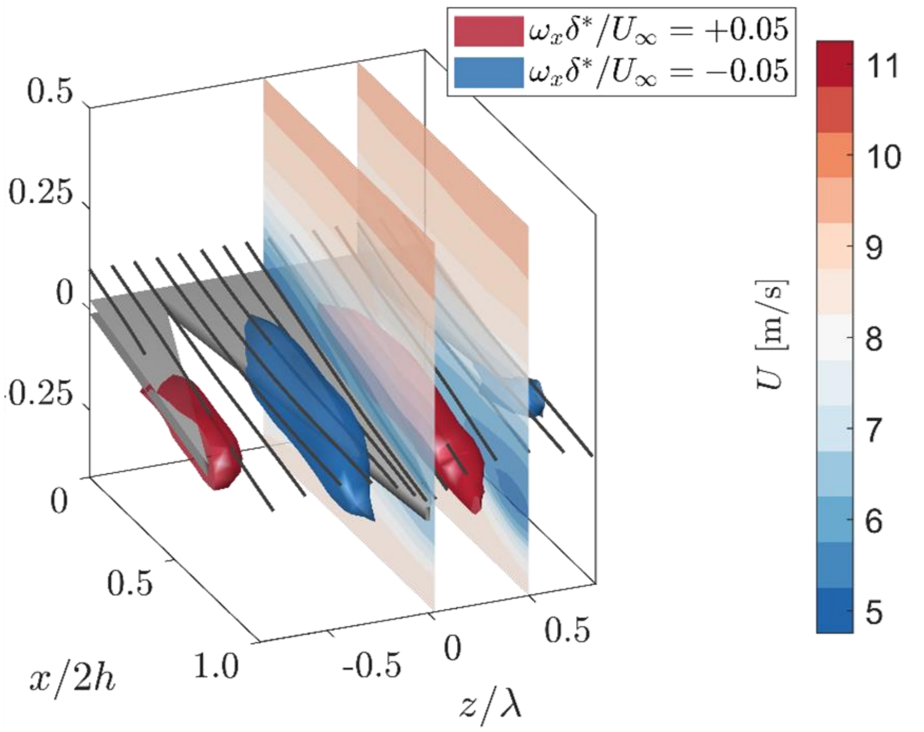

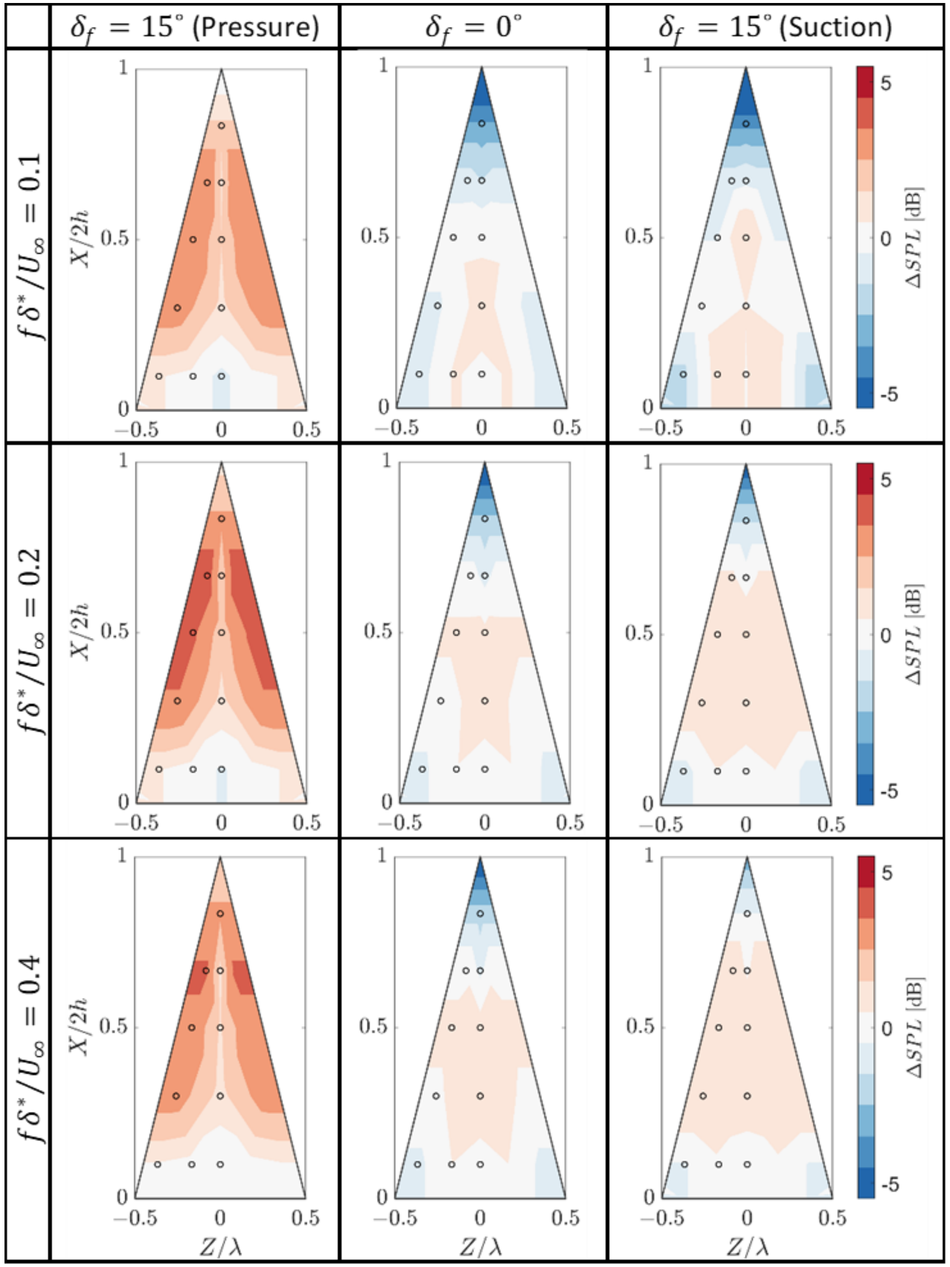

Far field noise measurements

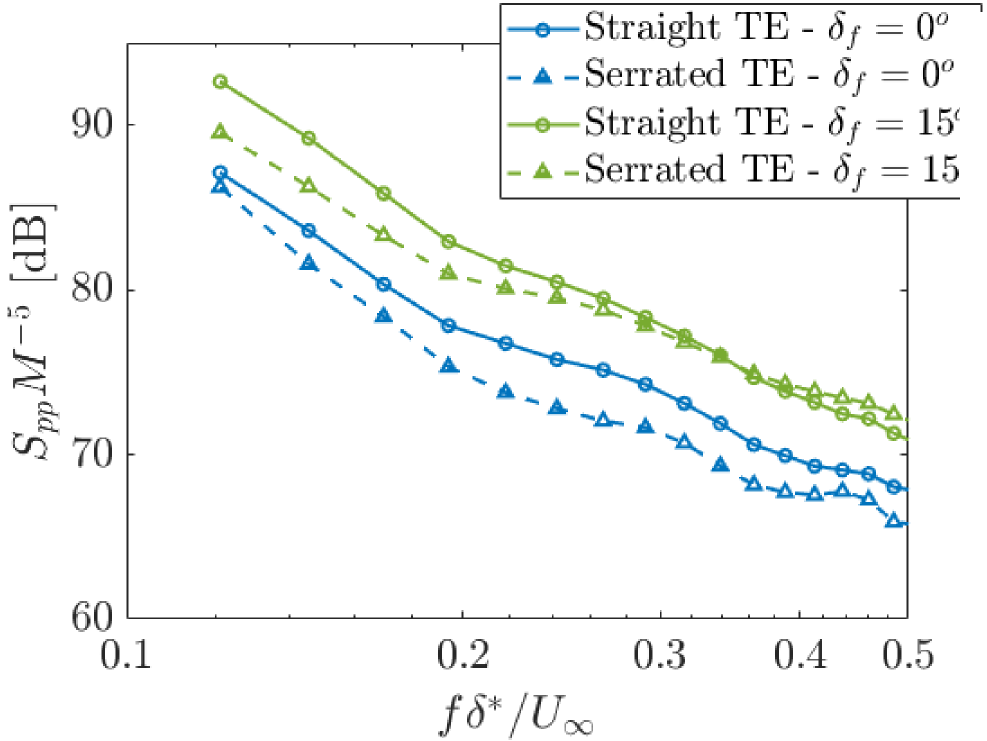

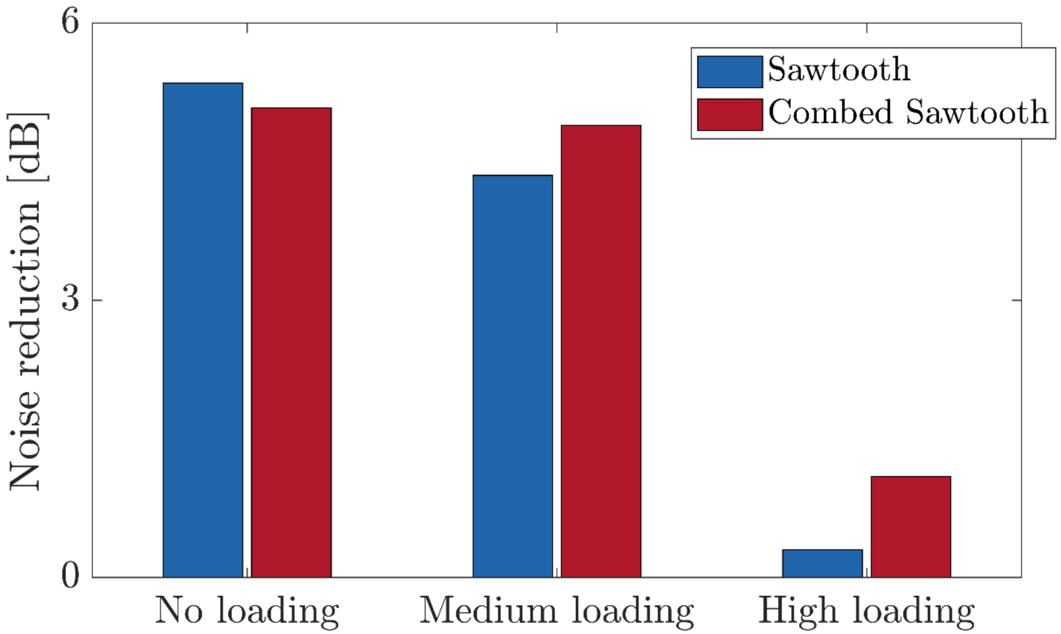

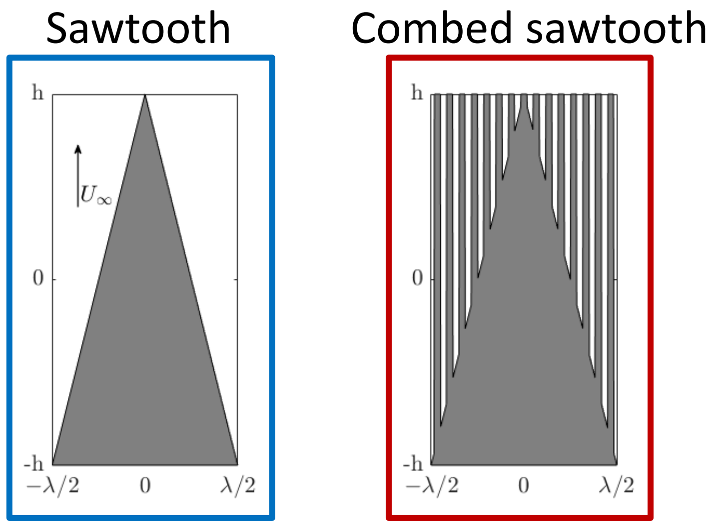

- Sawtooth serrations:
  - Better noise reduction without loading;
  - High sensitivity to the loading condition;
- Combed sawtooth:
  - Similar noise reduction levels without loading;
  - Less sensitive to increasing of aerodynamic loading.

Porous Trailing Edge

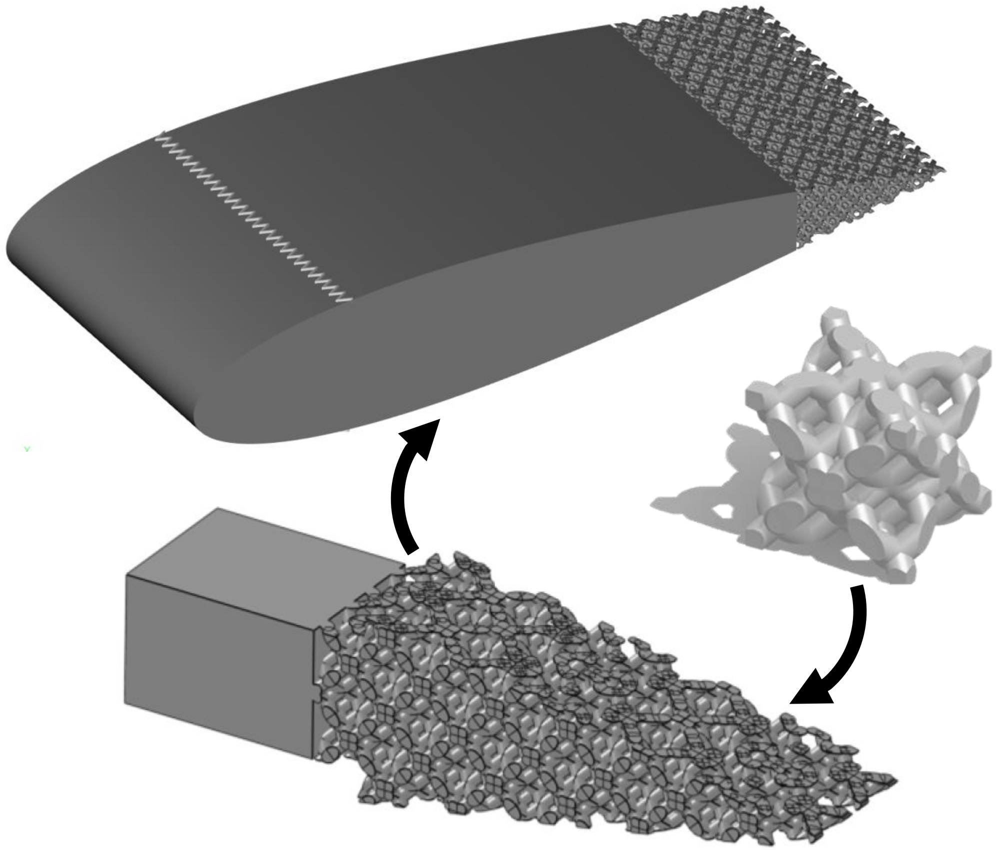

NACA 0018 with porous TE insert

- Porous trailing-edge (TE) has shown promising noise-reduction capability [1,2].
- Flow communication across the porous medium is essential for noise mitigation [2].
- Porous TE has lower scattering efficiency compared to the porous one [2].
- Which part of the porous TE is more important for promoting noise reduction?

[1] Geyer, T. F., & Sarradj, E. (2014). Trailing edge noise of partially porous airfoils. *In 20th AIAA/CEAS Aeroacoustics Conference* (p. 3039).
[2] Rubio Carpio, A., Avallone, F., Ragni, D., Snellen, M., & van der Zwaag, S. (2019). Mechanisms of broadband noise generation on metal foam edges. *Physics of Fluids*, 31(10), 105110

Porous Trailing Edge

SIMULIA PowerFLOW®

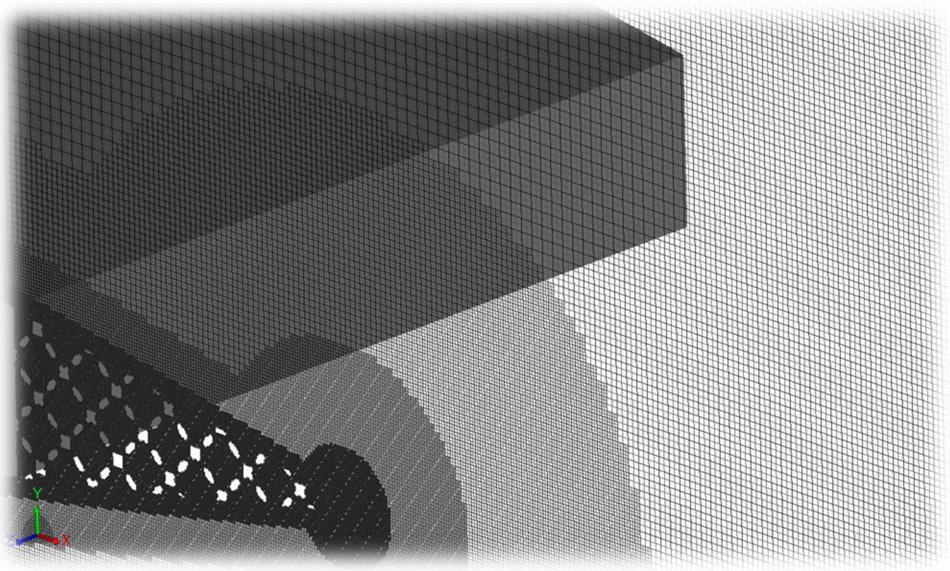

Mesh distribution in the simulation domain

- Porous trailing-edge (TE) has shown promising noise-reduction capability [1,2].
- Flow communication across the porous medium is essential for noise mitigation [2].
- Porous TE has lower scattering efficiency compared to the porous one [2].
- Which part of the porous TE is more important for promoting noise reduction?

[1] Geyer, T. F., & Sarradj, E. (2014). Trailing edge noise of partially porous airfoils. *In 20th AIAA/CEAS Aeroacoustics Conference* (p. 3039).
[2] Rubio Carpio, A., Avallone, F., Ragni, D., Snellen, M., & van der Zwaag, S. (2019). Mechanisms of broadband noise generation on metal foam edges. *Physics of Fluids*, 31(10), 105110

Diamond Trailing Edge

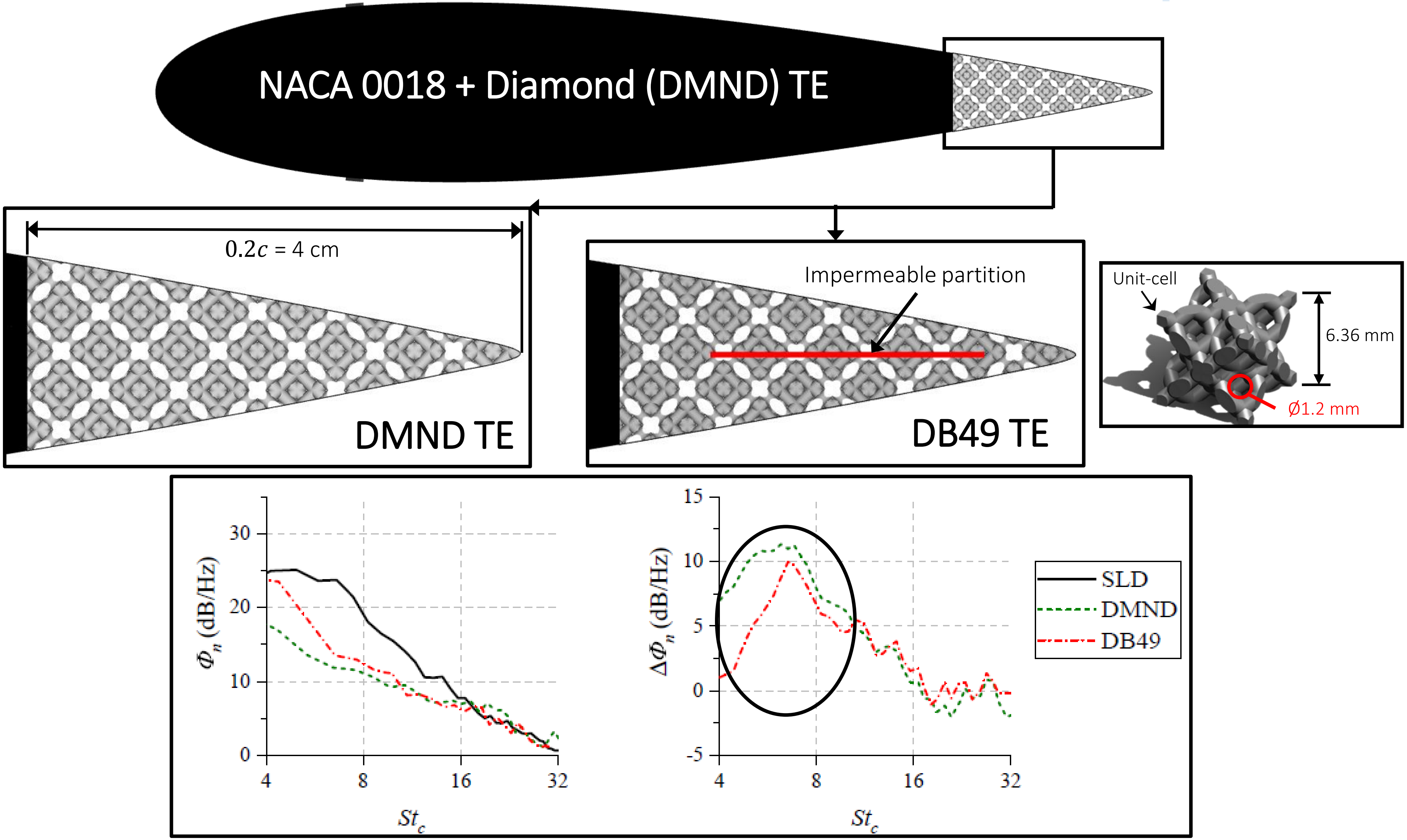

Correlation Statistics

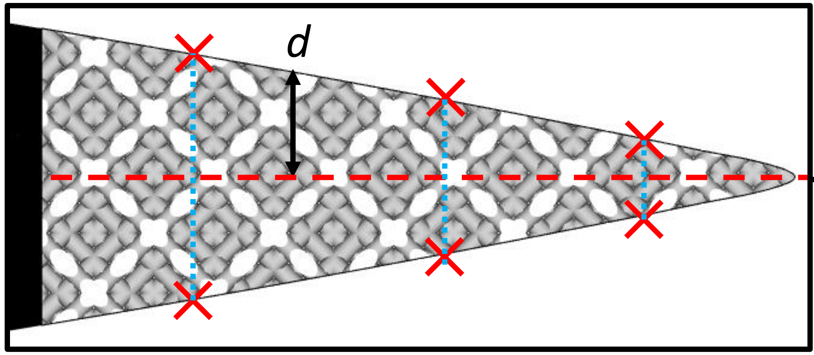

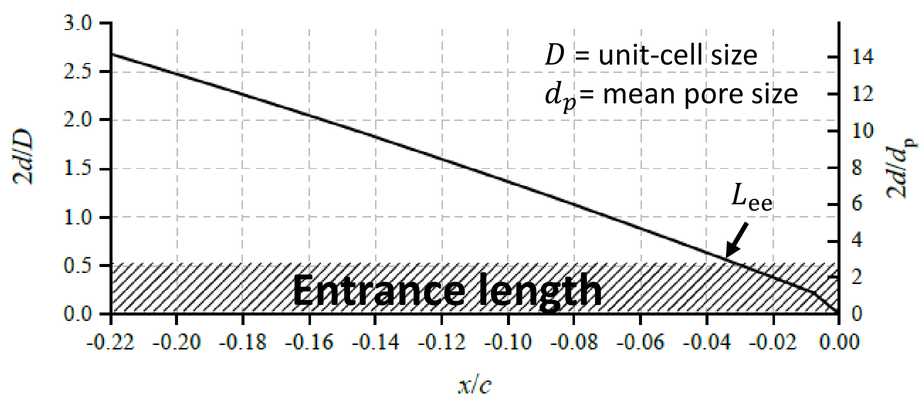

Local TE thickness normalised by unit-cell/pore dimension

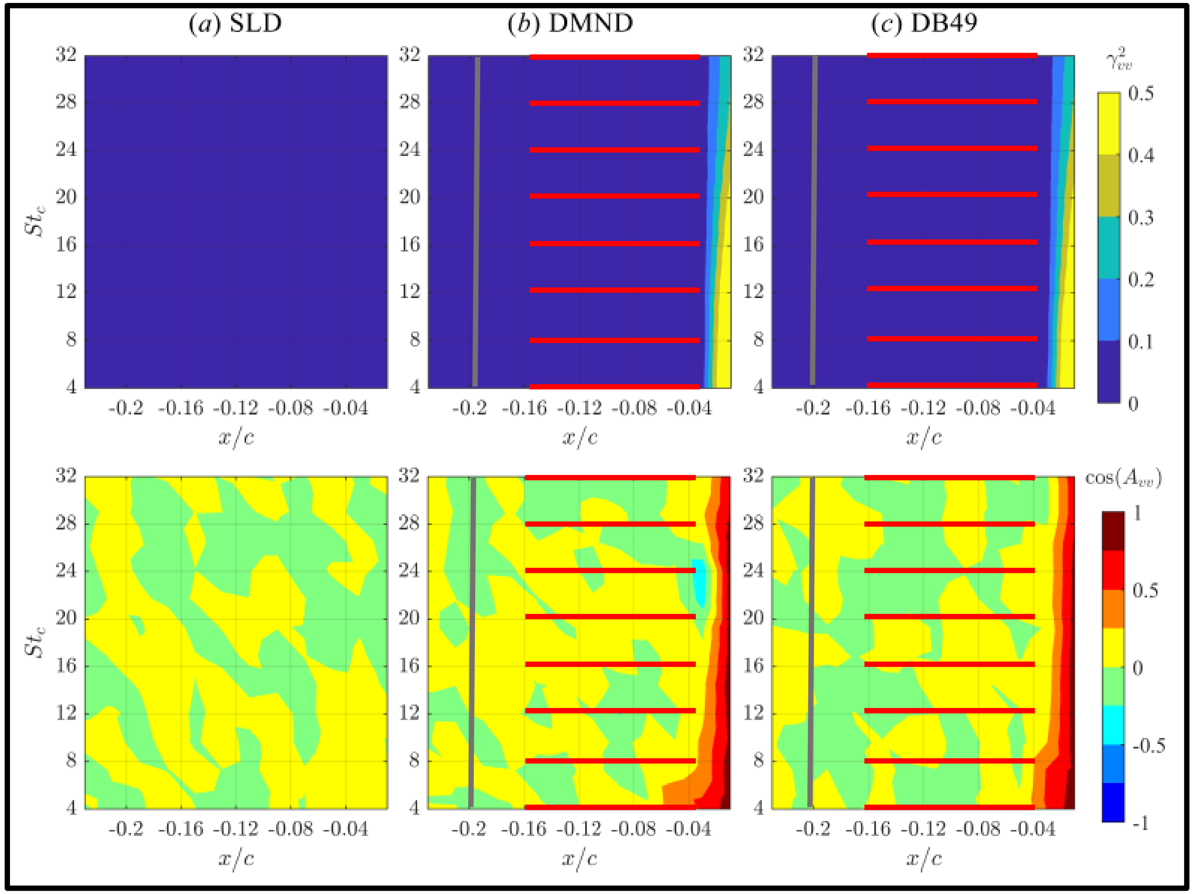

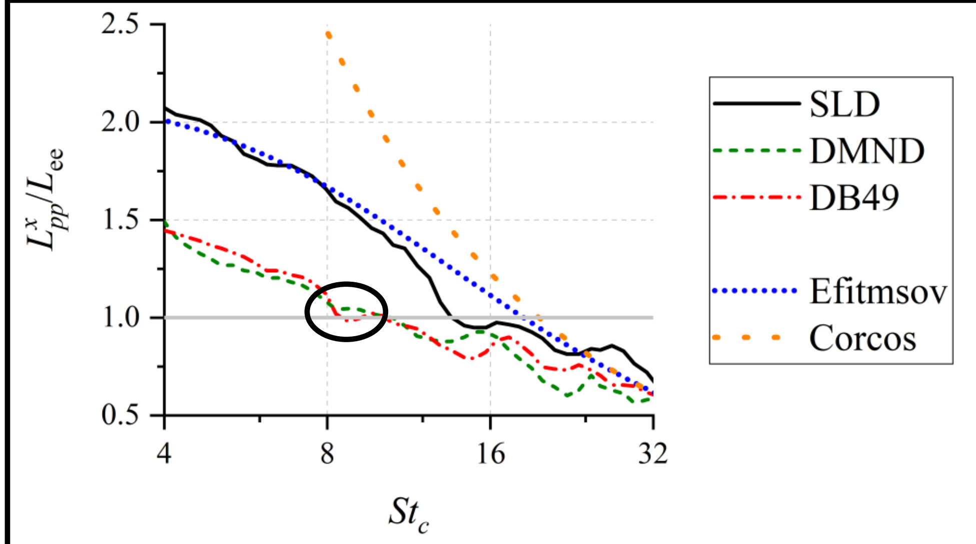

Streamwise correlation length of surface pressure fluctuations

Correlation Statistics

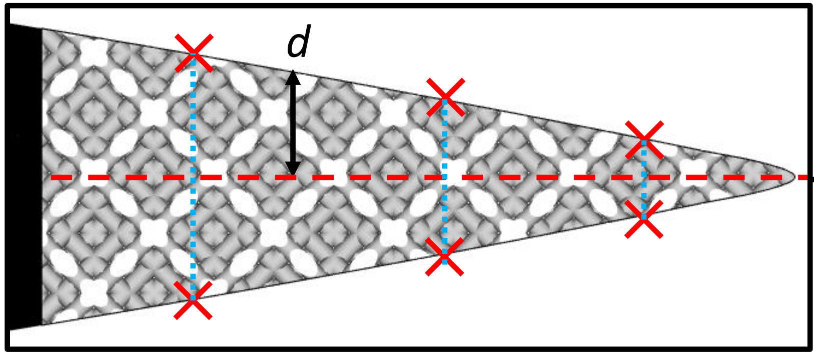

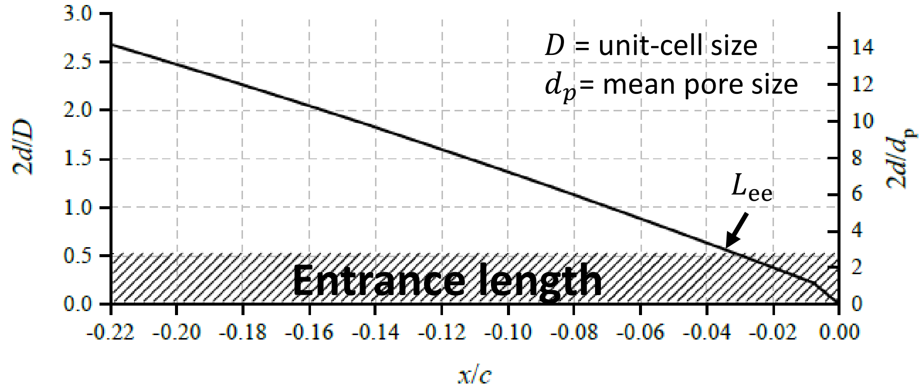

Local TE thickness normalised by unit-cell/pore dimension

A relatively thin and long porous TE extent might be desirable.

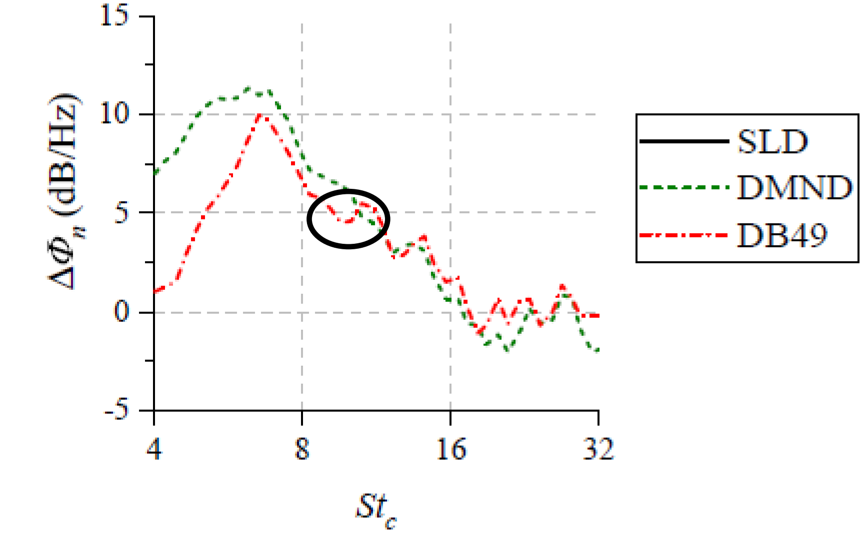

Noise reduction spectra

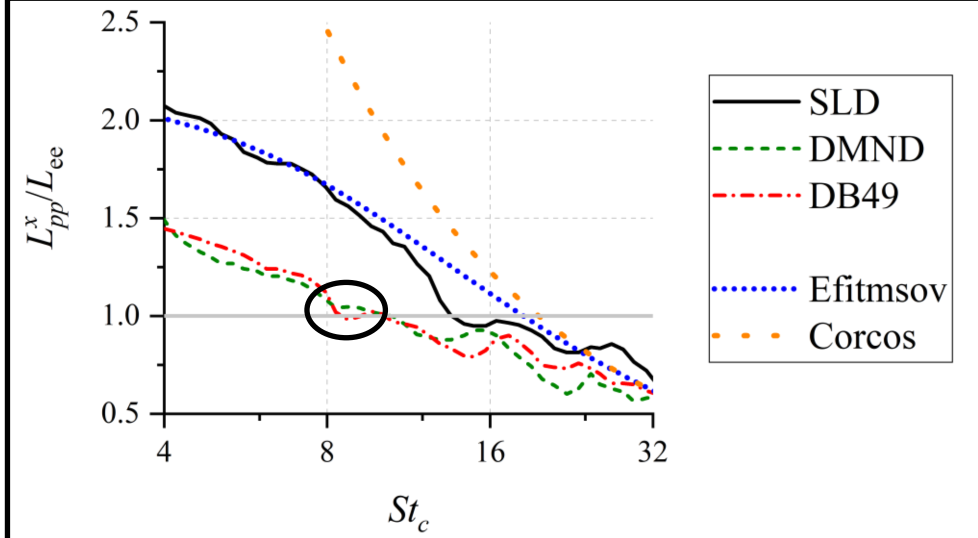

Streamwise correlation length of surface pressure fluctuations

1st Q/A SESSION

IV. SEPARATION CONTROL

RESEARCH BACKGROUND

- Design conditions : flow and acoustic analysis of wind turbine profiles/blades available.

Flow separation visualization

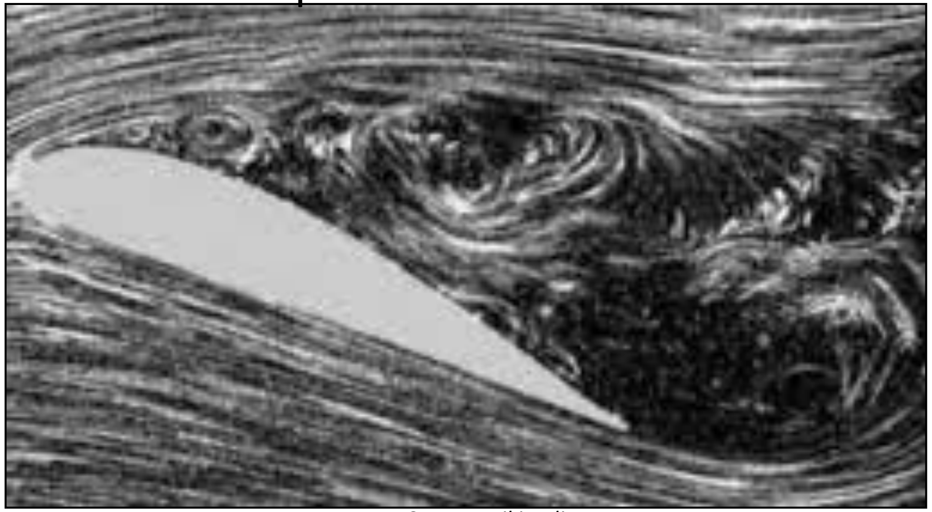

Source: wikipedia

<u>**Off design condition – boundary layer flow separation**</u>

- **Adverse pressure** gradients at high inflow angles and wind speeds.
- Causes **aerodynamic losses**, **stall** and **lower** performance.
- To tackle detached flow, various **flow control devices** have been used.

Souce: creativecommons.org

<u>**Flow control devices**</u>

- **Delay** and **reduce** separation thus **improving** aerodynamic performance.
- First proposed by Taylor (1948)[1] for aircrafts.
- Existing devices: Streamwise vortex generators (vane, delta, air jet etc.)

[1] Taylor, H. D., "The elimination of diffuser separation by vortex generators", United Aircraft Corporation Report No. R-4012-3, 1947

RESEARCH BACKGROUND

- Design conditions : flow and acoustic analysis of wind turbine profiles/blades available.

Off design condition – boundary layer flow separation

- **Adverse pressure** gradients at high inflow angles and wind speeds.
- Causes **aerodynamic losses**, **stall** and **lower** performance.
- To tackle detached flow, various **flow control devices** have been used.

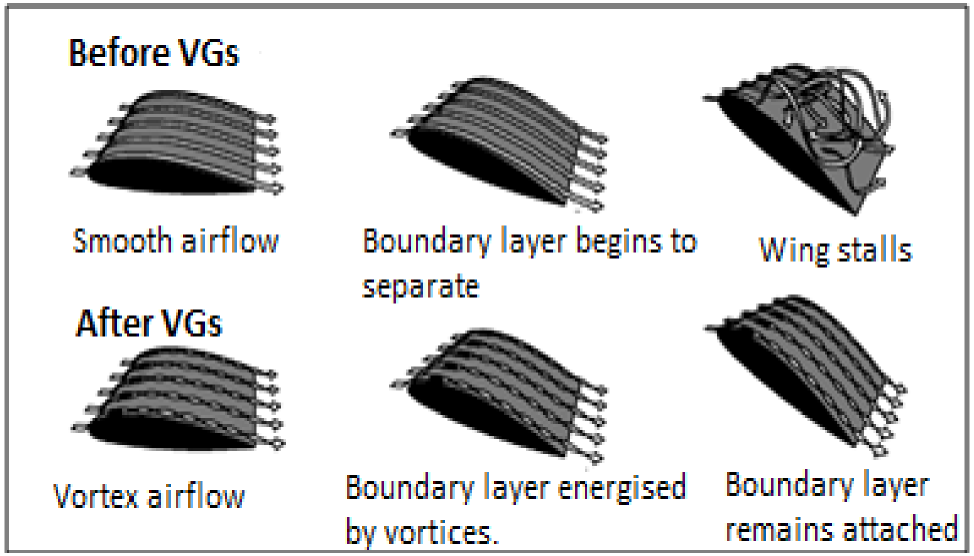

Source: wikipedia

Flow control devices

- **Delay** and **reduce** separation thus **improving** aerodynamic performance.
- First proposed by Taylor (1948)[1] for aircrafts.
- Existing devices: Streamwise vortex generators (vane, delta, air jet etc.)

Existing vortex generators

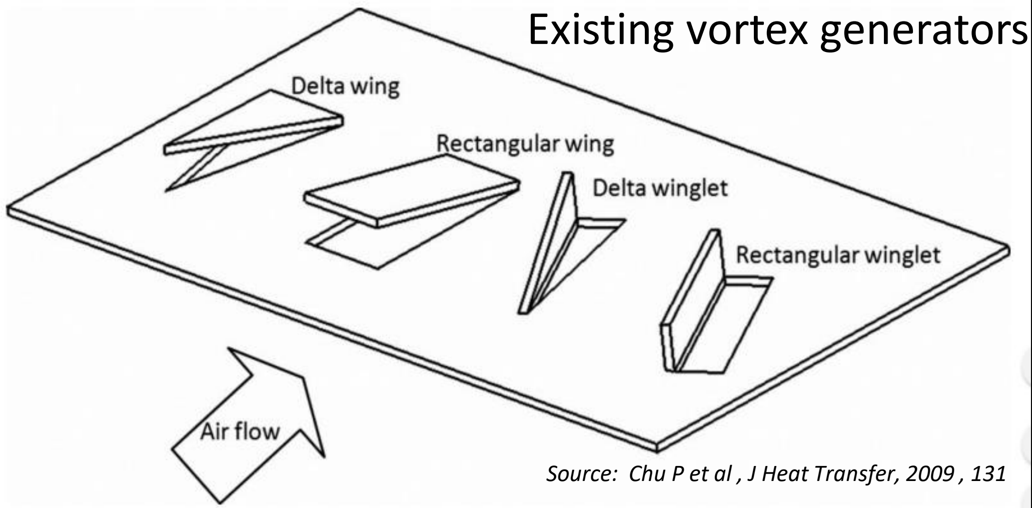

Source: Chu P et al , J Heat Transfer, 2009 , 131

[1] Taylor, H. D., "The elimination of diffuser separation by vortex generators", United Aircraft Corporation Report No. R-4012-3, 1947

RESEARCH INTRODUCTION

Off design condition : Novel flow control device **– Rod Vortex Generators (RVGs)**[1] for boundary layer separation.

RVGs investigated for **Helicopter** rotor blades[2], **Wind turbine profiles/rotors**[3].

Acoustic impact on wind turbine applications?

1. **Loading** noise due to pressure variations (dominant at low Mach).
2. **Thickness** noise due to rotation.
3. **Quadrupole** noise (neglected).

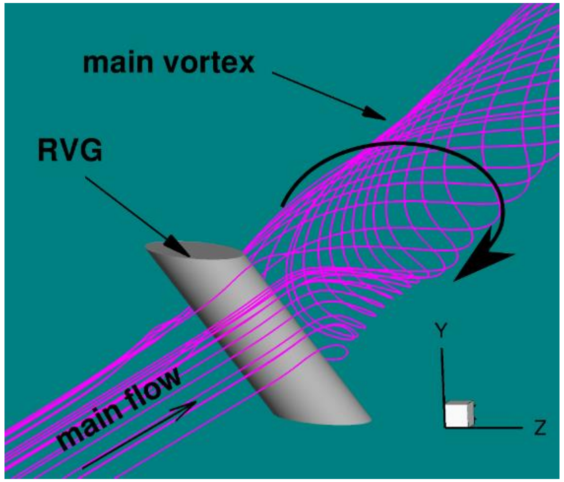

Streamwise vortex generated by a single RVG[3]

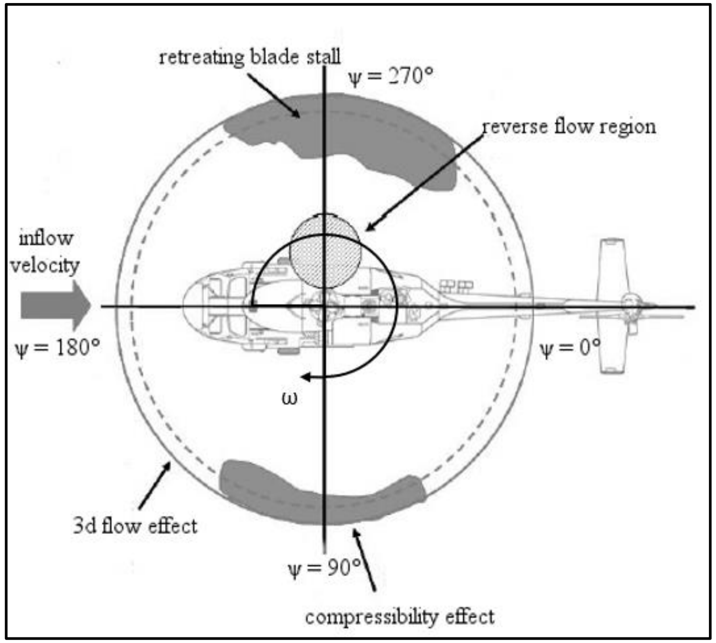

Limitations of helicopter operating in forward flight[2]

[1] P. Doerffer, 2009.
[2] F. Tejero et al. Journal Of American Helicopter Society, 2016.
[3] J Suarez et al. Wind Energy, 2018.

RESEARCH INTRODUCTION

<u>**Off design condition**</u> : Novel flow control device **– Rod Vortex Generators (RVGs)**[1] for boundary layer separation.

RVGs investigated for **Helicopter** rotor blades[2], **Wind turbine profiles/rotors**[3].

Acoustic impact on wind turbine applications?

1. **Loading** noise due to pressure variations (dominant at low Mach).
2. **Thickness** noise due to rotation.
3. **Quadrupole** noise (neglected).

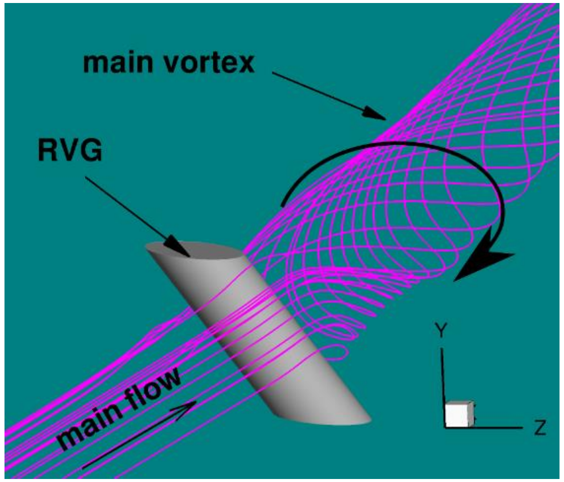

Streamwise vortex generated by a single RVG[3]

Contour plot of Mach number and streamlines at cross section of advancing helicopter rotor blade in forward flight

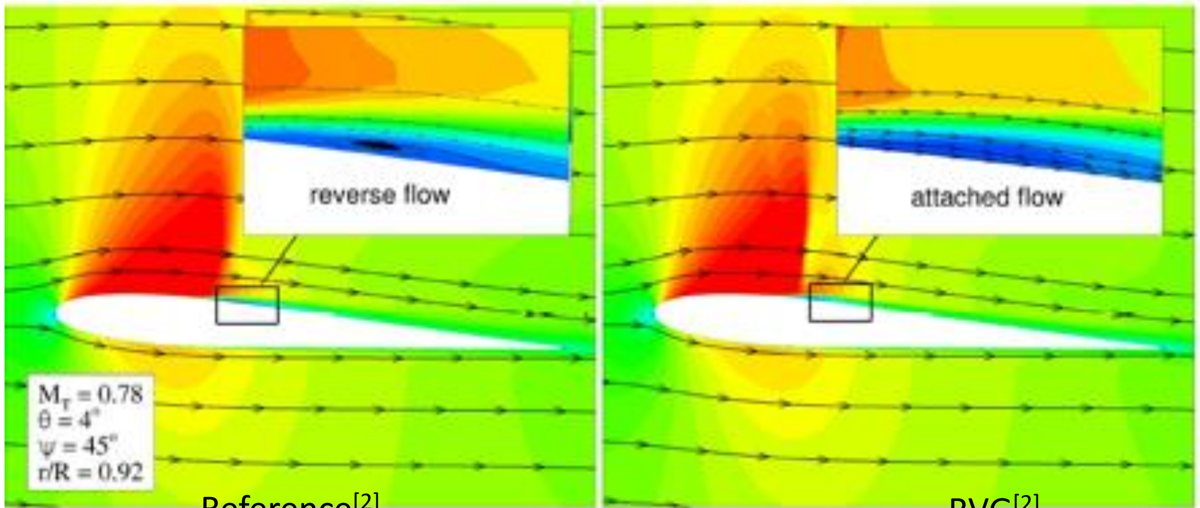

Reference[2] RVG[2]

[1] P. Doerffer, 2009.
[2] F. Tejero et al. Journal Of American Helicopter Society, 2016.
[3] J Suarez et al. Wind Energy, 2018.

RESEARCH INTRODUCTION

Off design condition : Novel flow control device **– Rod Vortex Generators (RVGs)**[1] for boundary layer separation.

RVGs investigated for **Helicopter** rotor blades[2], **Wind turbine profiles/rotors**[3].

Acoustic impact on wind turbine applications?

1. **Loading** noise due to pressure variations (dominant at low Mach).
2. **Thickness** noise due to rotation.
3. **Quadrupole** noise (neglected).

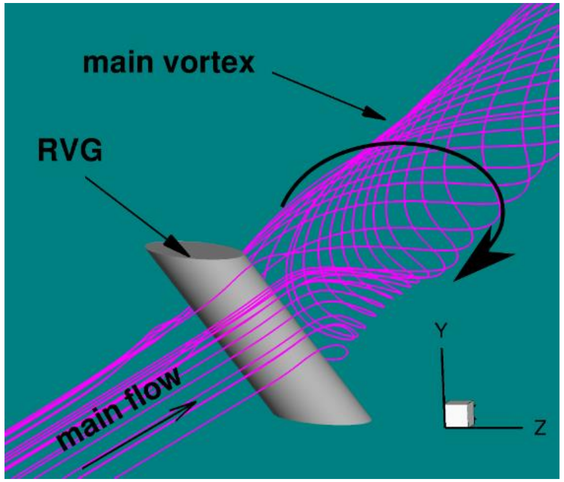

Streamwise vortex generated by a single RVG[3]

Contour maps of skin friction coefficient and flow streamlines for NREL Phase VI wind turbine rotor[3]

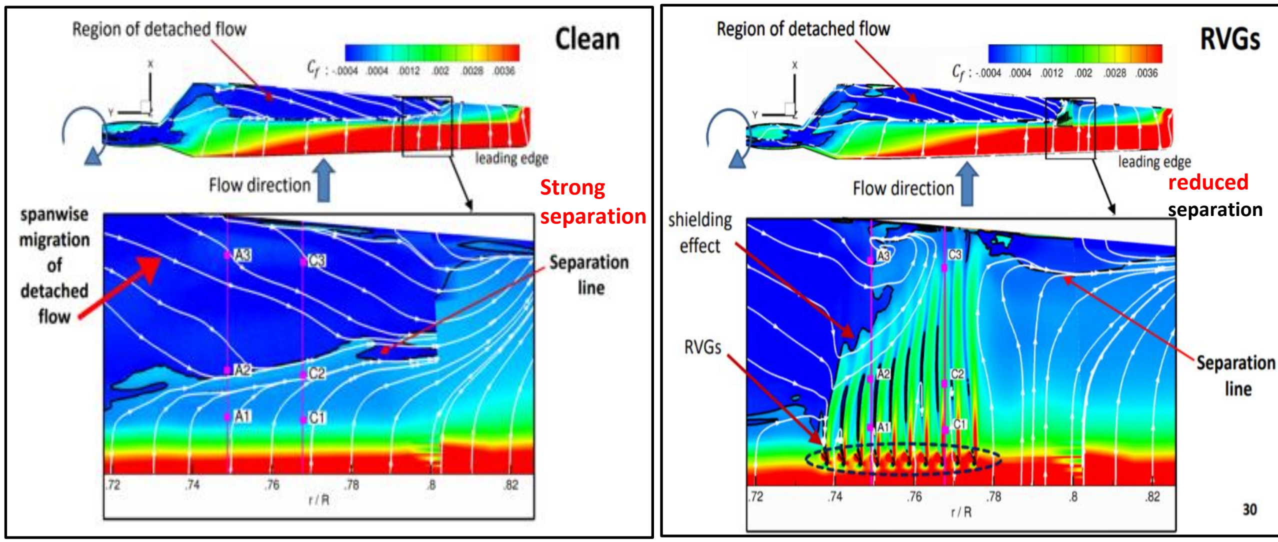

Reference[2]

RVG[2]

[1] P. Doerffer, 2009.
[2] F. Tejero et al. Journal Of American Helicopter Society, 2016.
[3] J Suarez et al. Wind Energy, 2018.

DESIGN OF RVGS FOR DU96-W-180 PROFILE

- Design of RVGs for measurements of a wind turbine profile **DU96-W-180** with/without RVGs at **TU Delft.**
- **Test section** : Anechoic vertical open-jet wind tunnel (rectangular section - 40 x 70 cm^2, contraction ratio of 15:1).
- **Numerical design** of **RVGs** :
  - Full wind tunnel approach – including sideplates, jet nozzle.
  - Profile : Chord = 0.15m, span = 0.4m, Reynolds number = 2.63 x 10^5.
  - Mesh : Hybrid mesh (Numeca Hexpress), RANS 3D simulations (Fine Open, EARSM model).

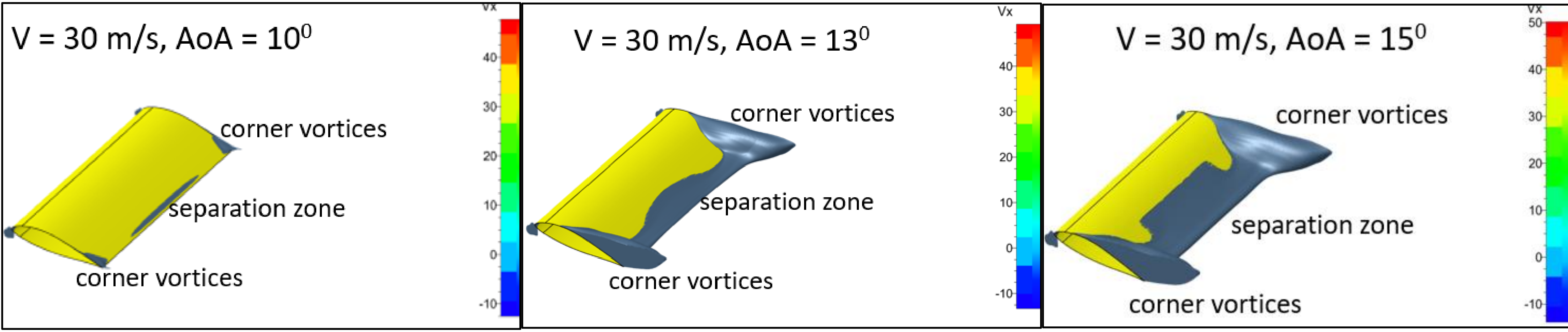

Separation zone and corner vortices grow along with increasing inflow angles

DESIGN OF RVGS FOR DU96-W-180 PROFILE

- Design of RVGs for measurements of a wind turbine profile **DU96-W-180** with/without RVGs at **TU Delft.**
- **Test section** : Anechoic vertical open-jet wind tunnel (rectangular section - 40 x 70 cm^2, contraction ratio of 15:1).
- **RVGs design parameters** :
  - Height = 2mm and 3mm.
  - Diameter = 0.8 mm.
  - Number of rods = 47.
  - Distance between the rods = 8 mm.

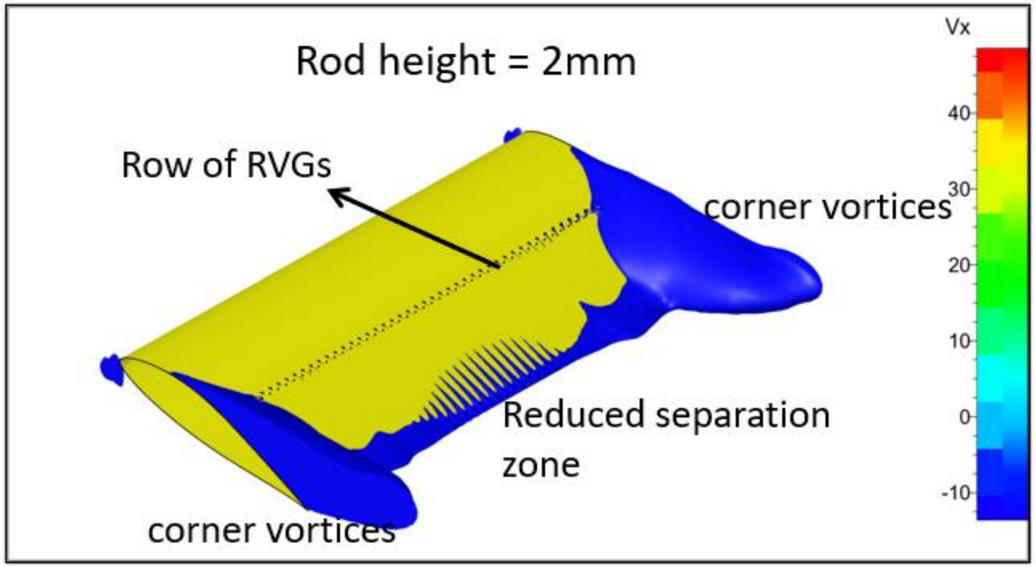

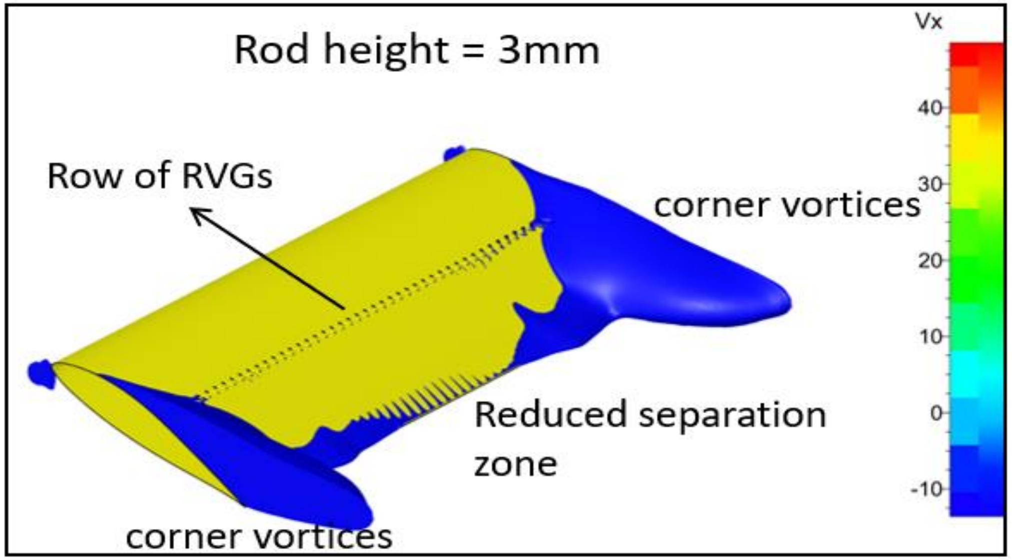

Reduced separation

EXPERIMENTAL CAMPAIGN (1)

Oil flow visualization for non-tripped DU96-W-180 profile at AoA = 17°

Reference

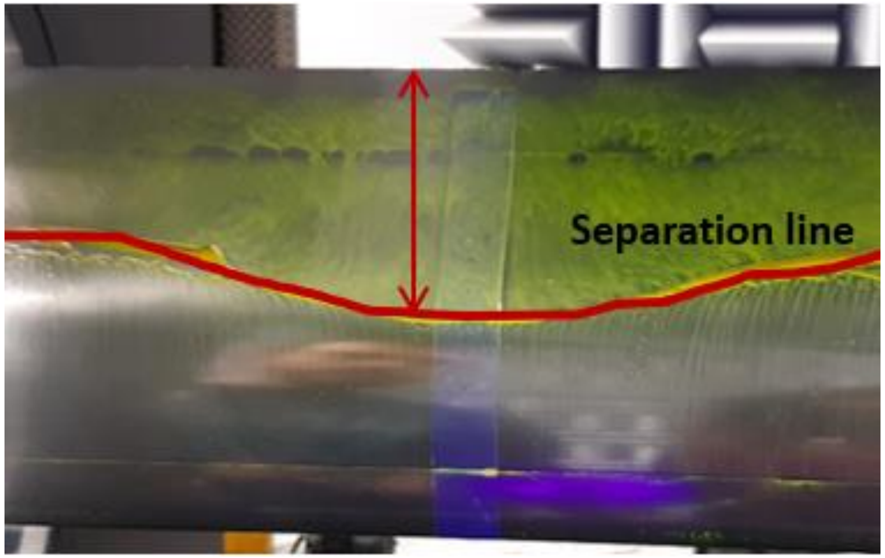

RVGs

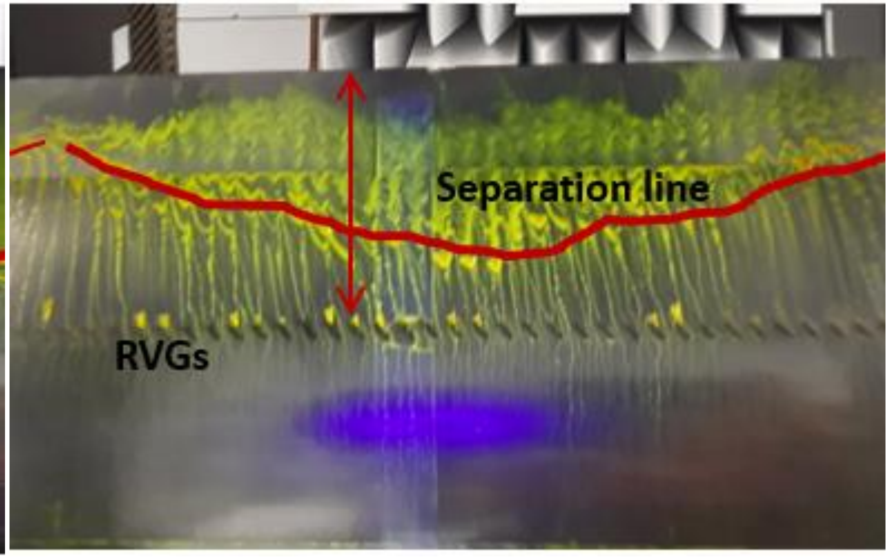

Acoustic beamforming for DU96-W-180 profile at AoA = 6°

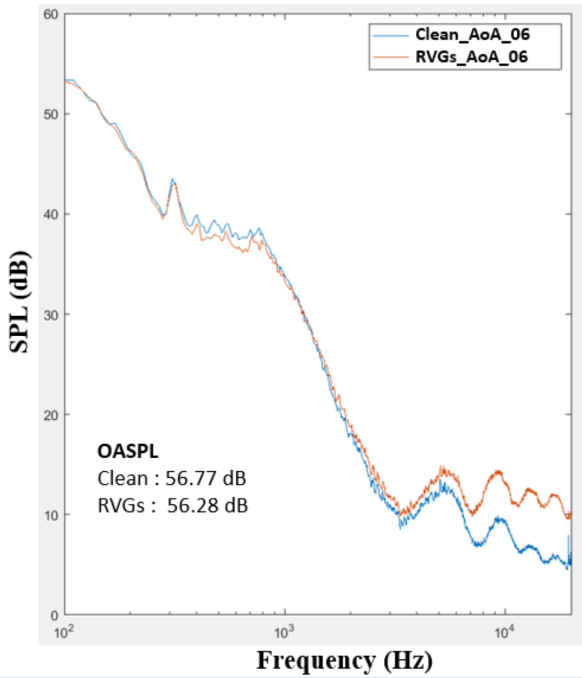

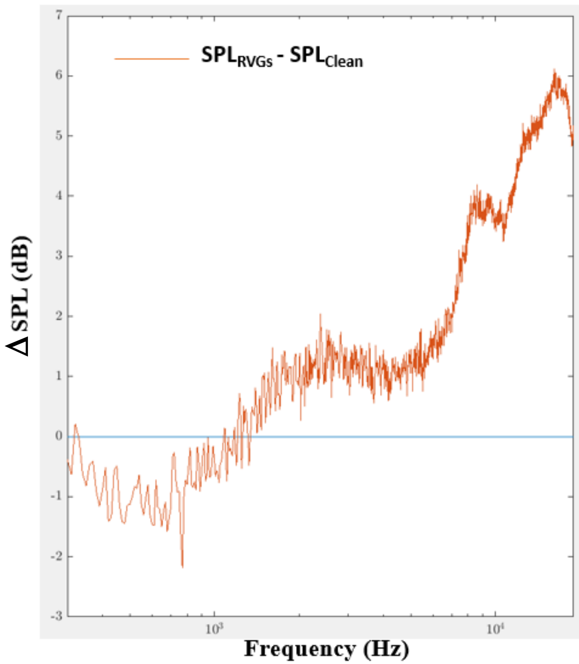

Sound pressure analysis

At low frequency : **SPL_{RVG} < SPL_{Clean}**

At mid frequency : **SPL_{RVG} ~ SPL_{Clean}**

At high frequency : **SPL_{RVG} > SPL_{Clean}**

EXPERIMENTAL CAMPAIGN (1)

Oil flow visualization for tripped DU96-W-180 profile at AoA = 6°

Reference

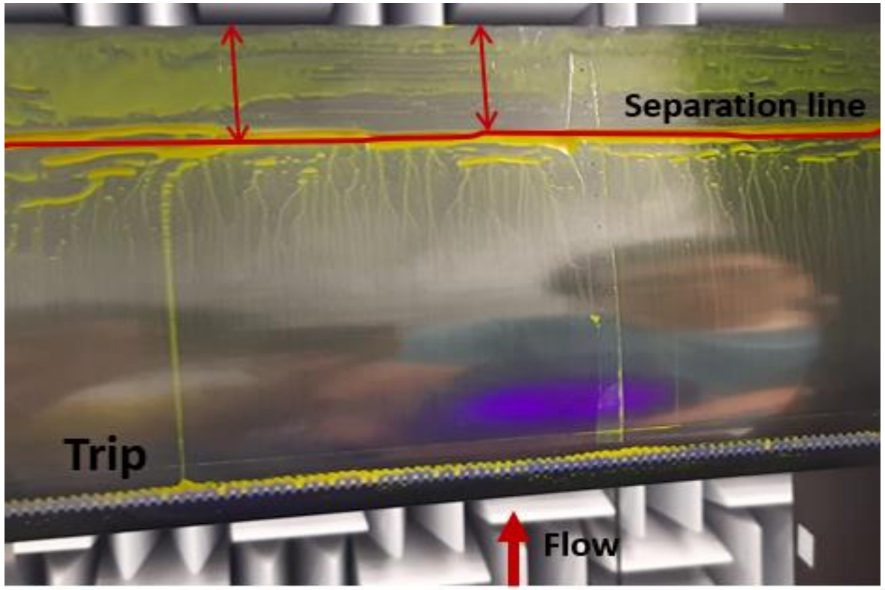

RVGs

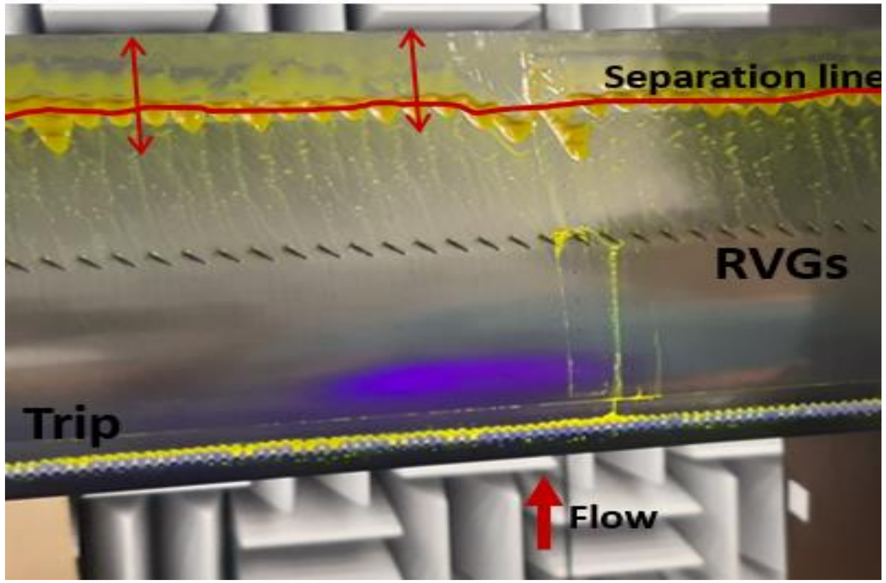

Acoustic beamforming for DU96-W-180 profile at AoA = 6°

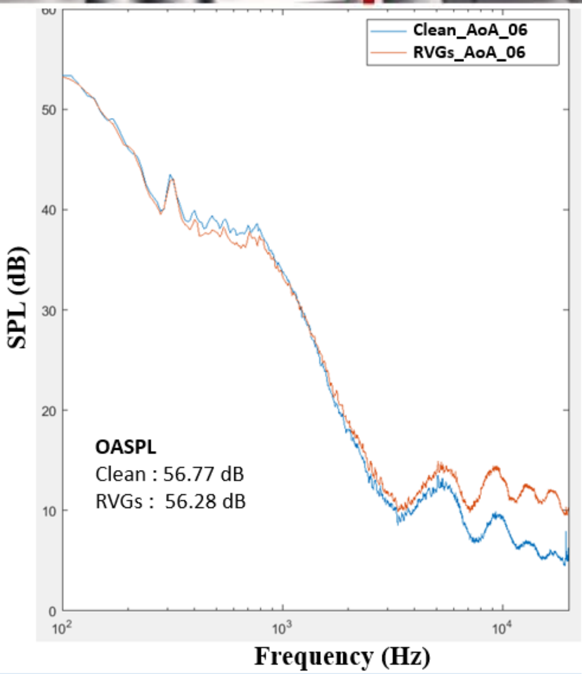

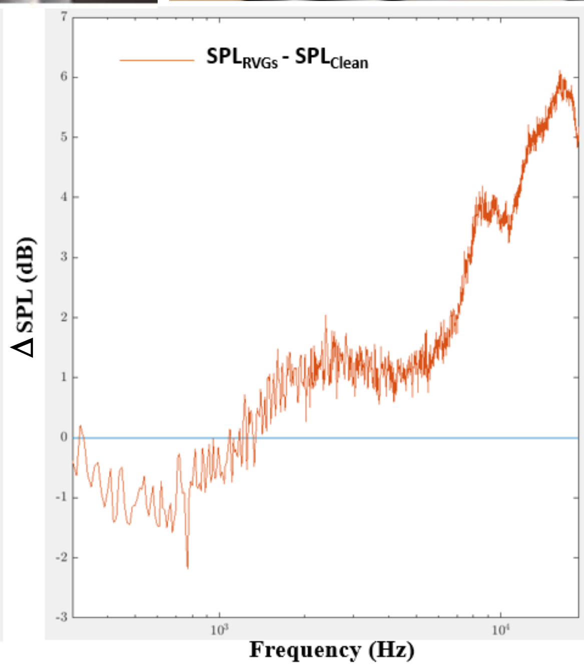

Sound pressure analysis

At low frequency :
SPL_{RVG} < SPL_{Clean}

At mid frequency :
SPL_{RVG} ~ SPL_{Clean}

At high frequency :
SPL_{RVG} > SPL_{Clean}

EXPERIMENTAL CAMPAIGN (2)

Acoustic beamforming for DU96-W-180 profile at AoA = 6°

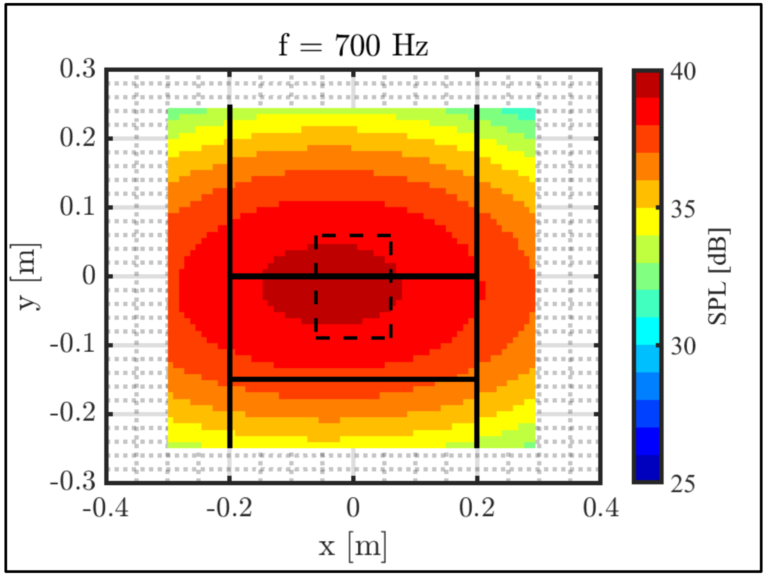

Reference

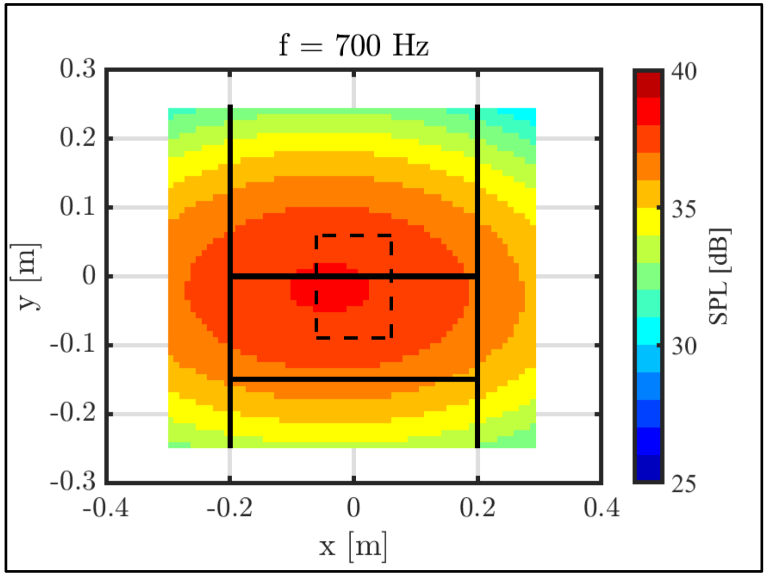

RVGs

Source maps for DU96-W-180 profile for AoA = 6° at low frequency

A noisier source map for the clean case at trailing edge

EXPERIMENTAL CAMPAIGN (2)

Acoustic beamforming for DU96-W-180 profile at AoA = 6°

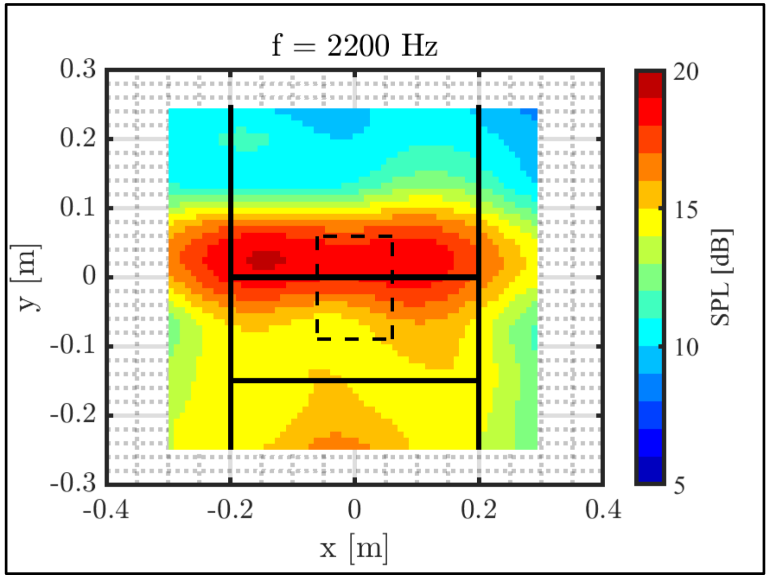

Reference

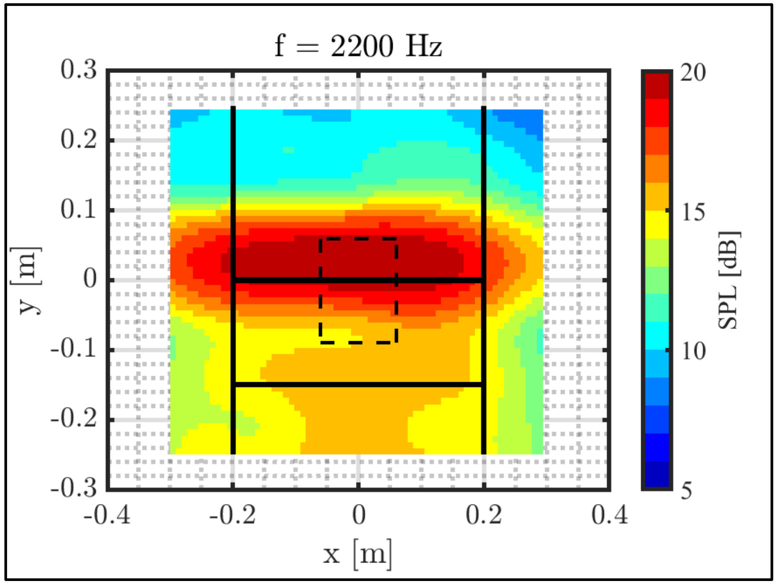

RVGs

Source maps for DU96-W-180 profile for AoA = 6° at mid frequency

A noisier source map for the RVGs case with source spreading at trailing edge
A noise source due to the jet is visible at the nozzle exit

EXPERIMENTAL CAMPAIGN (2)

Acoustic beamforming for DU96-W-180 profile at AoA = 6°

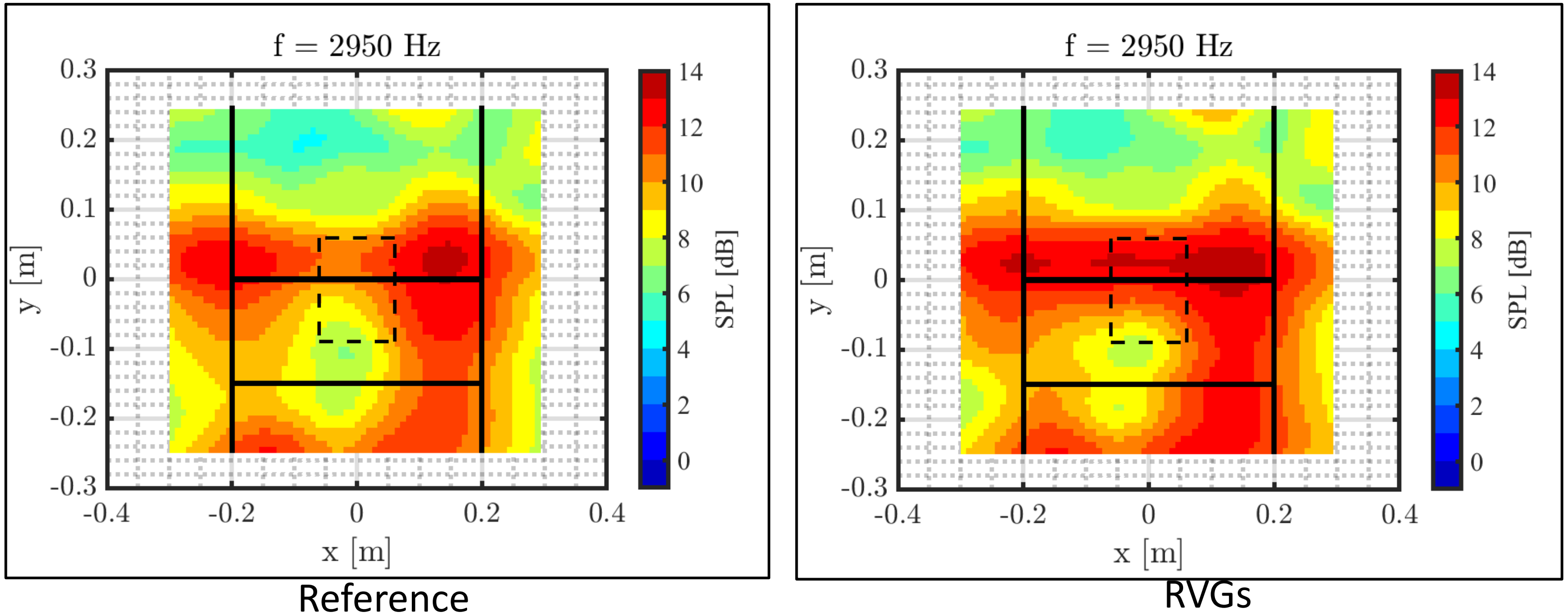

Source maps for DU96-W-180 profile for AoA = 6° at high frequency

A noisier source map for the RVGs case with source spreading at trailing edge
A noise source due to the jet is visible at the nozzle exit
Noise sources due to corner vortices at the side plates are also visible

AERO-ACOUSTIC CODE

Theory : Ffowcs Williams – Hawkings analogy (Farassat's formulations)

Acoustic pressure — *Observer time*

$$p'(\vec{x},t)=\frac{\partial}{\partial t}\iint_S\left[\frac{\rho_0 v_n}{r\left|1-M_r\right|}\right]_\tau dS-\frac{\partial}{\partial x_i}\iint_S\left[\frac{p_{ij}n_j}{r\left|1-M_r\right|}\right]_\tau dS+\frac{\partial^2}{\partial x_i\partial x_j}\iiint_V\left[\frac{T_{ij}}{r\left|1-M_r\right|}\right]_\tau dV$$

Monopole **(thickness term)** — **Dipole** **(loading term)** — **Quadrupole** **(volume term)**

Acoustic code :

1. **Development.**
2. **Validation**
3. **Applications**

Analytical

- **Stationary :**
  1. Monopole
  2. Dipole

Experiment +
Other codes

AERO-ACOUSTIC CODE

Theory : Ffowcs Williams – Hawkings analogy (Farassat's formulations)

Acoustic pressure — *Observer time*

$$p'(\vec{x},t) = \frac{\partial}{\partial t}\iint_S \left[\frac{\rho_0 v_n}{r|1-M_r|}\right]_\tau dS - \frac{\partial}{\partial x_i}\iint_S \left[\frac{p_{ij} n_j}{r|1-M_r|}\right]_\tau dS + \frac{\partial^2}{\partial x_i \partial x_j}\iiint_V \left[\frac{T_{ij}}{r|1-M_r|}\right]_\tau dV$$

Monopole (thickness term) — **Dipole (loading term)** — **Quadrupole (volume term)**

Acoustic code :

1. **Development.**
2. **Validation**
3. **Applications**

Analytical

- **Rotating :**
  3. Monopole
  4. Dipole
  5. Source-sink pair

Experiment + Other codes

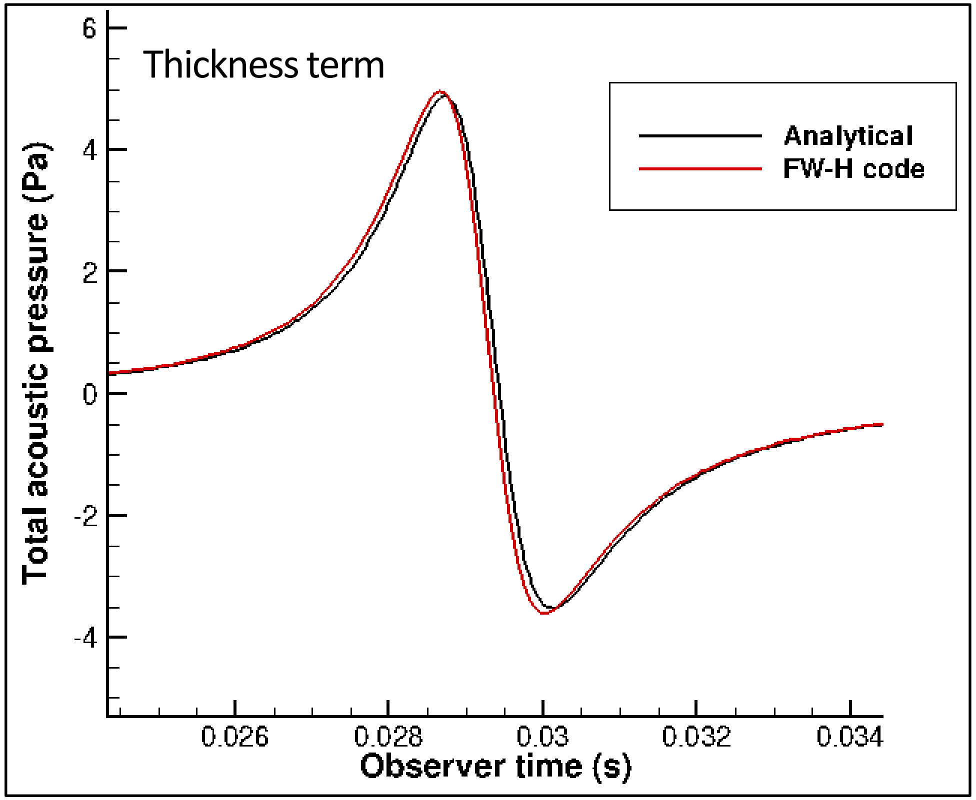

AERO-ACOUSTIC CODE

Theory : Ffowcs Williams – Hawkings analogy (Farassat's formulations)

Acoustic pressure — *Observer time*

$$p'(\vec{x},t) = \frac{\partial}{\partial t}\iint_S \left[\frac{\rho_0 v_n}{r|1-M_r|}\right]_\tau dS - \frac{\partial}{\partial x_i}\iint_S \left[\frac{p_{ij} n_j}{r|1-M_r|}\right]_\tau dS + \frac{\partial^2}{\partial x_i \partial x_j}\iiint_V \left[\frac{T_{ij}}{r|1-M_r|}\right]_\tau dV$$

Monopole **(thickness term)** — **Dipole** **(loading term)** — **Quadrupole** **(volume term)**

Acoustic code :

1. **Development.**
2. **Validation**
3. **Applications**

Analytical

- **Rotating :**
  3. Monopole
  4. Dipole
  5. Source-sink pair

Experiment + Other codes

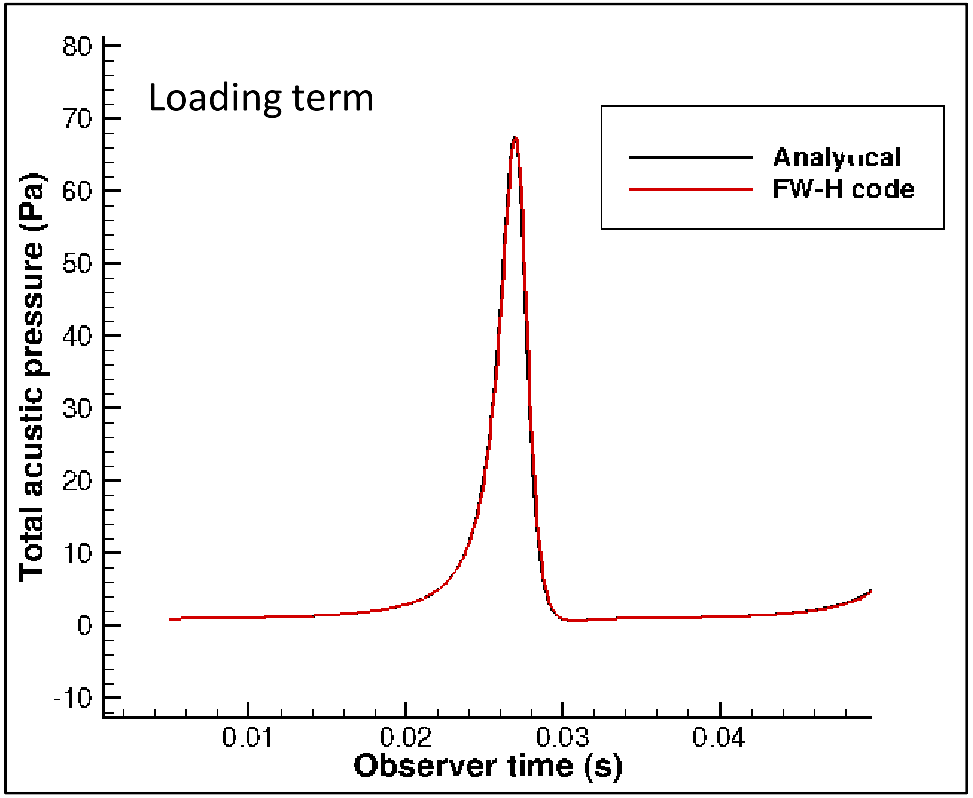

AERO-ACOUSTIC CODE

Theory : Ffowcs Williams – Hawkings analogy (Farassat's formulations)

Acoustic pressure *Observer time*

$$p'(\vec{x},t) = \frac{\partial}{\partial t}\iint_S \left[\frac{\rho_0 v_n}{r|1-M_r|}\right]_\tau dS - \frac{\partial}{\partial x_i}\iint_S \left[\frac{p_{ij} n_j}{r|1-M_r|}\right]_\tau dS + \frac{\partial^2}{\partial x_i \partial x_j}\iiint_V \left[\frac{T_{ij}}{r|1-M_r|}\right]_\tau dV$$

Monopole (thickness term) **Dipole (loading term)** **Quadrupole (volume term)**

Acoustic code :

1. **Development.**
2. **Validation**
3. **Applications**

Analytical

Experiment + Other codes

- **Helicopter** rotor

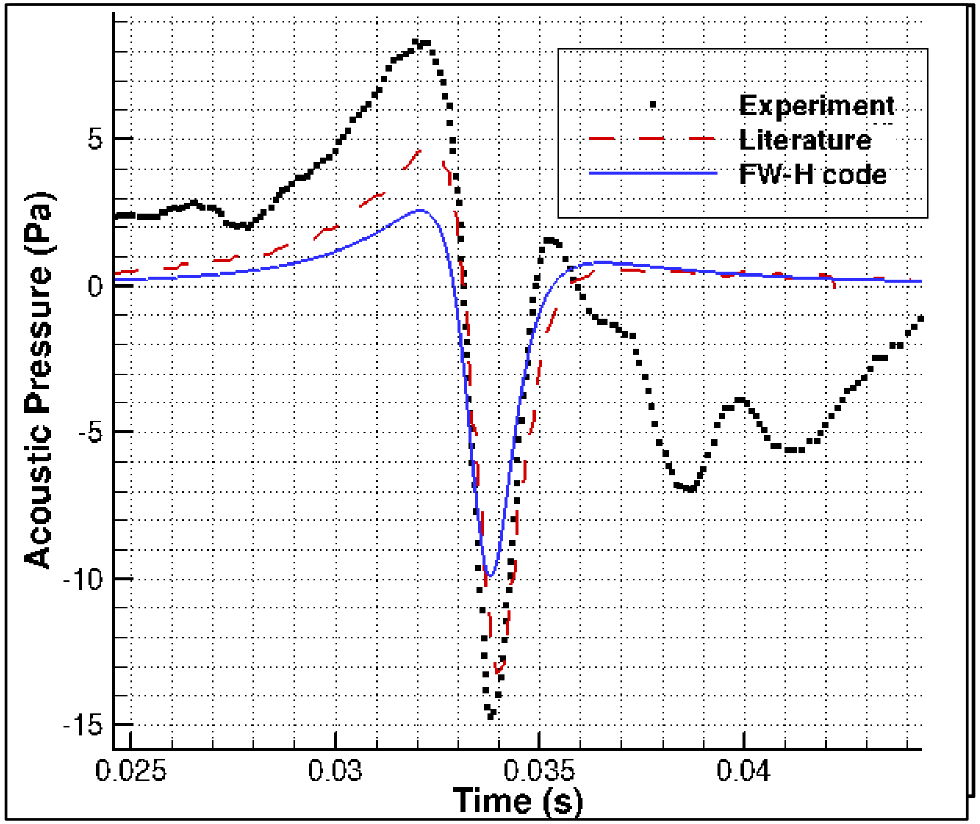

AERO-ACOUSTIC CODE

Theory : Ffowcs Williams – Hawkings analogy (Farassat's formulations)

Observer time

Acoustic pressure

$$p'(\vec{x},t)=\frac{\partial}{\partial t}\iint_S\left[\frac{\rho_0 v_n}{r|1-M_r|}\right]_\tau dS-\frac{\partial}{\partial x_i}\iint_S\left[\frac{p_{ij}n_j}{r|1-M_r|}\right]_\tau dS+\frac{\partial^2}{\partial x_i \partial x_j}\iiint_V\left[\frac{T_{ij}}{r|1-M_r|}\right]_\tau dV$$

Monopole (thickness term) — **Dipole (loading term)** — **Quadrupole (volume term)**

Acoustic code :

1. **Development.**
2. **Validation**
3. **Applications**
   - **Wind turbine blade** with RVGs

AERO - ACOUSTIC CODE : NREL PHASE VI WIND TURBINE ROTOR

- **Experiment**: NREL's Unsteady Aerodynamics Experiment on horizontal axis wind turbines[1]
  - Phase VI : 24 m x 36m wind tunnel
  - Rotor with 2 blades, 10 m diameter, rotational speed = 72 rpm

- **Pressure data** from steady flow simulations (**MAREWINT** project[2]) as input to the developed aero-acoustic code.

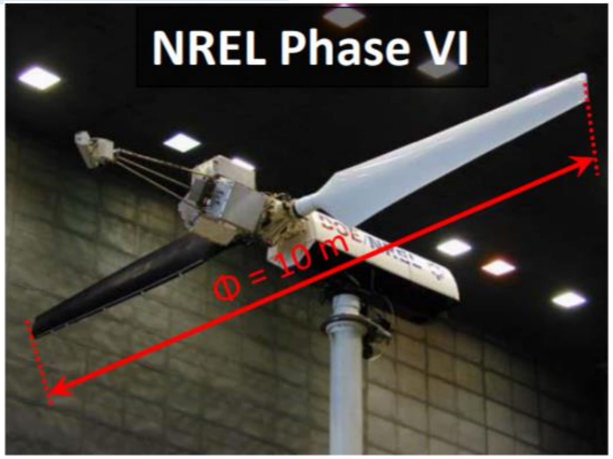

Preliminary results

Flow simulations[2] were validated against measurements[1]

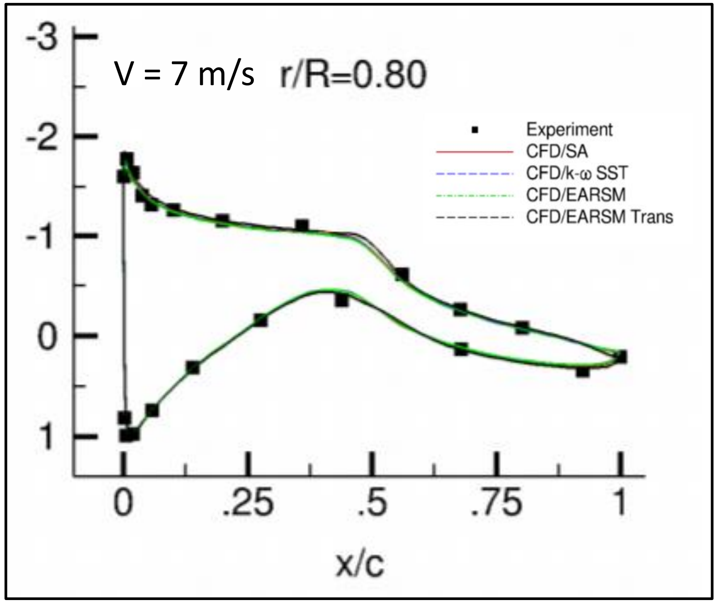

Pressure coefficient of NREL blade at flow velocity V = 7 m/s[3]

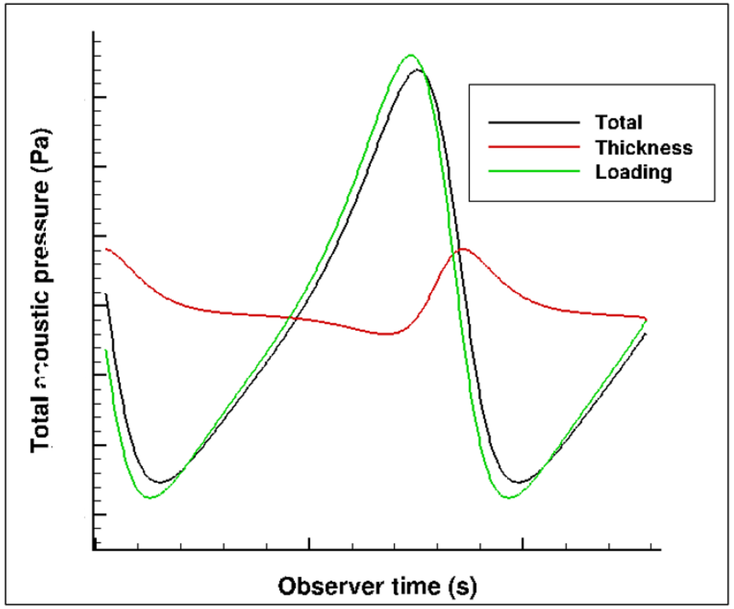

Acoustic pressure for clean NREL Phase VI blade

[1] M.M. Hand, et al. Unsteady Aerodynamics Experiment Phase VI: Wind Tunnel Test Configurations and Available Data Campaigns.
[2] J Suarez et al. Wind Energy, 2018

V. INDUSTRIAL PERSPECTIVE

Leading-edge serrations

Ziehl-Abegg, 2016

Zenger, Renz, and Becker 2017

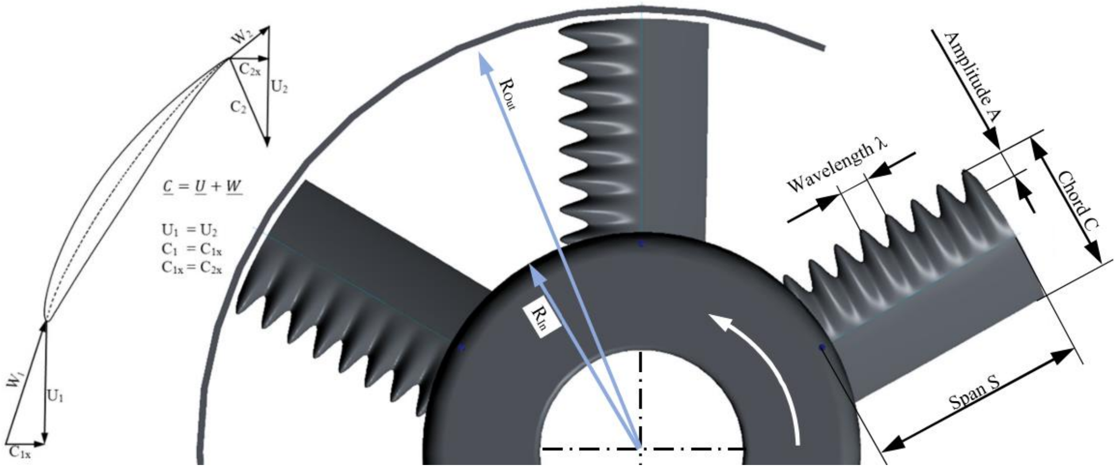

Zenger, Renz, and Becker, 2017

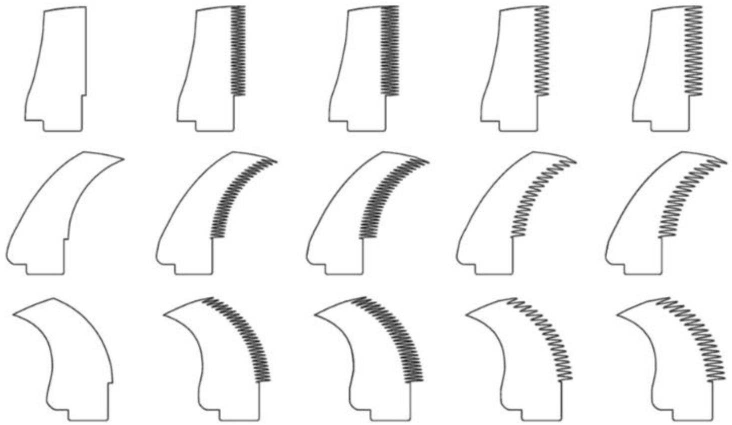

Krömer, Czwielong, & Becker, 2019

Trailing-edge serrations

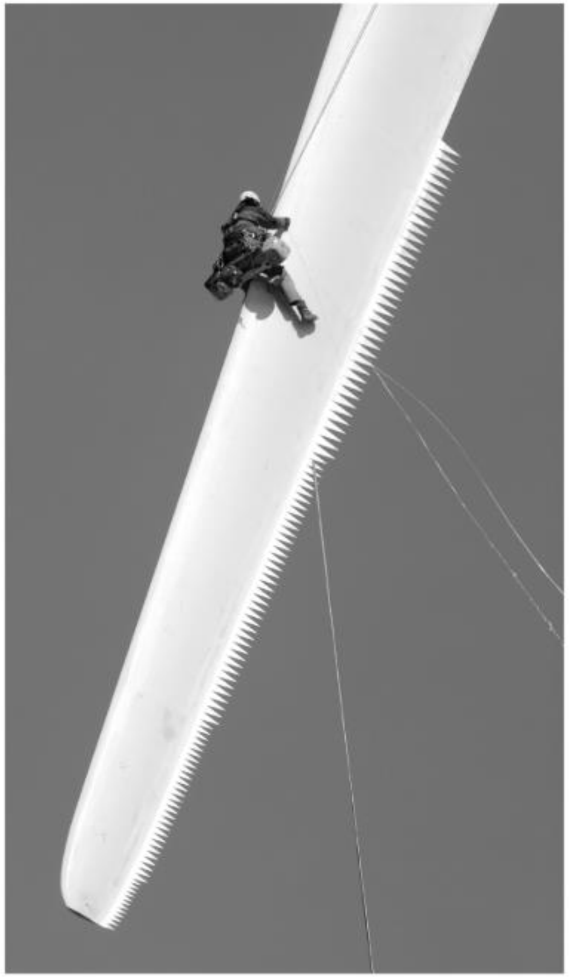

Oerlemans et al. 2009

Pagliaroli et al. 2018

Lee, Lim, & Lee, 2018

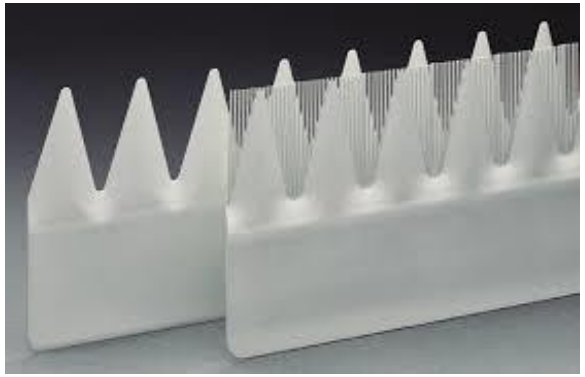

Siemens-Gamesa 2000

Ziehl-Abegg 2012

Vortex generators

Gloster Javelin FAW9 (BAE Systems), 1956

3M & EDF, 2014

Symphony SA-160, 2001

Lufthansa, 2014

Experiments on a plenum fan

- Diameter 361 mm
- Blade span 98 mm
- 7 blades
- N maxi = 1470 rpm

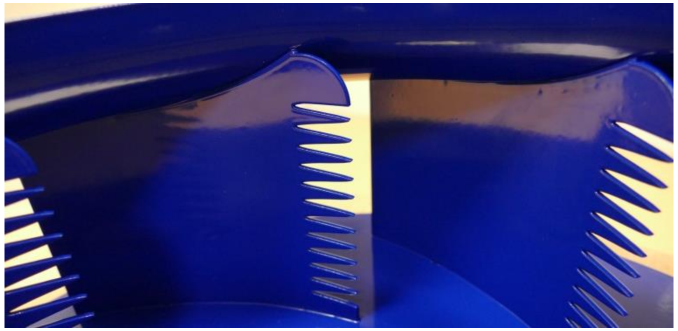

Nom	λ [mm]	h [mm]
LE_L8H11	8	11
LE_L16H11	16	11
LE_L16H22	16	22

Nom	λ [mm]	h [mm]
TE_L8H12	8	12
TE_L4H12	4	12
TE_L8H8	8	8

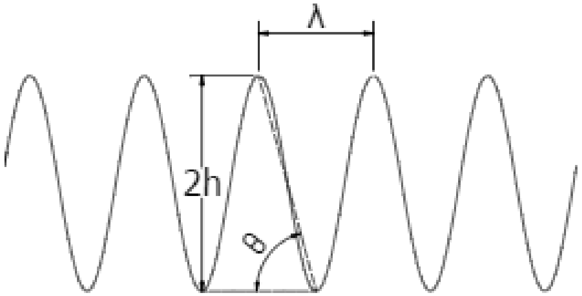

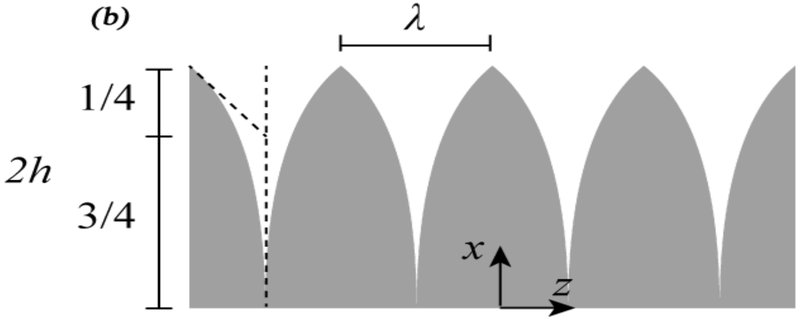

Leading edge, N=1440 rpm

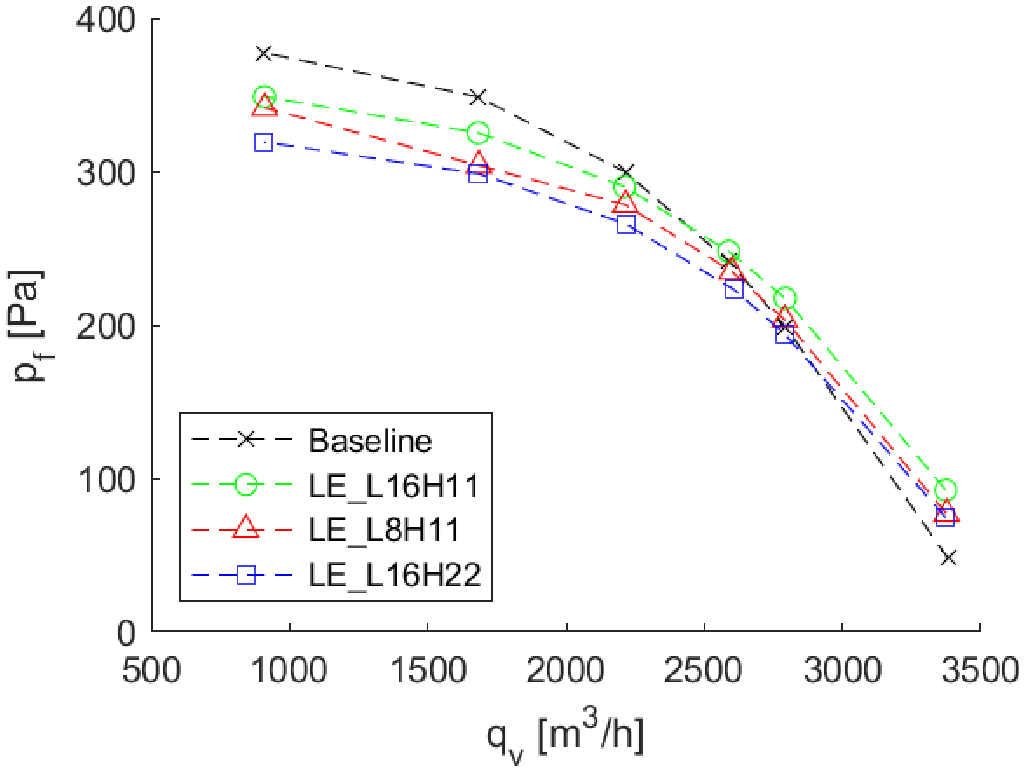

Pressure curves

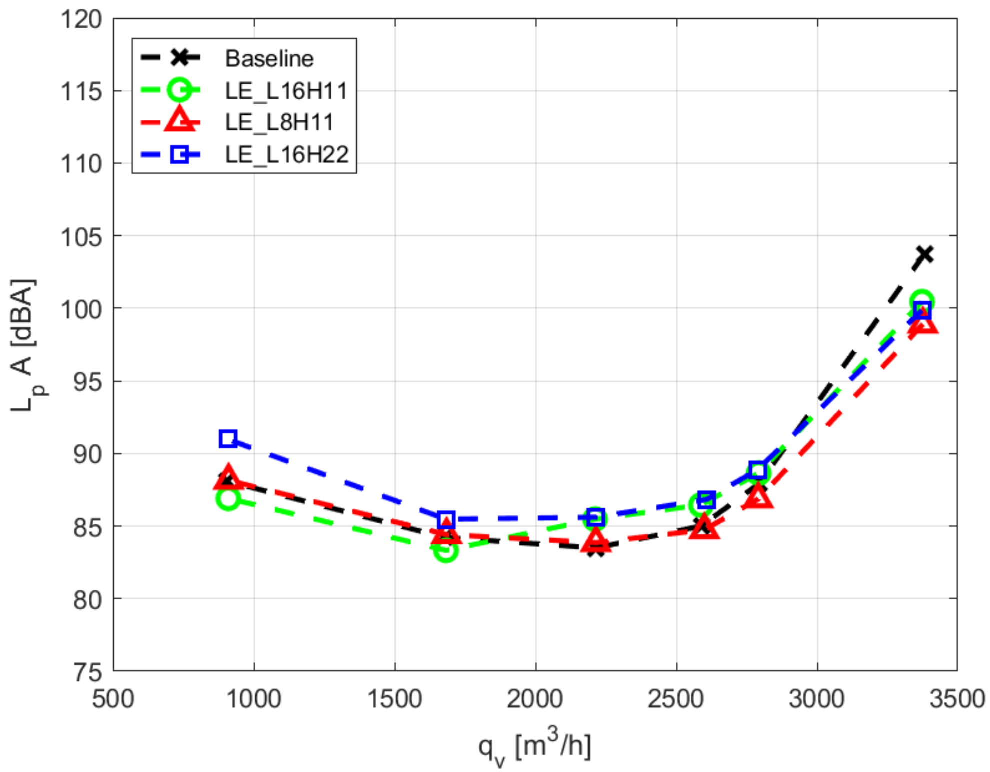

Specific sound levels at outlet

$$L_{p,specific} = L_p - 10\log(q_v) - 20\log(p_f)$$

Leading edge, BEP, N=1440 rpm

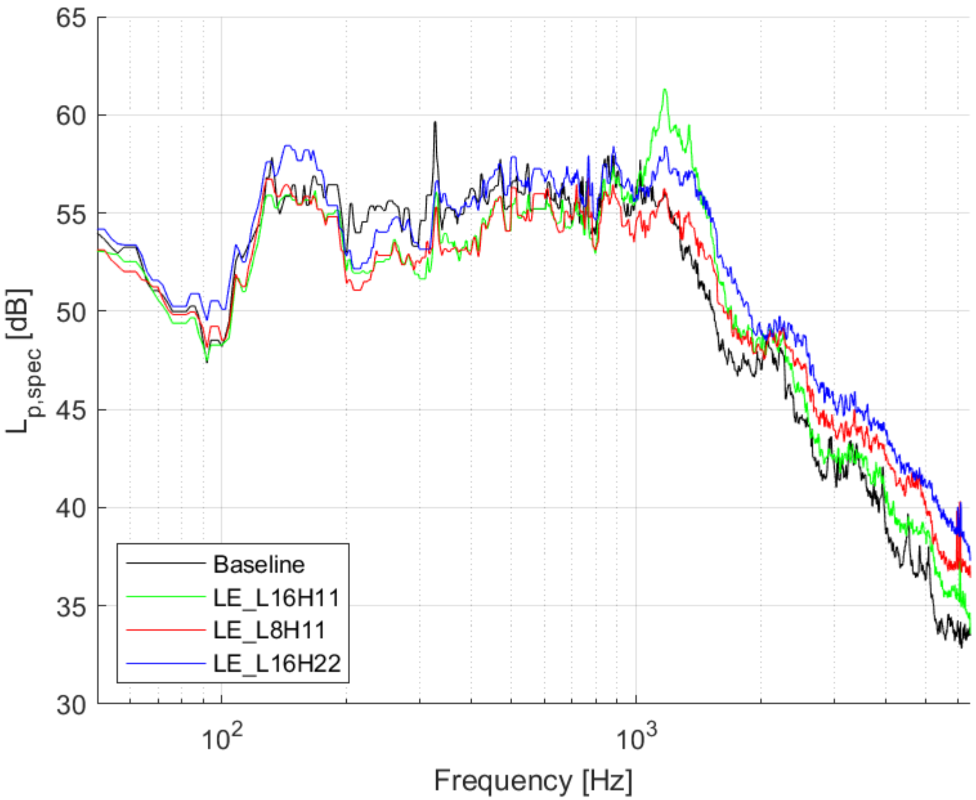

Specific noise spectra

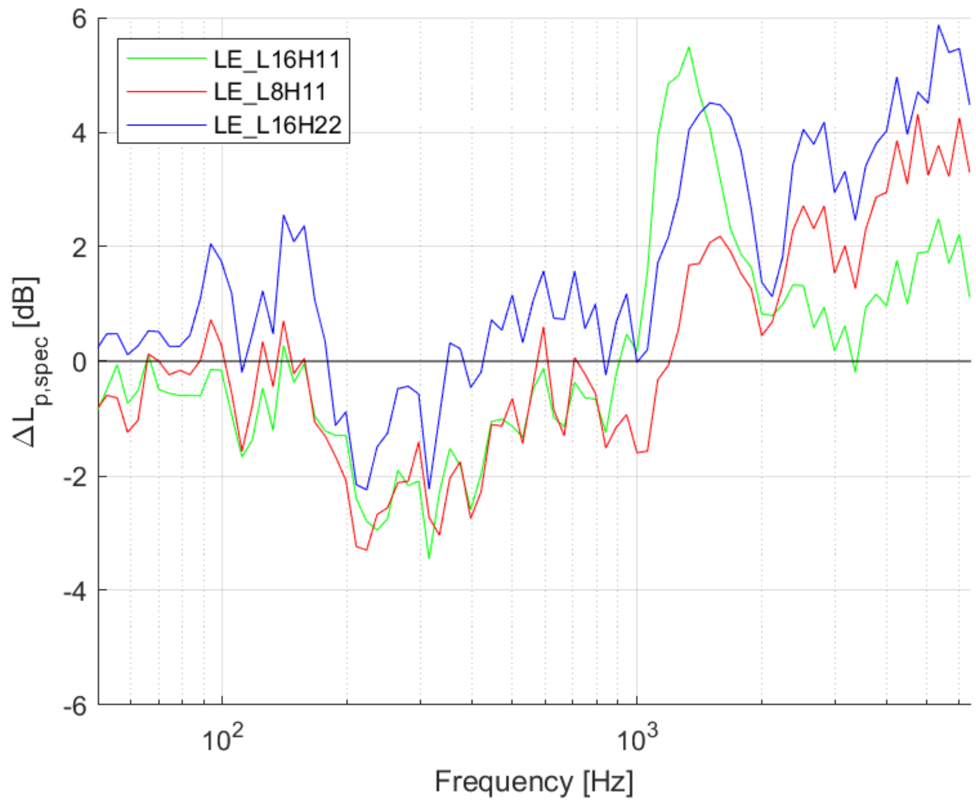

Specific noise reduction

Trailing edge, N=1440 rpm

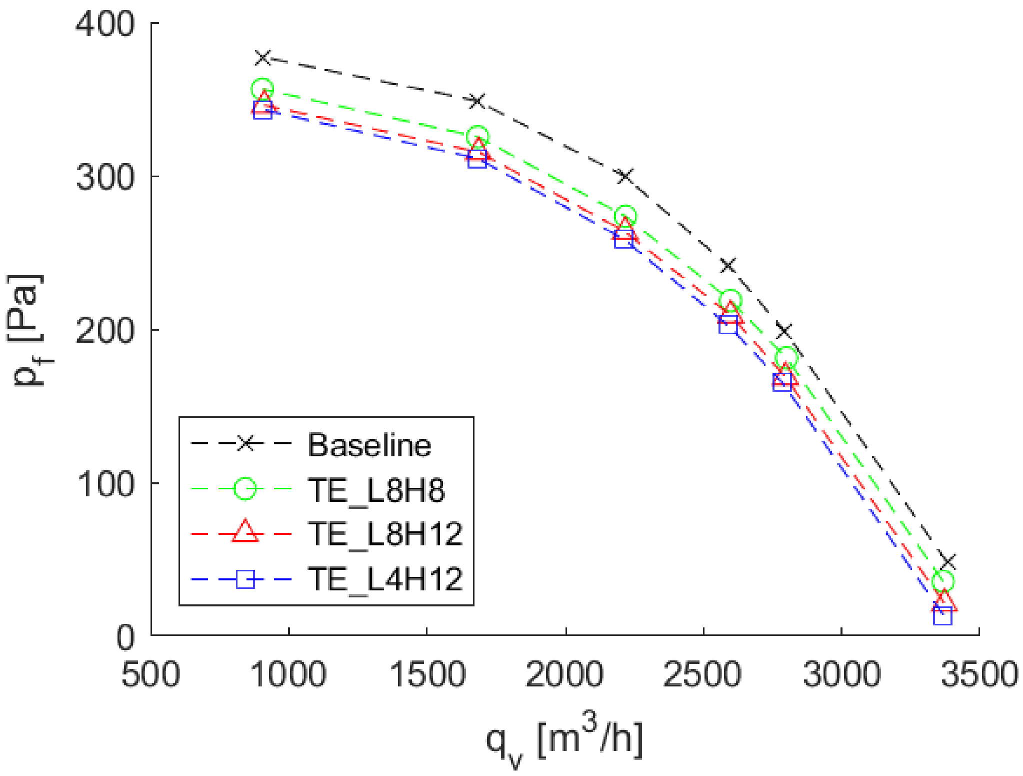

Pressure curves

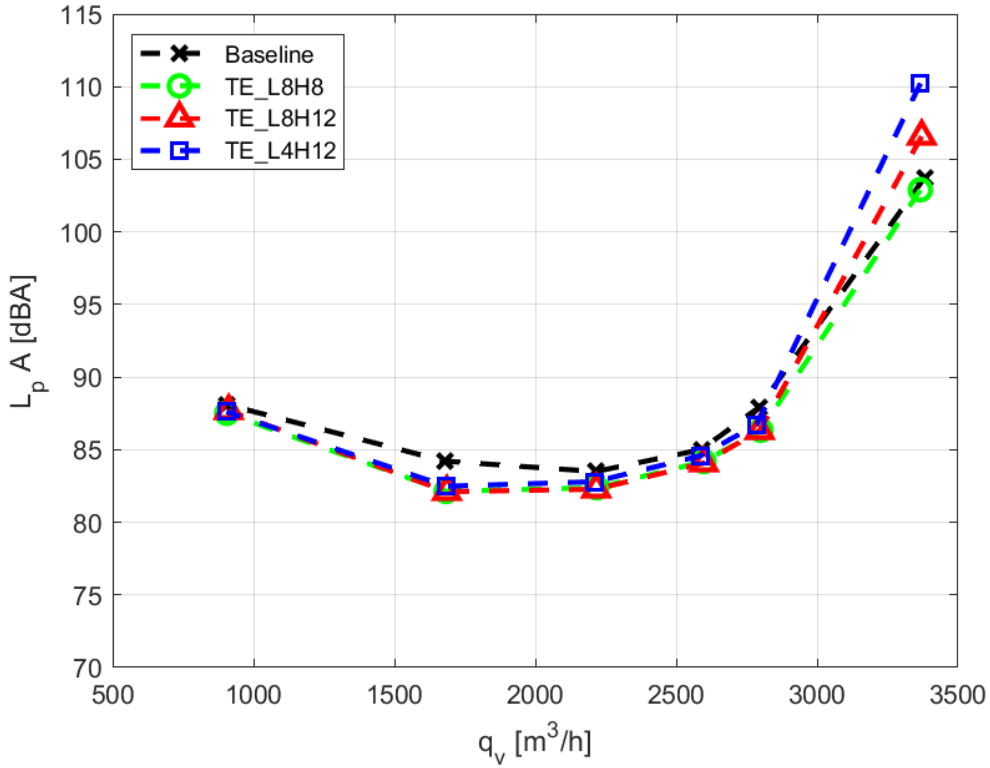

Specific noise levels at outlet

$$L_{p,specific} = L_p - 10\log(q_v) - 20\log(p_f)$$

Trailing edge, BEP, N=1440 rpm

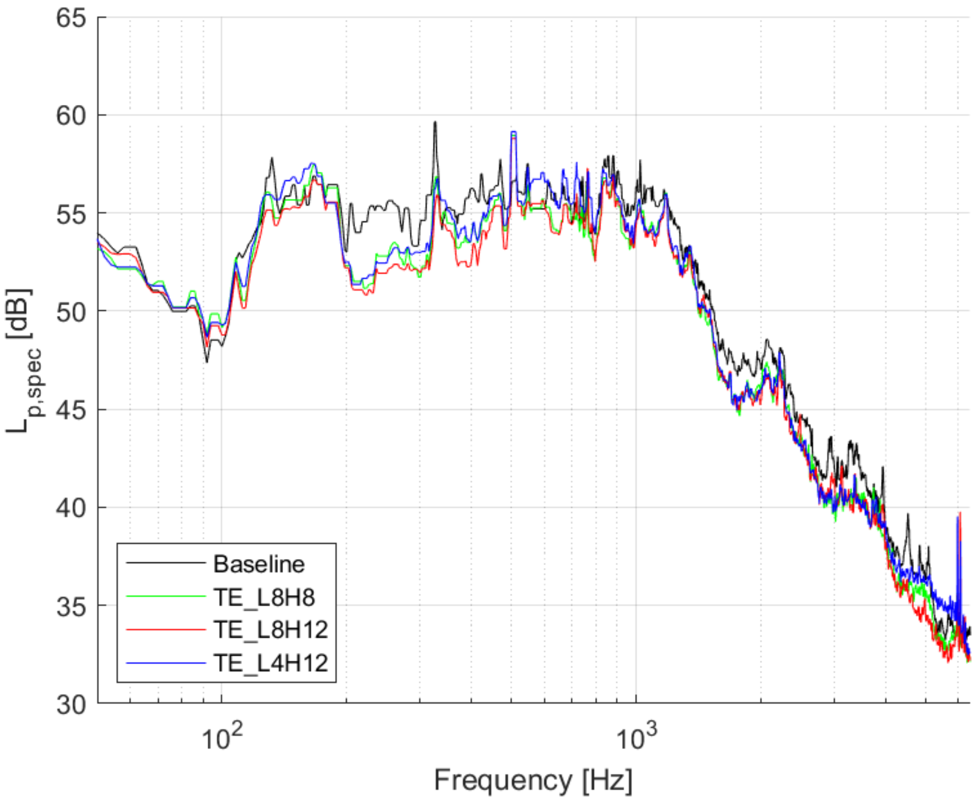

Specific noise spectra

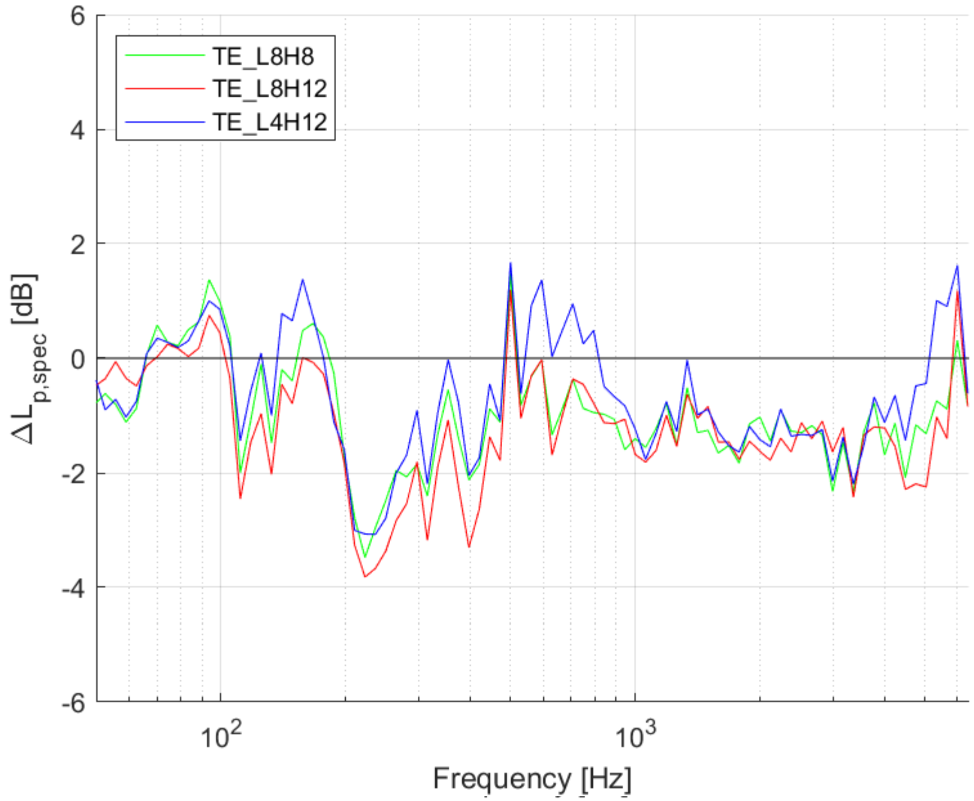

Specific noise reduction

Trailing edge, BEP, N=720 rpm

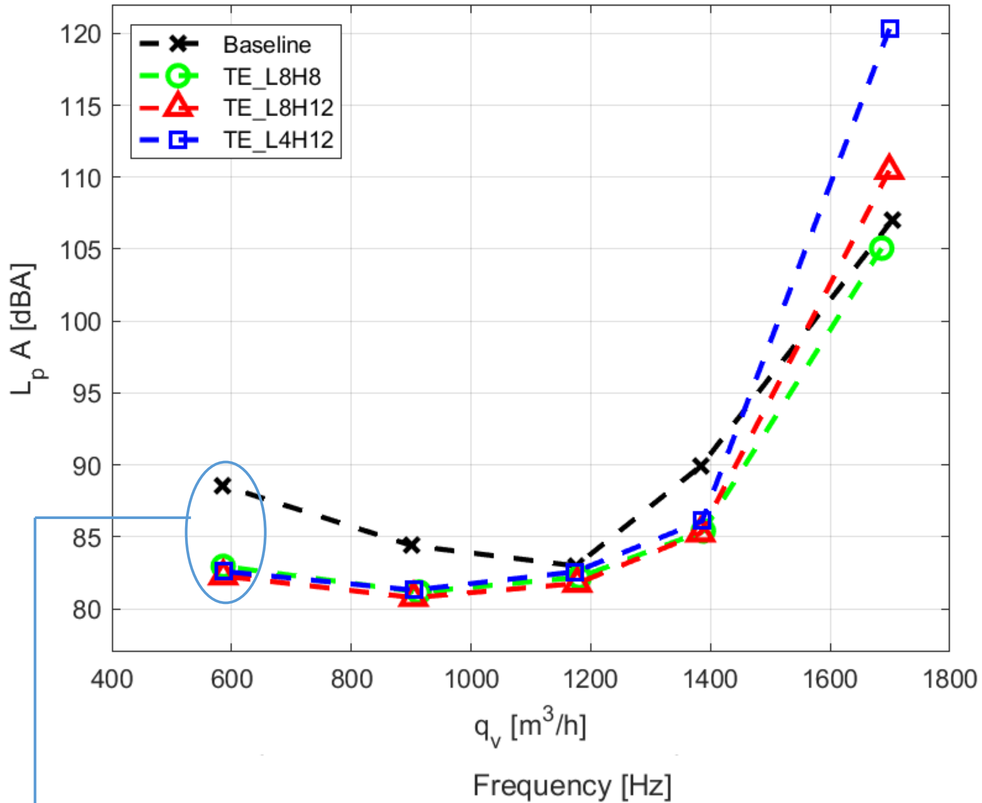

Specific noise levels at outlet

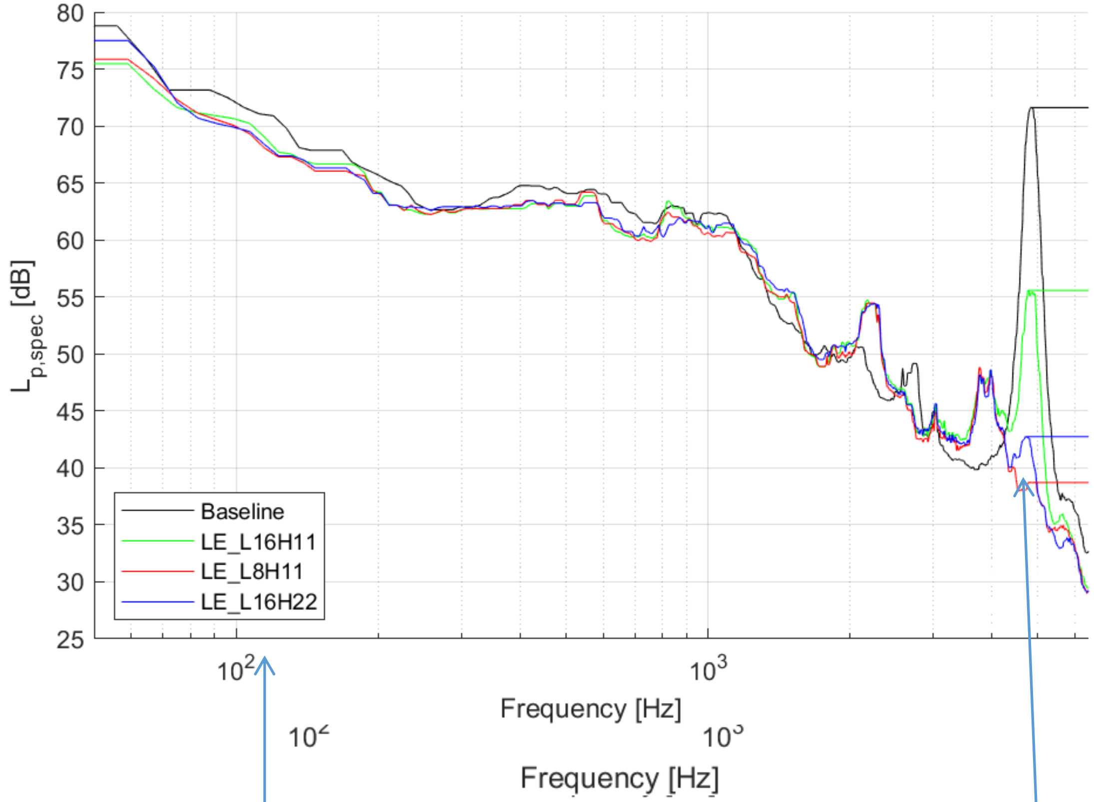

Specific noise spectra

Laminar boundary-layer vortex-shedding ??? $f \cdot \frac{e}{V} \approx 1$

VI. CONCLUDING REMARKS

What's next?

- Further investigation of the underlying physics of noise reduction by the use of serrations, porous materials, and vortex generators.

- To predict the impact of these novel noise mitigation techniques and their applications on an industrial scale.

Conclusion

WHY DID WE UNDERTAKE THIS ADVENTURE?

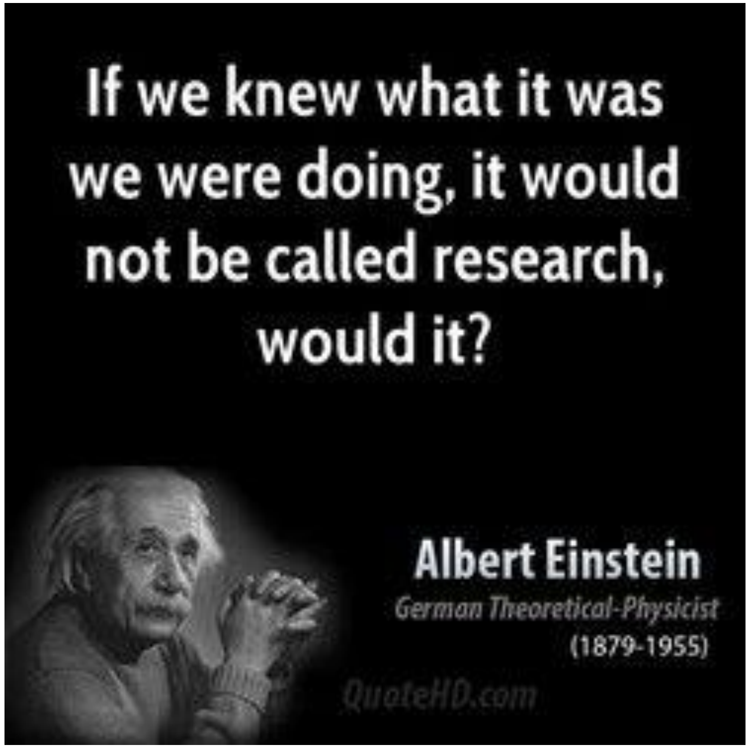

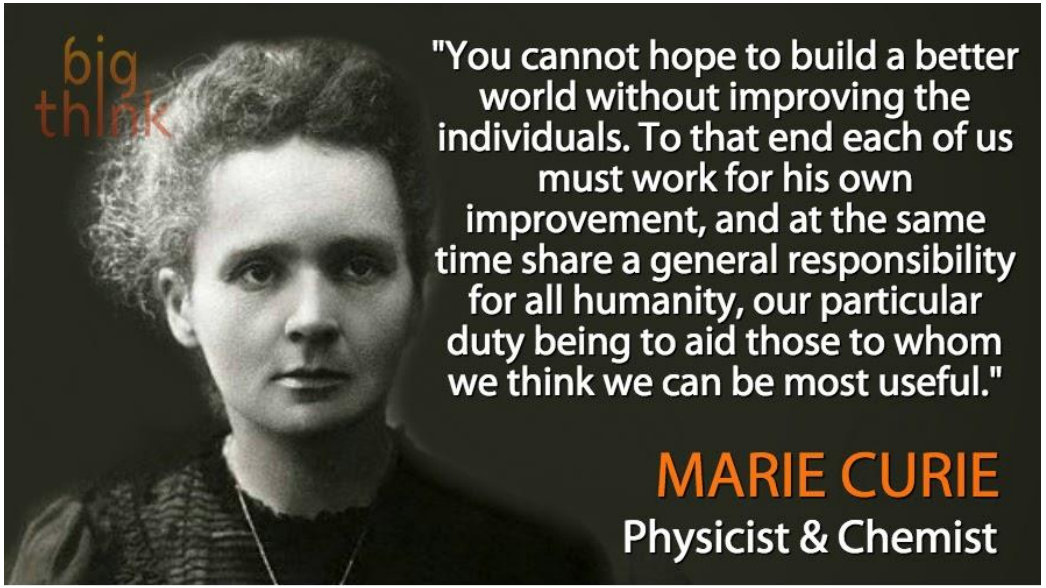

Smart ANSWER

HORIZON 2020 — MARIE CURIE ACTIONS

Thank you for your attention !

University of Southampton, Institute of Sound and Vibration Research — von KARMAN INSTITUTE FOR FLUID DYNAMICS — KU LEUVEN — EPFL — TU Delft — National Technical University of Athens

CETIAT ensemble, innover et valider — IMP PAN GDAŃSK — ÉCOLE CENTRALE LYON — LAUM — KTH VETENSKAP OCH KONST — Siemens PLM Software SIEMENS — SIEMENS Siemens Wind Power